

CALIBRATION OF THE PERFORMANCE MODELS OF THE AASHTOWARE PAVEMENT ME DESIGN SOFTWARE IN IDAHO

A Thesis

Presented in Partial Fulfillment of the Requirements for the

Degree of Master of Science

with a

Major in Civil Engineering

in the

College of Graduate Studies

University of Idaho

by

Mumtahir Hasnat

Major Professor: Fouad M.S. Bayomy, Ph.D., P.E.

Committee Members: Emad Kassem, Ph.D., P.E.; Ahmed A. Ibrahim, Ph.D., P.E.;

Christopher Williams, Ph.D.

Department Chair: Patricia J. S. Colberg, Ph.D., P.E.

August 2019

AUTHORIZATION TO SUBMIT THESIS

This thesis of Mumtahir Hasnat, submitted for the degree of Master of Science with a Major in Civil and Environmental Engineering and titled "CALIBRATION OF THE PERFORMANCE MODELS OF THE AASHTOWARE PAVEMENT ME DESIGN SOFTWARE IN IDAHO" has been reviewed in final form. Permission, as indicated by the signatures and dates below, is now granted to submit final copies to the College of Graduate Studies for approval.

Major Professor: _____ Date: _____
Fouad M.S. Bayomy, Ph.D., P.E.

Committee Members: _____ Date: _____
Emad Kassem, Ph.D., P.E.

_____ Date: _____
Ahmed A. Ibrahim, Ph.D., P.E.

_____ Date: _____
Christopher Williams, Ph.D.

Department
Chair: _____ Date: _____
Patricia J. S. Colberg, Ph.D., P.E.

ABSTRACT

The performance prediction models incorporated in the AASHTOWare Pavement ME Design software (PMED) were calibrated and validated using data primarily obtained from the Long-Term Pavement Performance (LTPP) program database. Therefore, the globally-calibrated models should be evaluated to determine whether they accurately predict field performance for Idaho local conditions. Otherwise, some pavements will be overdesigned and others under-designed, turning to either excessive costs or premature failure. This study aims to evaluate and improve the accuracy of the PMED asphalt and rigid pavement performance models for Idaho local conditions. A total of 34 flexible pavement and 39 rigid pavement sites were selected for conducting the local calibration effort. These sites represent different climate zones, traffic levels, pavement structures, and materials across Idaho. The required PMED inputs and the historical performance data for the selected sites were extracted from a variety of sources including project construction data, material testing records, Idaho Transportation Department (ITD) Transportation Asset Management System (TAMS). Each of the selected pavement sites were evaluated using PMED v2.5.3. The results showed a significant amount of bias and high standard error while comparing between the performance prediction and field observation. Therefore, to improve the accuracy of the software prediction with less bias and error, the PMED models were recalibrated and local factors were determined for both flexible and rigid performance models.

ACKNOWLEDGEMENTS

I would like to express my heartfelt gratitude to my supervisor Dr. Fouad M.S. Bayomy for his unconditional supports and inspirations that he showed throughout my graduate study. This would not be possible without the proper guidance of him. I am blessed to have an advisor like him who was always prompt and sincere in replying my questions and queries.

I would also like to acknowledge Dr. Emad Kassem, Dr. Ahmed Ibrahim and Dr. Cristopher Williams for being my committee members and advising me towards achieving the degree.

I am very much thankful to Dr. Ahmed Muftah, Research Fellow, who always encouraged me and helped me to every step of my graduate study here at U of I.

This study is a part of a research project that was sponsored by the Idaho Transportation Department (ITD) Special thanks are due to Mr. Mike Santi and Mr. James Poorbaugh of ITD. Their support and help in procuring pavement sections and performance data is greatly appreciated.

DEDICATION

To my beloved parents who sacrificed throughout their life.

TABLE OF CONTENTS

AUTHORIZATION TO SUBMIT THESIS	ii
ABSTRACT	iii
ACKNOWLEDGEMENTS	iv
DEDICATION	v
TABLE OF CONTENTS	vi
LIST OF TABLES	x
LIST OF FIGURES	xiv
CHAPTER 1: INTRODUCTION	1
1.1 Background	1
1.2 Problem Statement	2
1.3 Objectives	3
1.4 Thesis Organization.....	3
CHAPTER 2: LITERATURE REVIEW	5
2.1 AASHTOWare PMED Performance Prediction Models	5
2.1.1 Performance Prediction Models for Flexible Pavements	5
2.1.1.1 Rut Depth Prediction Models:.....	5
2.1.1.2 Load-Related Cracking (Fatigue) Models.....	7
2.1.1.3 Thermal Non-Load Related Cracking Model	10
2.1.1.4 Smoothness	11
2.1.2 Performance Prediction Models for Rigid Pavements.....	13
2.1.2.1 Transverse Slab Cracking Model	13
2.1.2.2 Joint Faulting Model	14
2.1.2.3 JPCP IRI Prediction Model.....	15
2.2 Local Calibration Effort of AASHTOWare PMED	16
2.2.1 Flexible Pavement.....	18
2.2.1.1 North Carolina.....	18
2.2.1.2 New Mexico	19
2.2.1.3 Minnesota.....	21
2.2.1.4 Washington	22

2.2.1.5 Arkansas	23
2.2.1.6 Arizona	24
2.2.1.7 Ohio	26
2.2.1.8 Tennessee	27
2.2.2 Rigid Pavement	28
2.2.2.1 Washington	28
2.2.2.2 Florida	29
2.2.2.3 Ohio	30
2.2.2.4 Utah	30
2.2.2.5 Iowa	31
2.2.2.6 Oregon	32
2.2.2.7 Colorado	32
2.2.2.8 Arizona	33
2.2.2.9 Louisiana	34
2.2.2.10 Kansas	35
2.2.2.11 Virginia	36
2.3 Conclusions	37
CHAPTER 3: METHODOLOGY FOR VERIFICATION AND LOCAL CALIBRATION OF PMED PERFROMANCE MODELS	43
3.1 Select Hierarchical Input level for Individual Input Parameter	43
3.1.1 Traffic Data	44
3.1.1.1 Vehicle Class Distribution	46
3.1.1.2 Monthly Adjustment Factors	48
3.1.1.3 Hourly Adjustment Factors	49
3.1.1.4 Number of Axles per Vehicle	50
3.1.1.5 Axle Load Spectra	50
3.1.2 Climate Data	50
3.1.3 Materials Data	53
3.1.3.1 Asphalt Concrete Layer Properties	53
3.1.3.2 Rigid Pavement Layer Properties	54
3.1.3.3 Base and Subbase Layer properties	56

3.1.3.4 Subgrade Layer Properties	56
3.2 Local Experimental Plan	57
3.3 Estimate Sample Size for Specific Distress Predictions Models	58
3.4 Projects Selection	59
3.5 Extract and Evaluate Distress and Project Data	64
3.6 Conduct Field and Forensic Investigation.....	65
3.7 Assess Local Bias Using Global Calibration Coefficients	65
3.8 Eliminate Local Bias of Distress and IRI Prediction Models.....	66
3.9 Assess the Standard Error of Estimate	66
3.10 Reduce Standard Error of the Estimate	67
CHAPTER 4: DEVELOPMENT OF THE PMED CALIBRATION FACTORS FOR FLEXIBLE PAVEMENT	68
4.1 Calibration of Rutting Models.....	68
4.1.1 Verification of Rutting Models Using Global Calibration Factors.....	68
4.1.2 Calibration of Rutting Models	69
4.1.3 Validation of Rutting Models	70
4.2 Calibration of Longitudinal Cracking (Top-Down) Cracking Model	71
4.2.1 Verification of Longitudinal Cracking Model Using Global Calibration Factors....	71
4.2.2 Calibration of Longitudinal Cracking Model	72
4.2.3 Validation of Longitudinal Cracking Model	73
4.3 Calibration of Alligator (Bottom-Up) Cracking Model	74
4.3.1 Verification of Alligator Cracking Model Using Global Calibration Factors	75
4.3.2 Calibration of Alligator Cracking Model.....	76
4.3.3 Validation of Alligator Cracking Model.....	77
4.4 Calibration of Transverse (Thermal) Cracking	77
4.4.1 Transverse Cracking Model at Level 3.....	78
4.4.1.1 Verification of Transverse Cracking Model at Level 3 Using Global Calibration Factors	78
4.4.1.2 Calibration of Transverse Cracking Model at Level 3.....	79
4.4.1.3 Validation of Transverse Cracking as Level 3.....	79
4.4.2 Transverse Cracking (Level 2)	80

4.4.2.1 Verification of Transverse Cracking Model at Level 2 Using Global Calibration Factors	80
4.4.2.2 Calibration of Transverse Cracking Model at Level 2.....	81
4.4.2.3 Validation of Transverse Cracking Model at Level 2.....	82
4.5 Calibration of International Roughness Index (IRI) Model	82
4.5.1 Verification of IRI Model Using Global Calibration Factors.....	83
4.5.2 Calibration of IRI Model	84
4.5.3 Validation of IRI.....	84
4.6 Calibration Results	85
CHAPTER 5: DEVELOPMENT OF THE PMED CALIBRATION FACTORS FOR RIGID PAVEMENT	87
5.1 Calibration of Joint Faulting Model	87
5.1.1 Verification of Joint Faulting Model Using Global Calibration Factors	87
5.1.2 Calibration of Joint Faulting Model.....	88
5.1.3 Validation of Joint Faulting	89
5.2 Calibration of Transverse Cracking Model	90
5.2.1 Verification of Transverse Cracking Model Using Global Calibration Factors	90
5.2.2 Calibration of Transverse Cracking Model	91
5.2.3 Validation of Transverse Cracking Model.....	92
5.3 Calibration of International Roughness Index (IRI) Model	93
5.3.1 Verification of IRI Model Using Global Calibration Factors.....	93
5.3.2 Calibration of IRI Model	94
5.3.3 Validation of IRI Model	95
5.4 Calibration Results	96
CHAPTER 6: SUMMARY, CONCLUSIONS, AND RECOMMENDATIONS	97
6.1 Summary	97
6.2 Conclusions	99
6.3 Recommendations	101
REFERENCES.....	102
APPENDIX	107

LIST OF TABLES

Table 2.1 Developed Calibration Factors for North Carolina.....	19
Table 2.2 Final Calibration Factors Determined in New Mexico for Flexible Pavements.....	21
Table 2.3 Summary Set of the Calibration Factors Established in Washington	23
Table 2.4 Established Calibration Factors in Arkansas for Flexible Pavement.....	24
Table 2.5 Established Calibration Factors for Two different Versions of MEPDG Software in Arizona.....	26
Table 2.6 A Summary of Local Calibration Factors in Tennessee	28
Table 2.7 Comparison of Nationally and Locally Calibrated Model.....	30
Table 2.8 Developed Local Calibration Factors for JPCP Predictions Models in Iowa	32
Table 2.9 Developed Local calibration Factors for JPCP in Arizona	34
Table 2.10 Developed Local Calibration factors for JPCP in Louisiana	35
Table 2.11 Developed Local Calibration Factors in Kansas.....	36
Table 2.12 Nationally Calibrated PMED Software’s Prediction Pattern on Flexible Pavement Sections for Different State Agency.	39
Table 2.13 Nationally Calibrated PMED Software’s Prediction Pattern on JPCP/CRCP Sections for Different State Agency.	40
Table 2.14 Reported Calibration Factors for Flexible Pavement Performance Models	41
Table 2.15 Reported Calibration Factors for Rigid Pavement Performance Models	42
Table 3.1 General Traffic Input Parameters for Idaho.....	45
Table 3.2 Vehicle Class Distribution of WIM Stations located in Idaho.....	48
Table 3.3 Monthly Adjustment Factors of WIM Stations located in Idaho.....	49
Table 3.4 Climate Stations for Selected Flexible Pavements in Idaho	51
Table 3.5 Climate Stations for LTPP Flexible Pavements.....	52

Table 3.6 Climate Stations for Rigid Pavements	52
Table 3.7 General Materials Inputs for AC Layer	54
Table 3.8 General Materials Inputs for PCC Surface Layer	55
Table 3.9 Base and Subbase Layer Properties Inputs	56
Table 3.10 Subgrade Layer Properties Inputs	56
Table 3.11 Experimental Sampling Matrix for Flexible Pavements.....	58
Table 3.12 Experimental Sampling Matrix for Rigid Pavements	58
Table 3.13 Required Minimum Number of Pavement Projects.....	59
Table 3.14 Selected Flexible Pavements in Idaho	61
Table 3.15 Selected LTPP Flexible Pavement Sections in Idaho	62
Table 3.16 Selected Rigid Pavement Sections in Idaho.....	62
Table 3.17 Selected LTPP Rigid Pavement Sections.....	63
Table 3.18 Suggested Calibration Coefficients to Eliminate Bias for Flexible and Rigid Pavement	66
Table 3.19 Suggested Calibration Coefficients to Reduce Standard Error of the Estimate (SEE) for Flexible and Rigid Pavement.....	67
Table 4.1 Summary of the Global Calibration Factors of Rutting Models	68
Table 4.2 Summary of the Local Calibration Factors of Rutting Models.....	70
Table 4.3 Summary for Rutting Models after Validation	71
Table 4.4 Summary of the Global Calibration Factors of Longitudinal Cracking Model	72
Table 4.5 Summary of the Local Calibration Factors of Longitudinal Cracking Model	73
Table 4.6 Summary for Longitudinal Cracking Model after Validation	74
Table 4.7 Summary of the Global Calibration Factors of Alligator Cracking Model	75
Table 4.8 Summary of the Local Calibration Factors of Alligator Cracking Model	76

Table 4.9 Summary for Alligator Cracking Model after Validation.....	77
Table 4.10 Summary of the Global Calibration Factors of Thermal Cracking (Level 3) Model	78
Table 4.11 Summary of the Local Calibration Factors of Thermal Cracking (Level 3) Model	79
Table 4.12 Summary for Thermal Cracking (Level 3) Model after Validation.....	80
Table 4.13 Summary of the Global Calibration Factors of Thermal Cracking (Level 2) Model	81
Table 4.14 Summary of the Local Calibration Factors of Thermal Cracking (Level 2) Model	82
Table 4.15 Summary of the Global Calibration Factors of IRI Model	83
Table 4.16 Summary of the Local Calibration Factors of IRI Model	84
Table 4.17 Summary of IRI Model after Validation.....	85
Table 4.18 Developed Local Factors for Flexible Pavement in Idaho.....	86
Table 5.1 Summary of the Global Calibration Factors of Joint Faulting Model	87
Table 5.2 Summary of the Local Calibration Factors of Joint Faulting Model	88
Table 5.3 Summary for Joint Faulting Model after Validation.....	89
Table 5.4 Summary of the Global Calibration Factors of Transverse Cracking Model	90
Table 5.5 Summary of the Local Calibration Factors of Transverse Cracking Model	92
Table 5.6 Summary of the Global Calibration Factors of IRI Model	93
Table 5.7 Summary of the Local Calibration Factors of IRI Model	94
Table 5.8 Summary of IRI Model after Validation.....	95
Table 5.9 Developed Local Factors for Rigid Pavement in Idaho.....	96

Table 6.1 Summary of Calibration Factors before and after Local Calibration for Flexible Pavement in Idaho.....	98
Table 6.2 Summary of Calibration Factors before and after Local Calibration for Rigid Pavement in Idaho.....	99
Table A.1 Site Specific Traffic Inputs for Idaho Local Pavements.....	107
Table A.2 Site Specific Traffic Inputs for LTPP Sections.....	108
Table A.3 Measured Rutting and IRI Data for Idaho Local Pavements.....	109
Table A.4 Measured Rutting and IRI Data for LTPP Sections in Idaho.....	112
Table A.5 Measured Longitudinal, Alligator and Thermal Cracking Data for Idaho Local Pavements.....	113
Table A.6 Measured Longitudinal, Alligator and Thermal Cracking Data for LTPP Sections in Idaho.....	115
Table A.7 Measured Faulting, Transverse Cracking and IRI Data for Rigid Sections in Idaho.....	116
Table A.8 Measured Faulting, Transverse Cracking and IRI Data for LTPP Rigid Sections in Idaho.....	120

LIST OF FIGURES

Figure 2.1 Summary of Agency PMED Implementation Status for Flexible Pavements.....	17
Figure 2.2 Summary of Agency PMED Implementation Status for Rigid Pavements	18
Figure 3.1 FHWA Vehicle Classification	47
Figure 3.2 Selected Flexible Pavement Sections in Idaho	63
Figure 3.3 Selected Rigid Pavement Sections.....	64
Figure 4.1 Predicted Vs. Measured Total Rutting Using Global Calibration Factors	69
Figure 4.2 Predicted Vs. Measured Total Rutting Using Local Calibration Factors	70
Figure 4.3 Predicted Vs. Measured Total Rutting Using Local Factors	71
Figure 4.4 Predicted Vs. Measured Longitudinal Cracking Using Global Calibration Factors	72
Figure 4.5 Predicted Vs. Measured Longitudinal Cracking Using Local Calibration Factors	73
Figure 4.6 Predicted Vs. Measured Longitudinal Cracking Using Local Factors	74
Figure 4.7 Predicted Vs. Measured Alligator Cracking Using Global Calibration Factors.....	75
Figure 4.8 Predicted Vs. Measured Alligator Cracking Using Local Calibration Factors	76
Figure 4.9 Predicted Vs. Measured Alligator Cracking Using Local Factors	77
Figure 4.10 Predicted Vs. Measured Transverse Cracking (Level 3) Using Global Calibration Factors	78
Figure 4.11 Predicted Vs. Measured Transverse Cracking (Level 3) Using Local Calibration Factors	79
Figure 4.12 Predicted Vs. Measured Transverse Cracking (Level 3) Using Local Factors.....	80
Figure 4.13 Predicted Vs. Measured Transverse Cracking (Level 2) Using Global Calibration Factors	81

Figure 4.14 Predicted Vs. Measured Transverse Cracking (Level 2) Using Local Calibration Factors	82
Figure 4.15 Predicted Vs. Measured IRI Using Global Calibration Factors	83
Figure 4.16 Predicted Vs. Measured IRI Using Local Calibration Factors	84
Figure 4.17 Predicted Vs. Measured IRI Using Local Factors	85
Figure 5.1 Predicted Vs. Measured Faulting Using Global Calibration Factors	88
Figure 5.2 Predicted Vs. Measured Faulting Using Local Calibration Factors	89
Figure 5.3 Predicted Vs. Measured Faulting Using Local Factors	90
Figure 5.4 Predicted Vs. Measured Transverse Cracking Using Global Calibration Factors..	91
Figure 5.5 Predicted Vs. Measured Transverse Cracking Using Local Calibration Factors ...	92
Figure 5.6 Predicted Vs. Measured Transverse Cracking Using Local Factors	93
Figure 5.7 Predicted Vs. Measured IRI Using Global Calibration Factors	94
Figure 5.8 Predicted Vs. Measured IRI Using Local Calibration Factors	95
Figure 5.9 Predicted Vs. Measured IRI Using Local Factors	96

CHAPTER 1: INTRODUCTION

1.1 Background

The American Association of State Highway and Transportation Officials (AASHTO) Guide for Design of Pavement Structures (1993) ⁽¹⁾ was the basis for designing new and rehabilitated highway pavements in the United States for many years. The AASHTO 1993 guide was developed based on empirical performance equations that were developed using the performance data that were collected back in late 1950's and early 1960's from the then named American Association of State Highway Officials (AASHO) Road Test. The test road was limited to a particular geographical and climatic conditions in Ottawa, Illinois. The first version of the design guide was released as an interim design guide in 1972. Over the years, AASHTO had improved and updated the design guide to reach its latest version of 1993. Although the AASHTO 1993 design guide has been updated and improved, this empirical-based design method has limitations such as 1) it was based on one single climatic area 2) the road tests did not include sophisticated material characterization 3) experiments included limited traffic load with specific vehicle type and weight ⁽²⁾. To overcome these limitations, AASHTO initiated the National Cooperative Highway Research Program (NCHRP) Project 1-37A to develop a mechanistic-based pavement design method ^(3,4).

The Guide for Mechanistic-Empirical Pavement Design of New and Rehabilitated Pavement Structures was the released product of the NCHRP 1-37A project. The guide was associated with a design software, MEPDG version 0.7 to facilitate the design procedure and pavement analysis ⁽³⁾. The MEPDG software, being a research product of NCHRP project 1-37A released in 2004, has gone through extensive reviews and testing to verify its applicability to field conditions. AASHTO adopted the guide and its accompanied software and released it as the AASHTOWare Pavement ME Design Software (PMED). The latest release is Version 2.5.3 for which this study is performed.

Pavement responses such as stresses, strains and deflection are calculated mechanistically by the PMED software following engineering mechanics concepts. After that, empirical distress transfer functions are employed to convert pavement responses to predict pavement performance over the service period. PMED has brought a radical change in designing

pavement. It is an advanced pavement design and analysis tool which is functioned by numerous trial and error efforts.

The distress models adopted in the PMED software were calibrated at the national level using pavement performance data from the national Long-Term Pavement Performance (LTPP) database ⁽⁵⁾. Hence, the software as released by AASHTO is calibrated at the global level. For the successful implementation of the PMED Software in different states, AASHTO recommends validating the globally calibrated performance prediction models to evaluate whether they can accurately predict the field conditions at the local level. If not, local calibration of these models is warranted.

1.2 Problem Statement

The AASHTOWare Pavement ME Design Software represents the recent advancements that occurred in the field of pavement design and analysis. It is a sophisticated tool which requires many inputs compared to the previously popular design method, the AASHTO 1993 design guide. The new PMED has been calibrated using data from all over North America which is accessible via the national LTPP database. Therefore, applying the design procedures as calibrated globally could produce unrealistic results for a given local condition. For example, the climate of Texas is different from the climate of Illinois, and so are the construction practices and traffic patterns or growth rate. Hence, same performance models with same calibration factors would not offer accurate, trustworthy and economical design in these two different states. Therefore, since the release of the PMED software by AASHTO, many states including Idaho have started extensive efforts to implement the new design procedures and develop local calibration factors for the performance models that are included in the PMED software.

The Idaho Transportation Department (ITD) maintains more than 12,200 lane-miles of roads. With a large roadway system and a limited budget, it is essential that proper pavement structures are designed and constructed to withstand anticipated traffic loads and climate conditions over the intended design life. Since 2008, ITD has been in the process of implementing Mechanistic-Empirical Design for Idaho local roads, which included developing traffic inputs database, characterizing material properties for both asphalt and concrete mixes, unbound aggregate layers, and subgrade soils ^(7, 8). In addition, a user's guide

was developed to assist ITD personnel with the implementation of the PMED⁽⁹⁾. This study is to complete the implementation process of the AASHTOWare Pavement ME Design software in Idaho and develop local calibration factors that are applicable to the local conditions in the state of Idaho.

1.3 Objectives

The primary objective of this research is to verify the globally calibrated distress models in the PMED software, and calibrate its prediction equations for Idaho conditions. In order to fulfil the major objective the following tasks have been carried out:

- Identifying set of pavement sections across the state to conduct calibration process
- Development of performance databases for both flexible and rigid pavement to house the design, construction and performance data collected for the identified sections
- Verification of the globally calibrated PMED distress models for both flexible and rigid pavements using the AASHTOWare Pavement ME Design Software V2.5.3 to Idaho local conditions
- Local calibration of the PMED distress models for flexible pavement
- Local calibration of the PMED distress models for rigid pavement
- Validation of the calibrated factors

1.4 Thesis Organization

This thesis consists of six chapters:

Chapter 1 presents the background of this research study, problem statement, objectives of the study, and thesis organization.

Chapter 2 provides a review of the distress prediction models for both flexible and rigid pavement in the ME software and a comprehensive relevant literature review highlighting the implementation efforts done by other state agencies.

Chapter 3 describes the methodology which has been followed to accomplish the research objectives.

Chapter 4 discusses the verification, calibration and validation results for flexible pavement.

Chapter 5 discusses the verification, calibration and validation effort related to the rigid pavement.

Chapter 6 presents the summary, conclusions and recommendations for future study.

CHAPTER 2: LITERATURE REVIEW

This chapter presents a review of the performance prediction models of both the flexible pavement and rigid pavements that are impeded in the AASHTOWare PMED software. A brief discussion about the previous local calibration studies conducted by other state agencies in the United States is also presented.

2.1 AASHTOWare PMED Performance Prediction Models

All the models that are impeded in the PMED design software have been documented in the AASHTO MEPDG Manual of Practice 2015 ⁽¹⁰⁾. A brief summary is presented here.

2.1.1 Performance Prediction Models for Flexible Pavements

2.1.1.1 Rut Depth Prediction Models:

Rutting or surface distortion is caused by the permanent vertical deformation in pavement sublayers including the Hot-Mix-Asphalt (HMA) surface layers, unbound base and/or subbase layers, and the subgrade roadbed soil. The AASHTOWare Pavement ME Design calculates rutting at mid depth of each sublayer and represents the total rutting as the summation of all these rutting at different depth. Repeated load permanent deformation tri-axial (RLPDT) tests are generally followed in the laboratory for both HMA mixtures and unbound materials to calculate the rate of plastic deformation. Then, the rut depth calculated from the laboratory derived relationships is compared to the field observed rut depth to determine an adjustment factor. Accumulated permanent deformation can be calculated using Equation 2.1 for all type of mixtures ⁽¹⁰⁾.

$$\Delta_{p(HMA)} = \frac{\varepsilon_{p(HMA)}}{\varepsilon_{r(HMA)}} \times H_{HMA} = \beta_{1r} k_z 10^{k_{1r}} n^{k_{2r}} \beta_{2r} T^{k_{3r}} \beta_{3r} \times H_{HMA} \dots \dots \dots (2.1)$$

where,

$\Delta_{p(HMA)}$ = Accumulated permanent deformation (in.) in the Asphalt Concrete (AC) layer/sublayer

$\varepsilon_{p(HMA)}$ = Accumulated strain (in./in.) in the Asphalt Concrete (AC) layer/sublayer

H_{HMA} = Thickness of the AC layer

$\varepsilon_{r(HMA)}$ = Resilient strain calculated in the middle of each HMA sublayer, in./in.

n = Number of axle-load repetitions

T = Pavement temperature, °F

k_z = confinement factor related to depth

$k_{1r,2r,3r}$ = Global field calibration factors ($k_{1r} = -2.45$, $k_{2r} = 3.01$, $k_{3r} = 0.22$) and

$\beta_{1r}, \beta_{2r}, \beta_{3r}$ = Local field calibration constants; based on global calibration, $\beta_{1r} = 0.4$, $\beta_{2r} = 0.52$, $\beta_{3r} = 1.36$

$$k_z = (C_1 + C_2 D) 0.328196^D \dots\dots\dots (2.2)$$

$$C_1 = -0.1039(H_{HMA})^2 + 2.4868H_{HMA} - 17.342 \dots\dots\dots (2.3)$$

$$C_2 = 0.0172(H_{HMA})^2 - 1.7331H_{HMA} + 27.428 \dots\dots\dots (2.4)$$

where,

D = Depth below the surface where strain to be determined, in. and

H_{HMA} = Total thickness of HMA, in.

In order to calculate permanent deformation within all unbound pavement sublayers and the foundation can be determined using Equation 2.5 ⁽¹⁰⁾.

$$\Delta_{p(soil)} = \beta_{s1} k_{s1} \varepsilon_v h_{soil} \left(\frac{\varepsilon_o}{\varepsilon_r}\right) e^{-\left(\frac{p}{n}\right)^\beta} \dots\dots\dots (2.5)$$

where,

$\Delta_{p(Soil)}$ = Permanent deformation occurs in layer/sublayer, inches

ε_r = Applied resilient strain to attain material properties ε_o , β , and ρ , inches/inches

ε_o = Intercept deduced from laboratory RLPDT tests, inches/inches

ε_v = Average vertical resilient strain in the layer/sublayer obtained by the structural response model, in./in.

n = Number of axle-load applications

h_{Soil} = Unbound layer/sublayer thickness, in.,

k_{s1} = National calibration factors; $k_{s1} = 0.965$ for coarse materials and 0.675 for fine-grained materials, and

β_{s1} = Local calibration coefficient, related to rutting occurs in the unbound layers; $\beta_{s1} = 1.00$; derived from the global calibration effort

$$\text{Log}\beta = -0.61119 - 0.017638(W_c) \dots \dots \dots (2.6)$$

$$p = 10^9 \left(\frac{C_0}{(1 - (10^9)\beta)} \right)^{\frac{1}{\beta}} \dots \dots \dots (2.7)$$

$$C_0 = \text{Ln} \left(\frac{a_1 M_r^{b_1}}{a_9 M_r^{b_9}} \right) \dots \dots \dots (2.8)$$

where,

W_c = Water Content, %

M_r = Resilient modulus of the unbound layer or sublayer, psi,

$a_{1,9}$ = Regression factors; $a_1 = 0.15$ and $a_9 = 20.0$, and

$b_{1,9}$ = Regression factors; $b_1 = 0.0$ and $b_9 = 0.0$.

2.1.1.2 Load-Related Cracking (Fatigue) Models

Due to the repeated traffic loading, load related cracking propagates either from top or bottom surface of an asphalt concrete layer. Therefore, PMED predicts two different forms of load-related cracking such as bottom up cracking (alligator cracking) and top down cracking (longitudinal cracking). In order to predict these two kinds of load related cracks, the required allowable number of axle load applications can be calculated as follows ⁽¹⁰⁾:

$$N_{f-HMA} = k_{f1}(C)(C_H)\beta_{f1}(\varepsilon_t)^{k_{f2}\beta_{f2}}(E_{HMA})^{k_{f3}\beta_{f3}} \dots \dots \dots (2.9)$$

where,

N_{f-HMA} = Allowable number of axle-load applications for a flexible pavement and HMA overlays

ε_t = Tensile strain at critical positions, inches/inches

E_{HMA} = Dynamic modulus of HMA measured in compression, psi

k_{f1}, k_{f2}, k_{f3} = Global field calibration factors ($k_{f1} = 3.75, k_{f2} = 2.87,$ and $k_{f3} = 1.46$), and

$\beta_{f1}, \beta_{f2}, \beta_{f3}$ = Mixture specific or local field calibration factors; derived from global calibration effort,

if $h_{ac} < 5$ in., then $\beta_{f1} = 0.02054$; where, h_{ac} = AC layer thickness

if $h_{ac} > 12$ in., then $\beta_{f1} = 0.001032$ or

if $5 \text{ in.} \leq h_{ac} \leq 12 \text{ in.}$, then $\beta_{f1} = (5.014 * \text{Pow}(h_{ac}, -3.416)) * 1 + 0$

$\beta_{f2} = 1.38, \beta_{f3} = 0.88$

$$C = 10^M \dots\dots\dots (2.10)$$

$$M = 4.84 \left(\frac{V_{be}}{V_a + V_{be}} - 0.69 \right) \dots\dots\dots (2.11)$$

where,

V_{be} = Effective asphalt content by volume, %,

V_a = Percent air voids in the HMA mixture, and

C_H = Thickness correction term, dependent on type of cracking

For bottom-up (alligator cracking):

$$C_H = \frac{1}{0.000398 + \frac{0.003602}{1 + e^{(11.02 - 3.49H_{HMA})}}} \dots\dots\dots (2.12)$$

For top-down (longitudinal cracking):

$$C_H = \frac{1}{0.01 + \frac{12.00}{1 + e^{(15.676 - 2.8186H_{HMA})}}} \dots\dots\dots (2.13)$$

where,

H_{HMA} = Total thickness of HMA, inches

Predictions of load-related cracking requires cumulative Damage Index (DI) at each critical location. The DI itself is just the summation of the incremental damages (ΔDI) occur with

time as shown in Equation 2.14 ⁽¹⁰⁾. While incremental damages can be estimated by dividing the actual number of axle loads by the allowable number of axle loads.

$$DI = \sum(\Delta DI)_{j,m,l,p,T} = \sum\left(\frac{n}{N_{f-HMA}}\right)_{j,m,l,p,T} \dots\dots\dots (2.14)$$

where,

n = Actual number of axle-load applications within a specific time period,

j = Axle-load interval,

m = Axle-load type (single, tandem, tridem, or quad),

l = Type of truck

p = Month, and

T = Median temperature for the five temperature intervals that subdivide each month, °F.

The following mathematical equation is used within PMED software to predict the alligator cracking area ⁽¹⁰⁾.

$$FC_{Bottom} = \left(\frac{1}{60}\right)\left(\frac{C_3}{1 + e^{(C_1 C_1^* + C_2 C_2^* \text{Log}(DI_{Bottom} * 100))}}\right) \dots\dots\dots (2.15)$$

where,

FC_{Bottom} = Area of alligator cracking that initiates at the bottom of the HMA layers, percent of total lane area

DI_{Bottom} = Cumulative damage index at the bottom of the HMA layers, and

$C_{1,2,3}$ = Transfer function regression constants; $C_3= 6,000$; $C_1=1.31$; and

if $h_{ac} < 5$ in., then $C_2 = 2.1585$; where h_{ac} = AC layer thickness

if $h_{ac} > 12$ in., then $C_2 = 3.9666$ or

if $5 \text{ in.} \leq h_{ac} \leq 12 \text{ in.}$, then $C_2 = (0.867 + 0.2583 * h_{ac}) * 1 + 0$

$$C_1^* = -2C_2^* \dots\dots\dots (2.16)$$

$$C_2^* = -2.40874 - 39.748 (1 + H_{HMA})^{-2.856} \dots\dots\dots (2.17)$$

The mathematical relationship used within PMED software to predict the longitudinal cracking length ⁽¹⁰⁾.

$$FC_{TOP} = 10.56 \left(\frac{C_4}{1 + e^{(C_1 - C_2 \text{Log}(DI_{TOP}))}} \right) \dots\dots\dots (2.18)$$

where,

FC_{Top} = Length of longitudinal cracks that initiate at the top of the HMA layer, ft/mile,

DI_{Top} = Cumulative damage index close to the top of the HMA surface, and

$C_{1,2,4}$ = Transfer function regression constants; $C_1= 7.00$; $C_2= 3.5$; and $C_4= 1,000$.

2.1.1.3 Thermal Non-Load Related Cracking Model

Temperature variation cause cracking in the pavement that is not load dependent. The non-load related cracking model is represented by Equation 2.19 ⁽¹⁰⁾.

$$\Delta C = A(\Delta K)^n \dots\dots\dots (2.19)$$

where,

ΔC = Cooling cycle caused crack depth change

ΔK = Change in the stress intensity factor due to a cooling cycle, and

A, n = HMA mixture related fracture parameters

According to the following two mathematical representations, A and n can be determined from the experimental results of the indirect tensile strength test and creep compliance test of the HMA.

$$A = k_t \beta_t 10^{[4.389 - 2.52 \text{Log}(E_{HMA} \sigma_m^n)]} \dots\dots\dots (2.20)$$

$$n = 0.8 \left[1 + \frac{1}{m} \right] \dots\dots\dots (2.21)$$

where,

k_t = Coefficient determined through global calibration for each input level

E_{HMA} = Indirect tensile modulus for HMA, psi,

σ_m = Tensile strength for mixture, psi,

m = The m-value derived from the indirect tensile creep compliance curve measured in the laboratory, and

β_t = Local or mixture calibration coefficient.

Simplified equation of stress intensity factor, K as shown in equation 2.22 is established using Theoretical finite element studies.

$$K = \sigma_{tip} [0.45 + 1.99 (C_o)^{0.56}] \dots\dots\dots (2.22)$$

where,

σ_{tip} = Far-field stress at depth of crack tip, psi, and

C_o = Current crack length, ft.

Degree of cracking predictions follows the below stated equation ⁽¹⁰⁾.

$$TC = \beta_{tl} N \left[\frac{1}{\sigma_d} \text{Log} \left(\frac{C_d}{H_{HMA}} \right) \right] \dots\dots\dots (2.23)$$

where,

TC = Thermal cracking witnessed, ft/mile

β_{tl} = Regression coefficient derived from global calibration; ($\beta_{tl}=400$)

$N[z]$ = Standard normal distribution evaluated at $[z]$,

σ_d = Standard deviation of the log of the depth of cracks in the pavement (0.769), in.,

C_d = Depth of crack, inches, and

H_{HMA} = HMA layers thickness, inches

2.1.1.4 Smoothness

The International Roughness Index (IRI) has been adopted as a universal indicator of how smooth or rough the pavement surface is. High IRI value indicates rough pavement, where low IRI indicates a smooth surface. Depending on the class of road, acceptable IRI values may range from as low as 70 to as high as 170. The prediction of pavement smoothness is

related to other types of distresses. Equation 2.24 and Equation 2.25 have been developed using the LTPP data and included within the AASHTOWare PMED to evaluate the international roughness index (IRI) for new HMA-surfaced pavements over the pavements service life ⁽¹⁰⁾.

$$IRI = IRI_0 + C_1(RD) + C_2(FC_{Total}) + C_3(TC) + C_4(SF) \dots\dots\dots (2.24)$$

where,

IRI_0 = Initial smoothness, inches/mile

SF = Site factor,

$$SF = Age^{1.5} \{ \ln[(Precip + 1)(FI + 1)_{P_{0.2}}] \} + \{ \ln[(Precip + 1)(PI + 1)_{P_{200}}] \} \dots\dots\dots (2.25)$$

FC_{Total} = Area of fatigue cracking (combined bottom-up, top-down, and reflection cracking in the wheel path), % of total lane area

TC = Length of transverse cracking, ft/mile, and

RD = Average rut depth, inches

$C_{1,2,3,4}$ = Calibration factors; $C_1 = 40.0$, $C_2 = 0.4$, $C_3 = 0.008$, $C_4 = 0.015$

where,

Age = Pavement age, year,

PI = Percent plasticity index of the soil,

FI = Average annual freezing index, °F days, and

$Precip$ = Average annual precipitation or rainfall, in.

$P_{0.2}$ = Percent passing the 0.02 mm sieve

P_{200} = Percent passing the 0.075 mm sieve

2.1.2 Performance Prediction Models for Rigid Pavements

AASHTOWare Pavement ME Design (PMED) software functions based on mainly three performance models for JPCP (Jointed Plain Concrete Pavement). These three models are briefly described in the following sub-sections.

2.1.2.1 Transverse Slab Cracking Model

Transverse cracking is considered as one of the prominent distresses that occur in rigid pavements. It appears as straight cracks that spread-out normal to the centerline of the pavements. Such cracks are initiated either at the top or bottom of the pavement and propagates on the other direction. Top-down cracking initiates from the top and propagate to other direction. It may happen when the bottom slab of the pavement becomes hotter than the top slab. On the other hand, bottom-up slab cracking is the phenomenon created once there is a higher positive temperature gradient present in the pavement (bottom portion is colder than the top). These both type of transverse slab cracking can lead to full deterioration of pavement. Transverse slab cracking depends on traffic loading, climate condition, material characteristics, and design criteria ⁽³⁾.

The PMED uses the model presented in Equations 2.25 and 2.26 to predict both top-down and bottom-up cracking ⁽¹⁰⁾:

$$TCRACK = (CRK_{Bottom-up} + CRK_{Top-down} - CRK_{bottom-up} \cdot CRK_{Top-down}) \cdot 100 \dots \quad (2.25)$$

$$Crack = \frac{100^{\log(N_{allowable})}}{1+C4 \cdot FD^{C5}} = \frac{100^{C1} \left(\frac{MR}{\sigma}\right)^{C2}}{1+C4 \cdot \left(\frac{N_{applied}}{N_{allowable}}\right)^{C5}} \dots \dots \dots (2.26)$$

where,

TCRACK = Total transverse cracking (% , all severities)

CRK = Predicted amount of transverse cracking (bottom-up and top-down)

FD = Damage due to fatigue

C1, C2 = Calibration coefficient constants, default C1 = 2.0, C2 = 1.22

C4, C5 = Calibration coefficient constants, default C4 = 0.52, C5 = -2.17

N_{allowable} = Allowable number of traffic repetitions

MR = Modulus of rupture, psi

σ = Applied stress at different conditions

2.1.2.2 Joint Faulting Model

Another type of pavement distress is joint faulting which is the cause of vertical pavement displacement across the joint due to repeated loading of wheels ⁽¹¹⁾. Joint faulting may vary from joint to another. It is predicted in a month to month basis incremental method in PMED. Equations 2.27 through 2.30 present the models used in PMED to predict joint faulting ⁽¹⁰⁾.

$$Fault_m = \sum_{i=1}^m \Delta Fault_i \dots \dots \dots (2.27)$$

$$\Delta Fault_i = (F3 + F4 \cdot FR^{0.25}) \cdot (FaultMax_{i-1} - Fault_{i-1})^2 DE_i \dots \dots \dots (2.28)$$

$$FaultMax_i = FaultMax_0 + F7 \sum_{k=1}^i DE_k \cdot \log(1 + F5 \cdot 5^{EROD})^{F6} \dots \dots \dots (2.29)$$

$$FaultMax_0 = (F1 + F2 \cdot FR^{0.25}) \delta_{curling} \left[\log(1 + F5 \cdot 5^{EROD}) \cdot \text{Log}\left(\frac{P_{200} \cdot WetDays}{P_s}\right) \right]^{F6} \dots \dots \dots (2.30)$$

where,

$Fault_m$ = Calculated mean joint faulting after the completion of month m, inches

$\Delta Fault_i$ = Change (incremental) in joint faulting during month i, inches

$FAULTMAX_i$ = Maximum mean transverse joint faulting for month i, inches

$FAULTMAX_0$ = Initial maximum mean transverse joint faulting, inches

$EROD$ = Erodibility factor

DE_i = Differential density of energy of subgrade deformation

$\delta_{curling}$ = Maximum mean monthly slab corner upward deflection

P_s = Overburden pressure on subgrade, lb

P_{200} = Percent subgrade material passing #200 sieve

$WetDays$ = Number of wet days calculated as annual average

$F_{1,2,3,4,5,6,7}$ = F1 = 0.595, F2 = 1.636, F3 = 0.00217, F4 = 0.00444, F5 = 250, F6 = 0.47, F7 = 7.3 (National calibration constants)

FR = Freezing index

2.1.2.3 JPCP IRI Prediction Model

The International Roughness Index (IRI) is a parameter describes the smoothness and ride quality of a pavement. It is dependent on the other two type of distress prediction models alongside with site factor and spalling. Equation 2.31 is used to predict IRI in PMED ⁽¹⁰⁾.

$$IRI = IRI_0 + J1 \cdot Crack + J2 \cdot Spall + J3 \cdot Fault + J4 \cdot SiteFactor \dots \dots \dots (2.31)$$

where,

IRI = Predicted IRI, inches/mile

IRI_0 = Initial IRI after construction, inches/mile

$Crack$ = Percent slabs with transverse cracks (all severities)

$Spall$ = Percentage of joints with spalling (medium and high severities)

$Fault$ = Total joint faulting cumulated per mi, inches

$J_{1,2,3,4}$ = Global calibration constants, $J1 = 0.8203$, $J2 = 0.4417$, $J3 = 1.4929$, $J4 = 25.24$

$$SiteFactor = AGE (1 + 0.5556 * FI) (1 + P_{200}) * 10^{-6} \dots \dots \dots (2.32)$$

where,

AGE = Age since construction, year

FI = Freezing index, °F-days

P_{200} = Percent subgrade material passing #200 sieve

$$Spall = \left(\frac{AGE}{AGE + 0.01} \right) \left(\frac{100}{1 + 1.005^{-12 * AGE + SCF}} \right)$$

where,

AGE = Age from the time when pavement was constructed, year

SCF = Scaling factor

$$SCF = -1400 + 350 \cdot AC_{PCC} \cdot (0.5 + PREFORM) + 3.4 f'c \cdot 0.4 - 0.2(FT_{cycles} \cdot AGE) + 43H_{PCC} - 536 WC_{PCC} \dots\dots\dots (2.33)$$

where,

AC_{PCC} = Air content for PCC mixture, %

AGE = Pavement Age, year

$PREFORM$ = 1 for preformed sealant; 0 if not

$f'c$ = Compressive strength, psi

FT_{cycles} = Number of freeze-thaw cycles calculated as annual average

H_{PCC} = Thickness of PCC slab, inches

WC_{PCC} = Water to cement ratio

2.2 Local Calibration Effort of AASHTOWare PMED

The AASHTOWare Pavement ME Design (PMED), formerly known as MEPDG, implementation effort has become a common topic discussed by state highway agencies. Hundreds of publications have been published in different transportation journals covering PMED and its implementation efforts. Local calibration of PMED software is a vital task in its implementation which follows the steps described in the NCHRP 1-40B project ⁽¹²⁾. These studies were used to learn from other states how to overcome challenges in the local calibration and successfully implement the mechanistic-empirical design in Idaho. Among these many publications, this part of the study highlights the most notable calibration efforts of 16 states covering both the flexible and rigid pavements.

Some state transportation agencies have implemented or have planned to implement Mechanistic-empirical concept for their local conditions. On the contrary, other states have no plans for the implementation. A recent survey, conducted by the AASTHTO Pavement ME National User Group shows that 13 and 14 states implemented the PMED for flexible and rigid pavement, respectively. However, few states disclosed no plan for the implementation ⁽¹³⁾. The remaining states are involved in conducting the calibration and implementation of both types of pavements within the coming five years. Figure 2.1 and

Figure 2.2 present the most recent map of PMED implementation all over the United States, respectively for flexible and rigid pavements.

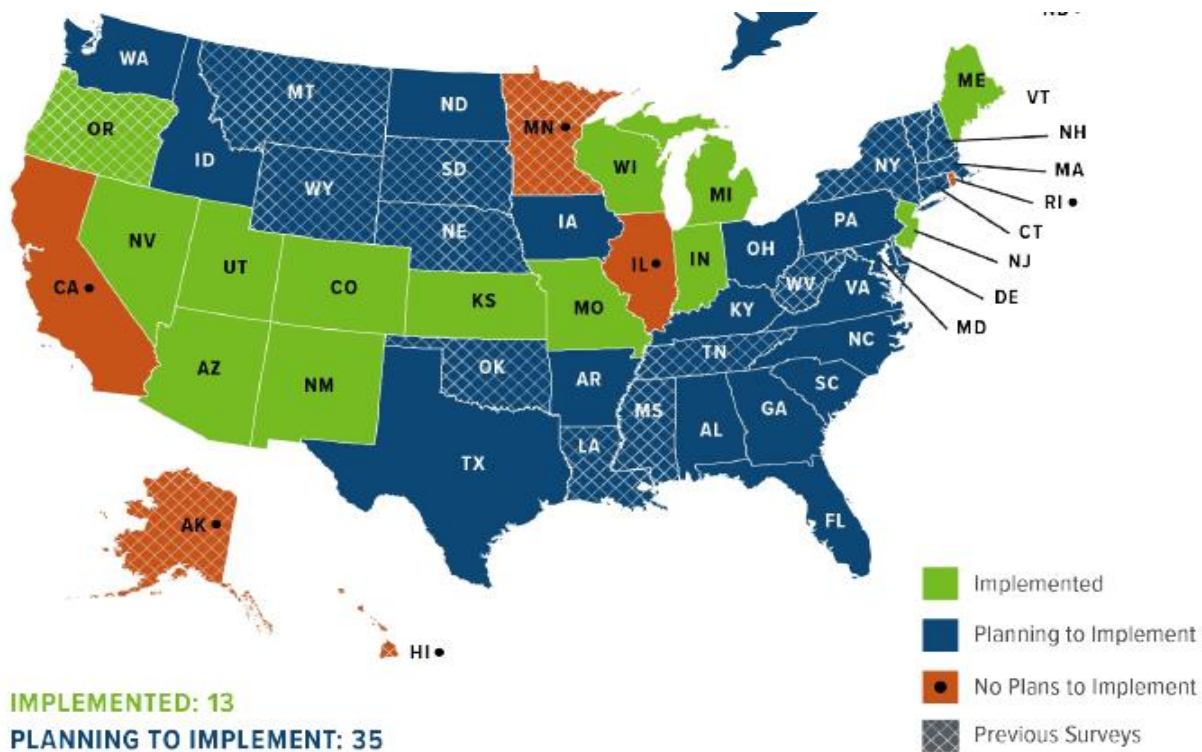


Figure 2.1 Summary of Agency PMED Implementation Status for Flexible Pavements ⁽¹³⁾

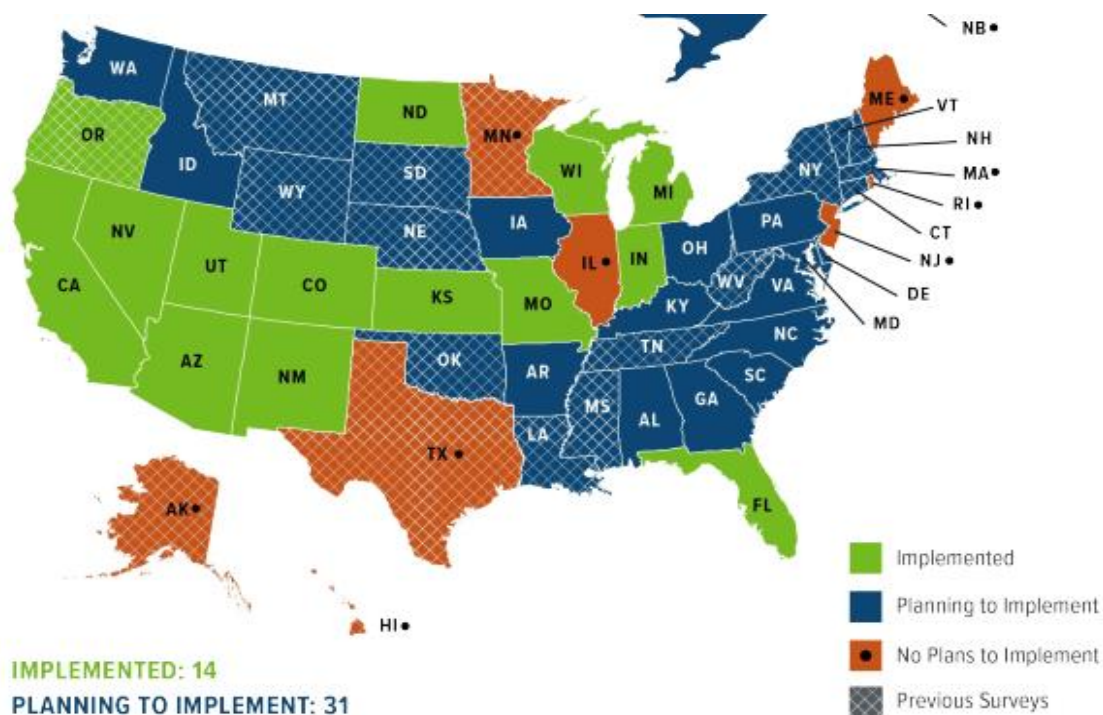


Figure 2.2 Summary of Agency PMED Implementation Status for Rigid Pavements ⁽¹³⁾

2.2.1 Flexible Pavement

This section discusses the implementation effort of the AASHTOWare Pavement ME Design by other state agencies for flexible pavement.

2.2.1.1 North Carolina

A study was conducted by Muthadi and Kim in 2008⁽¹⁴⁾ to locally calibrate the MEPDG for flexible pavement in the state of North Carolina. This study only considered the bottom-up cracking and the permanent deformation distress models to refine the MEPDG prediction accuracy through local calibration. The MEPDG version 1.0 was used in that process. A total of 53 flexible pavements were adopted from the LTPP database and the Pavement Management unit of the North Carolina Department of Transportation (NCDOT) to calibrate and validate the performance models. These pavement sections represent three different geographical regions (mountain, piedmont, and coastal) within North Carolina. Due to the inappropriate reporting unit of the rut depth measurement for NCDOT pavement sections, a discrepancy was observed between the predicted and measured rutting values. Therefore, the calibration effort for permanent deformation was done only considering LTPP sections.

Conversely, both the NCDOT and LTPP pavement sections were employed for the bottom-up cracking. The typical splitting method was employed, where 80% of the randomly selected projects were used to do the calibration and the left over 20% independent projects were set aside for validation purpose.

The verification results showed that bias existed between the predicted total rut depth and the measured value. The bottom-up cracking model under-predicted cracking.

The calibration effort for both these models nullified bias and significantly reduced the standard error of the estimate. Also, the null hypothesis was accepted that there was no differences between the predicted value and the measured data. However, the alligator cracking model yet showed poor prediction. The probable reason was thought that as the measurement method in North Carolina allowed them to capture only cracking in the outer wheel path, it provided lower measurement in general. Thus it was recommended to evaluate the distresses further, following the LTPP distress-identification manual ⁽¹⁵⁾. A Chi-square test was performed as well for both the models and it was found that the locally obtained standard error was comparable to that globally calibrated model. Moreover, the validation approach also recognized the calibration effort. Therefore, this study finally established following calibration factors set, highlighted in Table 2.1 ⁽¹⁴⁾.

Table 2.1 Developed Calibration Factors for North Carolina

Performance Model	Distress Type/Layer	Global Factors	Local Factors
Rutting	AC, (k1)	-3.35412	-3.41273
	Granular Base, (β_{s1})	2.03	1.5803
	Subgrade, (β_{s1})	1.67	1.10491
Fatigue Cracking	Bottom-Up Transfer Function (C_1, C_2, C_3)	1, 1, 6000	0.437199, 0.150494, 6000

2.2.1.2 New Mexico

Tarefder and Rodriguez-Ruiz performed a study on local calibration of the MEPDG software. ⁽¹⁶⁾ They used MEPDG version 1.0 with a total of 24 pavement sections in New Mexico to conduct the local calibration study for New Mexico. Among these pavement sections, 11 sections were extracted from the New Mexico Department of Transportation (NMDOT) sources, and the other 13 sections were from the LTPP database. This study

considered total rutting, alligator cracking, longitudinal cracking, and smoothness model to verify them using the globally calibrated factors and then if required would do the local calibration. The splitting method was adopted, whereas 19 projects were selected randomly to do the local calibration and the remaining 5 projects kept aside for the validation process.

The verification results revealed that, except the IRI model, the other three models showed bias in their respective prediction. For the permanent deformation, coefficient factors β_{r2} and β_{r3} were deemed most influential. Therefore, these two factors were adjusted at first for various combinations until the minimum sum of squared errors (SSE) and the mean residual error (MSE) obtained. Once these two factors were optimized, others factors (β_{r1} β_{GB} β_{SG}) for the permanent deformation model were adjusted in the similar way. It can be noted that as the NMDOT measured rutting was not consistent with the MEPDG reporting unit, the verification result showed that there was a different trend between the LTPP performance data and the converted NMDOT data. After calibration, the bias was reduced and the standard error was mitigated.

In the case of fatigue damage equation, the factors β_{f1} , β_{f2} , and β_{f3} could not be calibrated due to the unavailability of data to be compared with. Therefore, these coefficients were kept as default while calibrating the alligator cracking. The calibration factors C_1 and C_2 for the bottom up cracking prediction model were adjusted with the trial and error efforts.

Similarly, the longitudinal cracking model was calibrated adjusting C_1 and C_2 , though the researchers faced challenges as most of the measured values were identified almost zero. Among various combination of these two factors, $C_1 = 3$ and $C_2 = 0.3$ provided a significant improvement with the minimum SSE. Also, the calibration effort clustered the data points around the 45° line, hence reduced the bias.

For IRI model, only site factor was considered to adjust, and other new calibration factors for the distress models were used to run simulations. However, it was found that globally calibrated IRI model showed better prediction than the calibrated model. Table 2.2 presents the final results of the determined calibration factors in New Mexico.

This researchers realized that approximately 50 projects would be sufficient to further calibrate the MEPDG to predict distresses more precisely. This study also made a

recommendation to measure distresses in the appropriate unit which can be readily used to make comparison with the MEPDG prediction.

Table 2.2 Final Calibration Factors Determined in New Mexico for Flexible Pavements.

Performance Model	Distress Type/Layer	Global Factors	Local Factors
Total Rutting	AC, (β_{r1} , β_{r2} , β_{r3})	1.0, 1.0, 1.0	1.1, 1.1, 0.8
	Granular Base, (β_{s1})	1.0	0.8
	Subgrade, (β_{s1})	1.0	1.2
Fatigue Cracking	Bottom-Up Transfer Function (C_1 , C_2 , C_3)	1, 1, 6000	0.625, 0.25, 6000
	Top-Down Transfer Function (C_1 , C_2 , C_3 , C_4)	7, 3.5, 0, 1000	3, 0.3, 0, 1000
IRI	Smoothness (C_4)	0.015	0.015

2.2.1.3 Minnesota

Hoegh et al. in 2010 conducted the evaluation and local calibration of the MEPDG for asphalt pavement rutting model in Minnesota ⁽¹⁷⁾. The approach for local calibration was found unique compared to other studies. This study proposed a modified model for total rutting, rather than changing the globally calibrated model factors.

The Minnesota Road Research Project (MnROAD) facility contains an enriched database to perform the local calibration. As a result, a total of 12 main-line-HMA pavement test sections were selected, on which over 1300 measurements for rutting were recorded in the truck and passing lane. The MEPDG version 1.0 was run at 50% reliability level in this study.

Due to having limited knowledge about the rutting information correspondence to individual pavement layers, the MnROAD personnel were involved in several forensic investigations. The findings revealed that mostly rutting appeared in the upper parts of HMA layer, whereas the granular base and subgrade were found not affected.

In general, verification results with the global factors showed that the MEPDG over predicted total rutting for MnROAD pavements. But rutting prediction only for the HMA layer provided complex predictions. In other words, AC rutting predictions for some pavement sections matched well with the measured total rutting which supported the aforementioned forensic investigations, but again in some sections MEPDG significantly under-predicted. Further, this study discovered that the predictions for the base and subgrade rutting showed impractical high predictions in the first month of pavement life which led to the over

prediction of gross total rut depth. Therefore, it was decided to modify the total rut depth model excluding the predicted rutting in the base and subgrade layer after only the first month. As a consequence, MEPDG simulation results showed that the modified equation for total rutting provided a reasonable prediction with reduced bias.

2.2.1.4 Washington

Li et al in 2009 conducted calibration of the MEPDG for flexible pavement in Washington using MEPDG version 1.0⁽¹⁸⁾. The Washington pavement management system (WSPMS) has contained a rich historical database related to pavement structures, as well as for performance measurement, since 1969. Three different hierarchical input levels for materials, traffic, and climate were incorporated, but level 1 data for structural design inputs could not be processed well. However, in that regard, Level 2 and Level 3 provided adequate data input for model evaluation and calibration. For calibration, pavement sections from Western and Eastern Washington that experienced medium traffic (AADTT = 200 – 2000 AADTT) were selected, and all others pavement sections set aside for validation purpose. A combination of both the splitting and jackknife method were adopted in validation process.

The verification result showed a good relationship between the predicted and measured value of transverse cracking using the globally predicted factors; hence, transverse cracking model was not adjusted in this study. It was reported that due to some software bugs, the researchers could not calibrate the smoothness model. Therefore, except these two models, this study focused on the AC fatigue, alligator cracking, top-down cracking, and rutting models to calibrate.

An elasticity analysis was adopted to see the sensitivity of each altered calibration factor. Whereas zero elasticity indicates no difference between the default and the changed calibration coefficient, a positive value defines as the factor increases the estimation also increases, and a negative value indicates that with the factor increases, the estimated value conversely decreases. Also, this elastic analysis helped the researchers to decide the order of factors to be calibrated. For instance, as the longitudinal and alligator cracking models are dependent on the asphalt mixture fatigue model, the AC fatigue model should be calibrated prior to these models. Similar to the North Carolina study⁽¹⁴⁾. This study also recommended to calibrate the rutting model factors β_{r2} and β_{r3} first, and then β_{r1} . The calibration factors were

nominated on the basis of the least root-mean-square error (RMSE) between the WSPMS observed and the MEPDG predicted distress data on all calibration and validation sections. Like other studies ^(14, 16, 19), this research study also found that rutting phenomenon is more likely to occur in the HMA layer rather than in the base and subgrade layers. Hence, the factor related to the subgrade rutting model was set to zero. Overall, the calibration results showed reasonable predictive capability that matched well with the field measured values. The final results of the established calibration factors is presented in Table 2.3.

Table 2.3 Summary Set of the Calibration Factors Established in Washington

Performance Model	Distress Type/Layer	Global Factors	Local Factors
Rutting	AC, (β_{r1} , β_{r2} , β_{r3})	1.0, 1.0, 1.0	1.05, 1.109, 1.1
	Granular Base, (β_{s1})	1.0	1.0
	Subgrade, (β_{s1})	1.0	0
Fatigue Cracking	Fatigue Model, (β_{f1} , β_{f2} and β_{f3})	1.0, 1.0, 1.0	0.96, 0.97, 1.03
	Bottom-Up Transfer Function (C_1 , C_2 , C_3)	1, 1, 6000	1.071, 1, 6000
	Top-Down Transfer Function (C_1 , C_2 , C_3 , C_4)	7, 3.5, 0, 1000	6.42, 3.596, 0, 1000
IRI	Smoothness (C_1 , C_2 , C_3 , C_4)	40, 0.4, 0.008, 0.015	40, 0.4, 0.008, 0.015

2.2.1.5 Arkansas

Hall et al. in 2010 conducted initial local calibration for the flexible pavement in Arkansas ⁽¹⁹⁾. The Arkansas State Highway and Transportation Department (AHTD) prioritized their plans to implement MEPDG prior to this study realizing that LTPP sites from Arkansas were not included while establishing those national calibration factors.

A total of 26 flexible pavements over three different bases were adopted from the LTPP and PMS database of AHTD. These selected pavement sections represent five different geological areas within Arkansas. To run the simulation trials and therefore to evaluate and adjust the performance models, MEPDG version 1.100 was adopted. The splitting method was used, where randomly selected 20 sections (80% of all pavement sections) were identified for calibration, and the remaining 6 project sections (20% of all projects) were separated for the

validation process. This study considered five flexible performance models: top-down cracking, alligator cracking, transverse cracking, rutting, and IRI model.

The verification results of the nationally calibrated models showed poor prediction in general, particularly for the longitudinal and alligator cracking. The thermal cracking model is linked to the transverse cracking in MEPDG. However, prediction results showed that a use of properly identified performance grade (PG) binder-grade corresponded to Arkansas climate does not show any thermal cracking. On the other hand, field data revealed that there might be another kind of cracking mechanisms involved with the LTPP defined transverse cracking. Considering this vague issue, transverse cracking was not rectified in this study. In addition to that, no calibration effort for IRI model was reported as it is dependent on other distress performance predictions.

Once the calibration was done the predictive capability of longitudinal and alligator cracking was found improved. The Microsoft Excel Solver tool was utilized to minimize the sum of standard error (SSE) for these two models. In contrast, for the rutting model an iterative approach was followed to determine the calibration factors. Table 2.4 presents the final calibration set ⁽¹⁹⁾. Validation efforts on the remaining sites also endorsed the calibration factors. In order to conduct future calibration of transverse cracking model, it was recommended to identify thermal cracking as part of the distress identification in Arkansas.

Table 2.4 Established Calibration Factors in Arkansas for Flexible Pavement

Performance Model	Distress Type/Layer	Global Factors	Local Factors
Rutting	AC, (β_{r1} , β_{r2} , β_{r3})	1.0, 1.0, 1.0	1.2, 1, 0.8
	Granular Base, (β_{s1})	1.0	1.0
	Subgrade, (β_{s1})	1.0	0.5
Fatigue Cracking	Fatigue Model, (β_{f1} , β_{f2} and β_{f3})	1.0, 1.0, 1.0	1.0, 1.0, 1.0
	Bottom-Up Transfer Function (C_1 , C_2 , C_3)	1, 1, 6000	0.688, 0.294, 6000
	Top-Down Transfer Function (C_1 , C_2 , C_3 , C_4)	7, 3.5, 0, 1000	3.016, 0.216, 0, 1000

2.2.1.6 Arizona

Souliman et al. in 2010 established the local calibration factors for flexible pavement in Arizona. This study considered 39 LTPP pavement segments ⁽²⁰⁾. MEPDG version 1.0 was

used. This study mostly carried out level 2 and level 3 MEPDG input. Three major performance prediction models such as fatigue cracking (alligator and longitudinal cracking), rutting and roughness model were studied. In addition, as no subgrade modulus was reported against the LTPP sections, an estimation of Modulus of Resilience (M_r) value was attempted to be obtained from the correlation of a couple of empirical equations.

The verification results revealed that MEPDG under-predicted alligator cracking and AC rutting, and conversely over-predicted longitudinal cracking and subgrade rutting. For the IRI prediction model, using the MEPDG default initial IRI i.e. 63 in/mile yielded poor prediction. Therefore, this study tried to calculate initial IRI based on the back-calculation of time history plot of smoothness measurement. As no measured transverse cracking was reported in these LTPP sites, the calibration coefficient (C_3) related to transverse cracking was kept constant for the IRI model.

The objective of the calibration effort was to make the sum of standard error (SSE) to zero. Hence, the iterative approach with a different set of calibration factors was followed to calibrate all selected models (fatigue cracking, rutting and IRI). The calibration effort resulted in improved fatigue and rutting models at a satisfactory level. Although the improvement generated by the locally calibrated IRI model was not that evident, both the globally and locally calibrated models offered a good level of predictions with a comparison to the measured IRI.

In 2014, Darter et al. also locally adjusted flexible pavement performance models including the fatigue, alligator cracking, asphalt and subgrade permanent deformation models, and IRI model in Arizona. In this study, Darwin software version 3.1 was used, and calibration results showed reasonable prediction and accuracy ⁽²¹⁾. However, the associated calibration factors were found different compared to the previous study done by Souliman et al. (2010) Table 2.5 represents the comparison among the globally calibrated factors and locally calibrated factors from the above mentioned two studies in Arizona.

Table 2.5 Established Calibration Factors for Two different Versions of MEPDG Software in Arizona

Performance Model	Distress Type/Layer	Global Factors	Local Factors (20)	Local Factors (21)
Rutting	AC, ($\beta r1$, $\beta r2$, $\beta r3$)	1.0, 1.0, 1.0	3.63, 1.1, 0.7	0.69, 1.0, 1.0
	Granular Base, ($\beta s1$)	1.0	0.111	0.14
	Subgrade, ($\beta s1$)	1.0	1.38	0.37
Fatigue Cracking	Fatigue Model, ($\beta f1$, $\beta f2$ and $\beta f3$)	1.0, 1.0, 1.0	0.96, 0.97, 1.03	249.0087, 1.0, 1.2334
	Bottom-Up Transfer Function (C1, C2, C3)	1, 1, 6000	0.688, 0.294, 6000	1.0, 4.50, 6000
	Top-Down Transfer Function (C1, C2, C3, C4)	7, 3.5, 0, 1000	3.016, 0.216, 0, 1000	N/A
IRI	Smoothness (C ₁ , C ₂ , C ₃ , C ₄)	40, 0.4, 0.008, 0.015	5.455, 0.354, 0.008, 0.015	1.2281, 0.1175, 0.008, 0.0280

2.2.1.7 Ohio

Mallela et al. (2009) from the Applied Research Associates, Inc. developed the guidelines for implementing ME Design procedures in Ohio⁽²²⁾. A short number of LTPP sections for flexible pavement in Ohio were identified to evaluate the globally calibrated MEPDG models, such as alligator cracking, transverse cracking, rutting, and IRI model. MEPDG version 1.00 was used to conduct the process.

The bottom up cracking model was not adjusted due to shortage of field-data measurement to check the model adequacy. A non-statistical approach, rather than a statistical approach, had been followed because a majority of the measured transverse cracking values were found almost near to zero. This non-statistical method proved the appropriateness of globally calibrated transverse cracking model for Ohio road conditions. However, the researchers suggested reviewing the thermal cracking model using colder sites in Ohio prior to making any final conclusion.

Further, the verification results revealed that using the globally calibrated MEPDG prediction model for rutting provided overestimation of rut depth with a significant amount of bias.

Therefore an attempt to calibrate the rutting model was adopted, but due to a lack of diverse data sources, the exercise was considered as an example. The local calibration factors β_{r1} , β_{s1} , and β_{s2} associated respectively with the HMA rutting, base, and subgrade sub-model were adjusted. For IRI prediction model, poor goodness of fit with significant amount of bias was observed.

The calibration effort indicated that the recalibrated rutting prediction model did not show much improvement; bias was still high that implied the revised model to be defective. As a result, more comprehensive data sources and robust prediction analyses were advocated. On the contrary, recalibrated IRI model showed better agreement between the measured and predicted smoothness, and bias also mitigated at a reasonable level.

2.2.1.8 Tennessee

Gong et al. in 2017 established a method for local calibration of the AASHTOware PMED version 2.2 using data collected from Highway Pavement Management Application (HPMA) in Tennessee⁽²³⁾. Due to a limited number of records for the state routes, all the data were collected from interstates which included I-24, I-26, I-40, I-65, I-75, I-81, I-140, and I-240. A total of 158 pavement sections were elected. However, these sections were not utilized equally for all the performance predictions. Tennessee put much effort in implementing MEPDG which resulted in a database of dynamic modulus (E^*) and resilient modulus (M_R) of soil from 18 different sites. This study considered the alligator cracking, longitudinal cracking, and roughness model to be calibrated and subsequently validated. The transverse cracking model could not be adjusted due to inadequate available performance data. It should be noted here that the rutting model was calibrated in a different study⁽²⁴⁾. Curve fitting procedure in the MATLAB had been followed to reduce the variability between the measured and predicted cracking, i.e. both alligator and longitudinal cracking.

The results showed that the globally calibrated alligator cracking model under-estimated alligator cracking in Tennessee. Conversely, longitudinal cracking was over-predicted because the measured longitudinal cracking is much lower (8 ft/mile) than the design threshold value of 2000 ft/mile. The globally calibrated roughness model provided a reasonable prediction. However, using other calibrated distress functions and no adjustment

for IRI model coefficients showed even better result with reduced bias and less scattering pattern.

Validation approach was conducted using the popular Jackknife method. This study found the method as a powerful tool to identify outliers. In addition, the prediction capability of the considered models was found stable. This study also recommended adding an appropriate model for Asphalt Treated Base (ATB) as the total asphalt thickness (HMA surface + ATB) becomes too strong to be cracked. As a result, alligator cracking on these sections were found trivial. Table 2.6 presents the developed local calibration factors for flexible pavement performance models in Tennessee ⁽²³⁾.

Table 2.6 A Summary of Local Calibration Factors in Tennessee

Performance Model	Distress Type/Layer	Global Factors	Local Factors
Rutting	AC, (β_{r1} , β_{r2} , β_{r3})	1.0, 1.0, 1.0	0.111, 1.0, 1.0
	Granular Base, (β_{s1})	1.0	0.196
	Subgrade, (β_{s1})	1.0	0.722
Fatigue Cracking	Bottom-Up Transfer Function (C_1 , C_2 , C_3)	1, 1, 6000	1.023, 0.045, 6000
	Top-Down Transfer Function (C_1 , C_2 , C_3 , C_4)	7, 3.5, 0, 1000	6.44, 0.27, 204.54, 1000
IRI	Smoothness (C_1 , C_2 , C_3 , C_4)	40, 0.4, 0.008, 0.015	40, 0.4, 0.008, 0.015

2.2.2 Rigid Pavement

This section discusses the implementation effort of the AASHTOWare Pavement ME Design by other state agencies for rigid pavement.

2.2.2.1 Washington

Li et al. (2005) conducted the calibration of PCC models for the Washington State Department of Transportation (WSDOT ⁽²⁵⁾). MEPDG software version 0.6 was used in this process. Washington State Pavement Management System (WSPMS) was considered as the key source of data that represented different regions of the state. It has been found that almost 68% of WSDOT PCC pavements enclosed within the study were aged between 25 and 45 years and most of them placed without dowels.

As WSPMS did not differentiate between the longitudinal and transverse cracking data, researchers faced challenges on reporting the cracking data. Based on the observation of the historical performance data, they found that longitudinal cracking was more noticeable than transverse cracking in WSDOT PCC pavements. So, it was anticipated that two-thirds of all cracks would be longitudinal. As a result, estimated transverse cracking was adjusted to one-third of WSPMS captured values.

Generally, the national calibrated models over-predicted transverse cracking, and under-predicted the IRI. A different pattern was observed in the joint faulting prediction. This study discouraged the use of one set of calibration factors to the whole network of different dowel types in Washington because it would not show the actual distress scenario.

In the state of Washington, using of the studded tire wear is a substantial part in pavement roughness and deterioration. Since the software does not consider the effect of studded tires in the IRI model, under-prediction of IRI is observed compared to the actual field measurement. As a result, the researchers were unable to do the calibration for IRI model.

2.2.2.2 Florida

Texas Transportation Institute (TTI) researchers and engineers with the Florida Department of Transportation conducted the local calibration of MEPDG in a cooperative effort. MEPDG version 1.0 was used in this study ⁽²⁶⁾. The main objective of this research, in addition to the calibration, was to develop a database and establish typical thicknesses design tables. In the process, researchers verified the performance prediction using the nationally calibrated models and found that MEPDG under-predicted IRI and joint faulting. However, the transverse cracking was reasonably well predicted and no calibration effort was warranted. Researchers decided to have national calibration factors as the base or reference value and changed them to ± 40 percent to determine the sensitivity of the performance predictions to each calibration factor. Like other studies, they found calibration factors, F1 and F6 to be significant in influencing joint faulting and subsequently affecting IRI prediction model. The calibration effort was led to adjust two factors. Table 2.7 shows the locally calibrated factors for joint faulting and IRI respectively ⁽²⁶⁾. Calibration effort resulted in lower bias for both the models placing data points around the line of equality, although high scatter is observed.

Table 2.7 Comparison of Nationally and Locally Calibrated Model

Distress/Smoothness Model	Old National Factors	Calibrated Factors
Joint faulting (F1)	1.0184	2.00
IRI (C3)	1.4929	2.5

2.2.2.3 Ohio

Mallela et al. (2009) from the Applied Research Associates (ARA) conducted a study to propose guidelines for implementing the MEPDG in Ohio ⁽²²⁾. MEPDG version 1.00 was used. A limited number of LTPP sites were considered to do the verification of the globally calibrated models and calibrate them under the local condition of Ohio if needed. Both the statistical and non-statistical approaches were followed in this study to confirm the adequacy of the distresses or IRI prediction models compared to the measured field data. The global MEPDG transverse slab cracking prediction model was not calibrated in this study, because a non-statistical analysis for transverse cracking model showed reasonable accuracy between predicted and measured values. In the case of joint faulting, the model predicted well compared to the measured values. However, it is recommended to recalibrate the model on the availability of additional database with higher joint faulting intensity. IRI or ride quality model validation approach showed some bias. Hence, despite having a very good correlation between predicted and measured values, and less SSE, calibration effort was done. Changing the calibration factors (C1-C4) resulted in no bias and no major changes observed in R^2 and SSE. This study then conducted the recommended sensitivity analysis of the recalibrated IRI model, and it showed reasonably expected result. Joint spacing was found to be a more dominant influential parameter on IRI compared to other parameters such as concrete flexural strength, subgrade, etc. This study also recognized some limitations, that all the SPS projects used were mostly 10 years old, and the location of those projects does not represent the entire pavement or the climatic condition of Ohio.

2.2.2.4 Utah

Darter et al. (2009) conducted an effort to implement the MEPDG in Utah. The study included the calibration of performance models for both flexible and rigid pavements ⁽²⁷⁾. The

researchers selected a total of 30 projects from the LTPP road sections in Utah and UDOT pavement management system (PMS) that cover JPCP and JPCP subjected to Concrete Pavement Restoration (CPR). The project was originally performed in two phases, MEPDG version 0.8 was used in phase I, whereas phase II used version 1.0. The results revealed that the transverse slab cracking model had good predictions, and the statistical evaluation showed adequate goodness of fit with no significant bias. Regarding the faulting data, even though most of the measured mean joint faulting values were close to zero, the statistical analysis was done. The outcomes showed a good correlation between predicted and measured joint faulting value with slightly higher SEE and no bias. The same results were found in the IRI prediction model; MEPDG provided well adequate prediction and there was no need to calibrate the IRI model considering Utah local condition.

2.2.2.5 Iowa

Ceylan et al. conducted research in 2015 to improve the precision of the MEPDG performance models through calibration for Iowa road pavement condition ⁽²⁸⁾. This study used the MEPDG version 1.1 and the AASHTOWare pavement ME Design version 2.1.24 to check whether the predictions are compatible with each other. This research study identified 35 JPCP pavement sections within Iowa to represent local geographical condition under varied traffic loads. Among these pavement sections, 70% of these sections were utilized to conduct calibration, and 30% were withheld for validation purpose.

The verification results indicated that nationally calibrated faulting model significantly underpredicted faulting. Whereas the locally calibrated MEPDG provided noteworthy standard error, but it reduced the under-prediction trend, and the locally calibrated AASHTOWare Pavement ME Design showed reasonable predictions compared to others.

The transverse cracking model also refined through local calibration as nationally calibrated factors provided with an overestimation plot. It was supposed that higher joint spacing of 20 ft contributed to such predictions, where less than 20 ft for joint spacing is a typical practice in other LTPP test sites. IRI prediction model also presented a similar trend of overprediction while using the nationally calibrated factors. In order to avoid much efforts and costs, two approaches for the IRI model calibration were considered. Approach 1 was to consider the local calibration factors of other distress models to calibrate the IRI model. On the other hand,

Approach 2 is designed to use only the nationally calibrated distress models without considering their prediction accuracy. The researchers found that Approach 2 provided adequate predictions. Therefore, its calibration factors were selected as the final local calibration set for the IRI model. Also, it was realized that Approach 2 would save time and resources. Table 2.8 shows the developed local calibration factors for JPCP performance models ⁽²⁸⁾.

Table 2.8 Developed Local Calibration Factors for JPCP Predictions Models in Iowa

Performance Model	Calibration Parameters	Global Factors	Local Factors
Faulting	F1, F2, F3, F4, F5, F6, F7, F8	1.0184, 0.91656, 0.0021848, 0.0008837, 250, 0.4, 1.83312, 400	0.85, 1.39, 0.002, 0.274, 250.8, 0.4, 1.45, 400
Fatigue Cracking	C1, C2, C4, C5	2, 1.22, 1, -1.98	2.25, 1.4, 4.06, -0.44
IRI	J1, J2, J3, J4	0.8203, 0.4417, 1.4929, 25.24	0.11, 0.44, 0.01, 15.12

2.2.2.6 Oregon

In the year 2013, Williams et al. verified the PMED software models for Continuous Reinforced Concrete Pavements (CRCP) in Oregon. The MEPDG software Darwin M-E (version 1.1) was used in this study ⁽²⁹⁾. In this process, they used only four CRCP pavements and no JPCP was selected. The simulation runs were done at 50% and 90% reliability levels to demonstrate the effect of reliability. Summary of the Darwin M-E simulation for punchout of three CRCP sections revealed less estimation of punchouts as compared to the actual field measured values at the same corresponding age. The remaining section showed over prediction. Although the researchers were satisfied with the initial reasonable predictions, they were in agreement that it was challenging to comment about the adequacy of the nationally calibrated CRCP models for Oregon local condition based on only four sections.

2.2.2.7 Colorado

Mallela et al. conducted the implementation effort of the AASHTO Mechanistic-Empirical Pavement Design Guide for Colorado in 2013 ⁽³⁰⁾. MEPDG version 1.0 was used in this process to validate and calibrate performance models, if needed. Pavement Projects were selected from the Colorado Department of Transportation (CDOT) pavement management system and LTPP database. The researchers found a limited distribution of transverse

cracking and joint faulting which implied most of the measured cracking and joint faulting values were approximately zero. Hence, traditional statistical analysis was not possible to verify MEPDG global transverse cracking and joint faulting prediction models for Colorado conditions. They used the non-statistical analysis approach for verification. After verification, it was found that global calibration factors for both the models showed a reasonable relation between predicted and measured values with less bias. For that reason, local calibration for these two models in Colorado conditions was not warranted. Similarly, the globally calibrated JPCP smoothness model was verified by evaluating the goodness of fit and bias. Results revealed that MEPDG global IRI performance model predicted well compared to the measured IRI. Overall, in this study there is no calibration effort for JPCP Pavements has been found.

2.2.2.8 Arizona

Darter et al. (2014) attempted to calibrate and implement the MEPDG in Arizona. In this study 48 JPCP sections and only 2 CRCP sections were considered ⁽²¹⁾. The researchers designed their work method to evaluate first the global models, then if needed calibrate MEPDG with the 90% of selected projects and further validate the previously calibrated models with the remaining 10% of the projects.

The researchers verified all the distress models and IRI based on the goodness of fit and bias. Using the globally calibrated factors, if the simulation results provided a well representation of the goodness of fit and low bias, the researchers took the global factors: otherwise, they advanced for the local calibration. For Transverse cracking, using the global model for Arizona conditions provided poor goodness of fit with biased under-predicted result. The researchers investigated the probable cause for the poor prediction of transverse cracking and found that PCC slabs over the asphalt treated or aggregate bases gave reasonable predictions, while predictions for PCC slabs over lean concrete bases deemed problematic. Further, it was realized that due to the constructional practices in Arizona, the PCC slab and lean concrete base bonding and friction lost rapidly. Hence, the loss of bond between PCC slab and cement treated bases was assumed to occur at the age of zero years. On the other hand, joint faulting and IRI models showed over-prediction. Therefore, local calibration was warranted for these performance prediction models. After local calibration, results showed reasonable goodness

of fit and no significant bias for all these models. Table 2.9 highlights the local calibration factors for different models within Arizona local condition ⁽²¹⁾.

Table 2.9 Developed Local calibration Factors for JPCP in Arizona

Performance Model	Calibration Parameters	Global Factors	Local Factors
Faulting	F1, F2, F3, F4, F5, F6, F7, F8	1.0184, 0.91656, 0.0021848, 0.0008837, 250, 0.4, 1.83312, 400	0.0355, 0.1147, 0.00436, 1.1E-07, 20000, 2.0389, 0.1890, 400
Fatigue Cracking	C1, C2, C4, C5	2, 1.22, 1, -1.98	2, 1.22, 0.19, -2.067
IRI	J1, J2, J3, J4	0.8203, 0.4417, 1.4929, 25.24	0.60, 3.48, 1.22, 45.20

In the case of CRCP, due to insufficient data, local calibration could not be done. Although, the researchers were satisfied with the reasonableness of globally calibrated prediction models to Arizona-specific data inputs. However, it is advised to update these calibration factors with each updated version that AASHTO releases.

2.2.2.9 Louisiana

Louisiana Department of Transportation and Development (LADOTD) also implemented Pavement ME Design by evaluating and subsequently calibrating the globally calibrated models in 2014. This research recognized the importance of calibration of the MEPDG performance models as there was no LTPP section available when the national calibration of MEPDG models had been done ⁽³¹⁾. Pavement ME™ version 1.3 was adopted in this study. LADOTD Pavement management system (PMS) was employed to retrieve the historical pavement data. Following some selection criteria, in total 19 rigid pavement sections were identified with two pavement structure types, Portland cement concrete (PCC) over unbound base and PCC over asphalt mixture blanket as appropriate sections for evaluation. These road sections mostly represented interstate and highway sections in Louisiana.

From the initial evaluation of distress transfer functions and IRI, it is found that MEPDG over-predicted transverse slab cracking but under-estimated joint faulting for both PCC over unbound base and PCC over HMA blanket. However, it was deemed that MEPDG predicts IRI reasonably well for PCC over unbound base, but not well for PCC over HMA blanket. Therefore, local calibration for these aforementioned performance models was necessary. Reviewing previous studies and applying the judgment, the study mainly focused on adjusting the two most sensitive factors (C1 for transverse cracking and F6 for joint faulting model) for

local calibration process through trial and error approach. The locally calibrated models of MEPDG showed better performance prediction with significant improvement in bias and standard error for both types of pavements used in this research study. As a result, the researchers established the following values for these two factors presented in Table 2.10.

Table 2.10 Developed Local Calibration factors for JPCP in Louisiana

Distress/Smoothness Model	Global Factors	Calibrated Factors
Transverse Cracking (C1)	2	2.6
Joint Faulting (F6)	0.4	1.2

The Researchers also tried to compare design thicknesses obtained from the original AASHTO 1993 Guide and the MEPDG software. The results revealed that locally calibrated MEPDG provides thinner PCC slab compared to the AASHTO 1993 Guide. Moreover, this study also recognized the necessity of including longitudinal cracking in MEPDG as it is found more prominent in Louisiana than the typical transverse slab cracking. Some other challenges, for instance, missing data, inconsistency and lower distress data advocated to reevaluate the local calibration efforts within Louisiana condition.

2.2.2.10 Kansas

Kansas Department of Transportation (KDOT) also took an initiative to follow the trend of implementing the mechanistic-based design concept in Kansas. In 2015, Sun et al. conducted the calibration of the PMED for rigid pavements in Kansas⁽³²⁾. In the study, AASHTO ME Design Software, version 1.3 was used. Throughout Kansas road networks, a total of 32 rigid pavement projects comprising of different materials, traffic loading and environmental conditions were nominated. These various input data were retrieved from the pavement management system (PMS) database of KDOT. As the researchers found adequacy of the data sources, no further field or forensic investigation of input values was done. Selected project sections generally consisted of three chemically based layers. In this study, joint faulting and IRI prediction models were considered only. Transverse cracking was not considered as part of the MEPDG calibration. Researchers used base layer CEMBAS (Cement treated base) and DBWED (Drainage base with edge drains) for local calibration, and PCCDCB (Drainable cement treated base under PCC) base layer was used for validation.

The simulation results revealed that with a comparison to the field measurements, MEPDG nationally calibrated models over-predicted joint faulting but under-predicted IRI. After local calibration, bias between predicted and measured values was reduced significantly, and researchers found that joint faulting was not influenced by different types of chemically stabilized base layers. Table 2.11 shows the final established local calibration factors for rigid pavements in Kansas ⁽³²⁾.

Table 2.11 Developed Calibration Factors in Kansas

Performance Model	Calibration Parameters	Global Factors	Local Factors
Faulting	F3, F6, F7	0.0021848, 0.4, 1.83312	0.00164, 0.15, 0.01
IRI	J3, J4	1.4929, 25.24	9.38, 70

2.2.2.11 Virginia

Smith et al. conducted the local calibration of the AASHTOware Pavment ME design software for the Transportation Department of Virginia (VDOT) in 2015 ⁽³³⁾. The Pavement ME Design, version 1.3 was used. This study utilized the VDOT's Pavement Management System (PMS) records. JPCP predication models (Transverse slab cracking and joint faulting) were not included due to the limited number of sections in Virginia. From the category of concrete pavements only CRCP punchout and smoothness prediction model were considered in this study. The Jackknife statistical approach was taken rather than the typical splitting-sampling method for the CRCP local calibration.

Verification results indicated that globally calibrated prediction model over-predicted punchout by 8 punchouts per mile. Therefore, local calibration was conducted. The adjusted punchout model seemed to be reasonable with no bias, though it showed higher SEE than that recommended by the AASHTO local calibration guide. On the other hand, IRI was under-predicted by the global IRI model. But, researchers preferred to use global calibration coefficients for IRI prediction over local calibration coefficients. Because after the local calibration endeavor they found a significant increase in the standard error over the globally predicted model. However, bias was reduced to a negligible level.

2.3 Conclusions

Based on the literature review, many studies specified the two main issues that should be addressed for the successful implementation of the PMED. The first is providing comprehensive representative inputs when you have limited information about the selected projects, and the second is the readiness of field data in a format similar to the software output. Respectively, Tables 2.12 and 2.13 show nationally calibrated MEPDG software's prediction pattern on flexible sections and JPCP/CRCR sections for different state agencies and versions they used to evaluate the PMED predictions. Unreasonable results or predictions have driven state agencies to calibrate PMED locally. Reviewing those states' endeavors, it is found that local calibration of PMED software represents reasonable results more than nationally calibrated PMED model. Agencies that had conducted local calibration were recommended to reanalyze or re-evaluate PMED against more projects with adequate database and advanced PMED software version. Table 2.14 and Table 2.15 represent the developed local calibration factors for flexible pavement and rigid pavement performance models, respectively ⁽²⁸⁾. Based on the presented literature review, some notable findings are stated below:

Flexible Pavement

- Rutting essentially occurs in the upper layer of HMA, while base and subgrade are not influenced much. But in general, PMED model for total rutting over-predicts considering the rutting calculation from base and subgrade. Therefore, it is recommended to have field cores and trenches for getting rutting measurement associated with each individual layer.
- Fatigue damage model is related to both alligator and longitudinal cracking models. Hence, it is recommended to calibrate fatigue model prior to these two models.
- One of the studies recommended including proper Asphalt Treated Base (ATB) model, because the total asphalt thickness (HMA surface + ATB) becomes too strong to be cracked. As a result, alligator cracking on those sections were found negligible.

Rigid Pavement

- Locally calibrated PMED design requires less or equal PCC thickness compared to the AASHTO 1993 Guide.

- Calibration factor: C1 for transverse cracking and F6 for joint faulting model deemed to be the most sensitive coefficients for local calibration process.
- In Washington and Louisiana, longitudinal cracking is found dominant over transverse cracking. Therefore, researchers felt the urge to include the longitudinal cracking model for rigid pavement in the PMED.
- States that use studded tire may underestimate IRI due to disregarding the effect of the studded tire on the ride quality of pavement.

Table 2.12 Nationally Calibrated PMED Software’s Prediction Pattern on Flexible Pavement Sections for Different State Agency.

State Agency	Flexible pavements - Performance Prediction Patterns					Version Used
	Alligator Cracking	Longitudinal Cracking	Transverse Cracking	Total Rutting	IRI	
North Carolina	Under	N/A	N/A	Over	N/A	MEPDG version 1.00
Washington	Under	Under	Match Well	Under	Not Match Well	MEPDG version 1.00
Ohio	N/A	N/A	Well Match	Over	Not Match Well	MEPDG version 1.00
Minnesota	N/A	N/A	N/A	Over	N/A	MEPDG version 1.00
Arkansas	Not Match Well	Not Match Well	Under	Over	Over	MEPDG version 1.100
Arizona	Under	Over	N/A	Over	Match Well	MEPDG version 1.00
New Mexico	Under	Not Match Well	N/A	Over	Match Well	MEPDG version 1.00
Tennessee	Under	Over	N/A	Over	Match Well	AASHTOWare MEPDG Version 2.2

Table 2.13 Nationally Calibrated PMED Software’s Prediction Pattern on JPCP/CRCP Sections for Different State Agency.

State Agency	JPCP			CRCP		Version Used
	Transverse Slab Cracking Prediction	Joint Faulting Prediction	IRI Prediction	Punchouts Prediction	IRI Prediction	
Arizona	Under	Over	Over	Well	Well	Darwin M-E version 3.1
Iowa	Over	Under	Over	N/A	N/A	AASHTOWare PMED version 2.1.24
Louisiana	Over	Under	Well	N/A	N/A	PMED version 1.3
Washington	Over	Over	Under	N/A	N/A	MEPDG version 1.0
Oregon	N/A	N/A	N/A	Well**	N/A	Darwin M-E version 1.1
Kansas	N/A	Over	Under	N/A	N/A	AASHTO ME Design version 1.3
Colorado	Well*	Well*	Well*	N/A	N/A	MEPDG version 1.0
Ohio	Well*	Well	Not Well Match	N/A	N/A	MEPDG version 1.0
Virginia	N/A	N/A	N/A	Over	Under	AASHTOWare PMED 1.3
Utah	Well	Well*	Well	N/A	N/A	Phase 1: MEPDG version 0.8 Phase 2: MEPDG version 1.0
Florida	Well	Under	Under	N/A	N/A	MEPDG software version 1.0

*Measured values were almost zero.

** Researchers felt reasonable prediction though found both under and over prediction in different pavements.

Table 2.14 Reported Calibration Factors for Flexible Pavement Performance Models

Performance Model	Calibration Parameters	National Calibration Factors (NCF) ⁽³⁴⁾	NC	NM	WA	AR	ARZ	TN
Fatigue	β_{f1}	1	0.437199	N/A	0.96	N/A	249.0087	N/A
	β_{f2}	1	0.150494	N/A	0.97	N/A	1	N/A
	β_{f3}	1	1	N/A	1.03	N/A	1.2334	N/A
Alligator Cracking	C_1	1	N/A	0.625	1.071	0.688	1	1.023
	C_2	1	N/A	0.25	1	0.294	4.5	0.045
	C_3	6000	N/A	6000	6000	6000	6000	6000
Longitudinal Cracking	C_1	7	N/A	3	6.42	3.016	N/A	6.44
	C_2	3.5	N/A	0.3	3.596	0.216	N/A	0.27
	C_3	0	N/A	0	0	0	N/A	0
	C_4	1000	N/A	1000	1000	1000	N/A	204.54
Total Rutting	β_{r1}	1	-3.41273	1.1	1.05	1.2	0.69	0.111
	β_{r2}	1	1.5606	1.1	1.109	1	1	NCF
	β_{r3}	1	0.479244	0.8	1.1	0.8	1	NCF
	β_{r4}	1	1.5803	0.8	1	1	0.14	0.196
	β_{r5}	1	1.10491	1.2	0	0.5	0.37	0.722
IRI	C_1	40	N/A	NCF	N/A	N/A	1.2281	NCF
	C_2	0.4	N/A	NCF	N/A	N/A	0.1175	NCF
	C_3	0.008	N/A	NCF	N/A	N/A	0.008	NCF
	C_4	0.015	N/A	0.015	N/A	N/A	0.028	0.015

Table 2.15 Reported Calibration Factors for Rigid Pavement Performance Models

Performance Model	Calibration Parameters	ONCF⁽³⁴⁾	NNCF⁽³⁵⁾	AZ	CO	IA	LA	OH
Transverse Slab	<i>C1</i>	2	2	NNCF	NNCF	2.17	2.6	ONCF
	<i>C2</i>	1.22	1.22	NNCF	NNCF	1.32	ONCF	ONCF
	<i>C4</i>	1	0.52	0.19	NNCF	1.08	ONCF	ONCF
	<i>C5</i>	-1.98	-2.17	-2.067	NNCF	-1.81	ONCF	ONCF
Mean Joint Faulting	<i>F1</i>	1.0184	0.595	0.0355	0.5104	2.0427	ONCF	ONCF
	<i>F2</i>	0.91656	1.636	0.1147	0.00838	1.83839	ONCF	ONCF
	<i>F3</i>	0.00218 5	0.00217	0.00436	0.00147	0.00438 2	ONCF	ONCF
	<i>F4</i>	0.00088 4	0.00444	1.10E- 07	0.00834 5	0.00177 3	ONCF	ONCF
	<i>F5</i>	250	250	20000	5999	ONCF	ONCF	ONCF
	<i>F6</i>	0.4	0.47	2.0389	0.8404	0.8	1.2	ONCF
	<i>F7</i>	1.83312	7.3	0.189	5.9293	ONCF	ONCF	ONCF
	<i>F8</i>	400	400	NNCF	NNCF	ONCF	ONCF	ONCF
IRI	<i>J1</i>	0.8203	0.8203	0.6	NNCF	0.04	ONCF	0.82
	<i>J2</i>	0.4417	0.4417	3.48	NNCF	0.02	ONCF	3.7
	<i>J3</i>	1.4929	1.4929	1.22	NNCF	0.07	ONCF	1.711
	<i>J4</i>	25.24	25.24	45.2	NNCC	1.17	ONCF	5.703

- ONCF = Old National Calibration Factors

- NNCF = New National Calibration Factors

CHAPTER 3: METHODOLOGY FOR VERIFICATION AND LOCAL CALIBRATION OF PMED PERFORMANCE MODELS

This chapter describes the methodology for the verification and local calibration of the PMED performance models. The process follows the guidelines provided in the AASHTO guide for the local calibration of the PMED software ⁽¹²⁾.

3.1 Select Hierarchical Input level for Individual Input Parameter

There are three levels of data input option available in the PMED software. These hierarchical input levels are incorporated to provide the user with the maximum flexibility in attaining the project design inputs based on its significance and economic consideration. Following are the brief description of these three levels.

Level 1: this level of data (traffic, climate, and material properties) input shows the maximum amount of accuracy, as this data input can be available directly from the lab experiment or field test. It implies the highest knowledge of material characteristics and traffic conditions. As a result, it requires significant amount of cost and effort at this level on the basis of project importance.

Level 2: represents the intermediate level of data input. It is basically dependent on the correlations or regression equations of Level 1 experimental databases. Level 2 can be selected by the user to represent the regional database of a local agency.

Level 3: this is the most uncertain data input level which is mainly based on the user-defined default values. These default values are selected based on engineering experiences and national averages of certain parameters. This level of input can be used with low risk and low volume roads when design inputs are not available.

The objective of step 1 is to select the hierarchical input levels for present and future model validation and calibration. This step covers three categories of data inputs including traffic data, climate data, and materials properties data.

3.1.1 Traffic Data

Traffic is one of the essential inputs to be considered in the PMED software. The software allows the user to input three different levels of traffic data. Level 1 defines project specific data, including details of traffic volume and load pattern at or near the project location. Level 2 describes traffic data originated from Weigh-in-Motion (WIM) stations or other sources, such as Automatic Traffic Recorders, Portable Traffic Counts, Manual Traffic Classification Counts, Automatic Vehicle Classification sites. Level 3 represents default values embedded in the software or statewide default values which do not require site-specific data. Regarding traffic, Level 1 and Level 3 of hierarchical inputs have been considered in this study.

Phase reports of the selected sections provided by ITD, supplied the general traffic parameters. The phase report contains Annual Average Daily Traffic (AADT), growth rate, operational speed, and directional truck distribution. The general traffic input parameters used in the study are shown in Table 3.1. However, the AASHTOWare PMED software requires additional traffic inputs such as Axle load distribution and truck volume distribution which were not found readily available in these phase reports or in any other documents provided.

Table 3.1 General Traffic Input Parameters for Idaho

Input Group	Input Parameters	Value Used	Input Level
AADTT	Two-way AADTT	Actual project value	Level 1
	Number of lanes	Actual project value	Level 1
	Percent trucks in design direction	Actual project value	Level 1
	Percent trucks in design lane	Actual project value	Level 1
	Operational speed (mph)	Actual project value	Level 1
Axle Configuration	Average axle width (ft)	8.5	Level 3
	Tandem axle spacing (in)	51.6	Level 3
	Dual tire spacing (in)	12	Level 3
	Quad axle spacing (in)	49.2	Level 3
	Tire pressure (psi)	120	Level 3
	Tridem axle spacing (in)	49.2	Level 3
Lateral Wander	Design lane width (ft)	12	Level 3
	Mean wheel location (in)	18	Level 3
	Traffic wander standard deviation (in)	10	Level 3
Wheelbase	Average spacing of long axles (ft)	18	Level 3
	Average spacing of medium axles (ft)	15	Level 3
	Average spacing of short axles (ft)	12	Level 3
	Percent trucks with long axles	61	Level 3
	Percent trucks with medium axles	22	Level 3
	Percent trucks with short axles	17	Level 3
Growth Rate (%)		Actual project value	Level 1

In addition to actual design phase reports, traffic inputs are generated through WIM stations in Idaho ⁽⁹⁾. ITD research project RP193 developed a comprehensive traffic database based on 21 Weigh in Motion (WIM) stations around the state ⁽⁷⁾. Detailed Descriptions of the WIM stations with functional classes can be found in Table 58 and Table 59 of the RP193 project report ⁽⁷⁾.

In this study, we considered the axle load data as exited in the traffic database for various WIM stations as level 1. In cases where WIM station was not found for a project location, the

nearest WIM station had been adopted, assuming that the monthly traffic adjustment factors and vehicle class distribution etc. would be the same. Otherwise, Idaho default traffic distribution was considered based on the Idaho PMED User Guide ⁽⁹⁾. For the LTPP sections, traffic data was analyzed to be used as level 1 data.

3.1.1.1 Vehicle Class Distribution

Vehicle Class distribution (VCD) characterizes the percentage of truck traffic by vehicle class within the initial year AADTT. It can be noted here that FHWA considers class 4 through 13 as truck, as shown in Figure 3.1. It is recommended to have level 1 VCD data where the road of interest is functioned with heavy seasonal recreational and agricultural traffic. Table 3.2 represents the VCD from each of 21 WIM stations across Idaho. It is observed that in Idaho FHWA vehicle class 9 is most predominant and then is followed by vehicle Class 5.






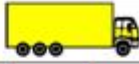










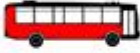

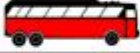



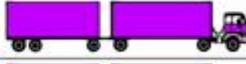

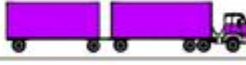



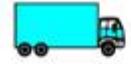



Class 1 Motorcycles		Class 7 Four or more axle, single unit	
Class 2 Passenger cars		Class 8 Four or less axle, single trailer	
			
			
			
Class 3 Four tire, single unit		Class 9 5-Axle tractor semitrailer	
			
			
Class 4 Buses		Class 10 Six or more axle, single trailer	
			
			Class 11 Five or less axle, multi trailer
Class 5 Two axle, six tire, single unit		Class 12 Six axle, multi-trailer	
			
			Class 13 Seven or more axle, multi-trailer
Class 6 Three axle, single unit			
			
			

Figure 3.1 FHWA Vehicle Classification (Source: https://www.fhwa.dot.gov/policyinformation/tmguidetmg_2013/vehicle-types.cfm)

Table 3.2 Vehicle Class Distribution of WIM Stations located in Idaho ⁽⁷⁾

WIM Site ID	FHWA Vehicle Class									
	4	5	6	7	8	9	10	11	12	13
79	1.77	21.2	2.13	0.5	8.35	49.07	5.19	1.11	1.01	9.67
93	0.99	11.21	1.31	0.11	4.09	52.9	12.73	0.76	0.59	15.33
96	1.94	45.59	6.6	0.95	7.64	27.43	6.73	0.18	0.32	2.62
115	2.62	29.15	7.15	10.82	5.31	33.57	7.92	0.26	1.03	2.18
117	1.03	5.96	3.86	7.2	4.56	52.35	15.06	1.45	1.33	7.2
118	2.5	48.01	11.18	14.05	4.19	8.84	10.52	0.02	0.04	0.65
128	1.25	16.44	1.75	0.22	5.49	54.73	9.96	2.28	1.54	6.34
129	5.1	37.84	6.61	0.64	7.29	22.21	11.36	0.45	0.17	8.33
133	1.34	46.53	10.18	7.73	7.54	18.56	5.12	0.08	0.01	2.92
134	2.15	21.28	1.9	0.36	5.51	61.01	3.43	0.19	0.27	3.91
135	1.84	42.4	4.74	0.82	9.71	30.16	7.54	0.53	0.08	2.19
137	5.37	8.56	10.73	0.32	6.94	52.33	8.71	0.61	0.18	6.26
138	1.14	3.82	2.39	0.03	5.18	72.76	6.35	2.23	0.58	5.54
148	2.11	7.69	13.66	1.16	5.02	24.87	41.78	0	0.12	3.59
155	17.94	7.73	11.46	3.1	8.46	16.75	15.21	2.07	2.33	14.95
156	1.01	4	5.12	0	4.96	39.99	12.72	0	0.08	32.12
171	1.17	3.37	1.51	0.24	3.46	69.49	9.24	1.64	1.48	8.41
179	0.35	10.37	9.84	0.53	2.64	35.85	13.36	0	0	27.07
185	0.26	4.77	9.1	0.45	8.05	46.29	21.53	0	0	9.55
192	3.4	4.9	2.18	0.6	7.24	75.47	3.68	0.5	0.26	1.78
199	2.98	38.76	9.94	12.49	5.12	11.9	11.67	0.68	1.06	5.4

3.1.1.2 Monthly Adjustment Factors

Traffic volume Monthly Adjustment Factors (MAF) represents the proportion of truck traffic loadings for each vehicle class type throughout the year. PMED default MAF value was set as 1.0 for all the months and for all vehicle class type in each global calibration effort. The reason for this is that the selected road segments were from either mainly interstate systems or

primary arterials where seasonal variation was not observed considerably in traffic operation. However, as developed in RP193, the monthly adjustment factors (MAF) show variation within months and within vehicle classes as well. Table 3.3 shows the average MAF of all the WIM stations located in Idaho. It can be observed that in the summer period the monthly adjustment factors are higher, which is expected.

Table 3.3 Monthly Adjustment Factors of WIM Stations located in Idaho ⁽⁷⁾

Month	Vehicle Class									
	4	5	6	7	8	9	10	11	12	13
January	0.74	0.86	0.91	1.04	0.64	0.98	0.88	0.9	0.93	1.12
February	0.83	0.82	0.87	0.63	0.67	1	0.96	0.91	0.67	0.96
March	0.77	0.8	0.83	0.75	0.86	0.95	1.1	0.97	1.48	1.01
April	0.91	0.85	0.86	1.2	1.0	0.95	1.1	0.93	0.79	0.88
May	1.12	0.98	0.9	1.63	1.07	0.95	1.1	1.07	1.2	0.8
June	0.99	1.01	0.84	0.72	1.17	0.94	0.84	1.42	1.69	0.81
July	1.49	1.33	1.3	1.09	1.53	0.97	0.85	1.66	1.08	0.88
August	1.46	1.21	1.45	1.21	1.42	0.98	1.01	0.81	0.96	0.99
September	1.31	1.14	1.29	0.98	1.18	1.06	1.08	0.88	0.71	0.93
October	0.94	1.08	1.26	0.92	1.03	1.16	1.13	0.6	0.76	1.13
November	0.72	0.99	0.75	0.98	0.79	1.07	0.92	0.82	0.67	1.09
December	0.72	0.93	0.74	0.85	0.64	0.99	1.03	1.03	1.06	1.4

3.1.1.3 Hourly Adjustment Factors

Hourly adjustment factor is used only for rigid pavement design and analysis. In order to calculate the incremental pavement damage due to thermal gradient phenomenon, such as slab curl/warp, the PMED software requires the hourly frequency of traffic loading ⁽³⁶⁾. However, hourly traffic distribution factors have minimal influence on flexible pavement performance. The ITD research project RP193 was exclusively dedicated to the flexible pavement, hence hourly adjustment factors were not analyzed. However, analyzing or processing hourly adjustment factors for rigid pavement is out of the scope of this study. Therefore, PMED

default values have been adopted as level 3, which can be seen in Table 15 of the ITD research project report RP211B ⁽⁹⁾.

3.1.1.4 Number of Axles per Vehicle

AASHTOWare PMED software requires the average number of axles per vehicle and axle load spectra which assist to calculate average pavement damage induced in pavement structure by each vehicle class ⁽³⁷⁾. The developed statewide estimates for the number of single, tandem, tridem, and quad axles per truck for Idaho were extracted from Table 81 of the RP193 project report ⁽⁷⁾.

3.1.1.5 Axle Load Spectra

AASHTOWare PMED software also requires axle load spectra which makes it more unique than other design methods. Axle load spectra are the frequency of total axle load applications used to distribute the total number of axles within four axle types (single, tandem, tridem, and quad) and vehicle class for individual months of the year. TrafLoad software developed under NCHRP Project 1-39 was employed to create the axle load spectra files in the RP193 ⁽⁷⁾.

3.1.2 Climate Data

Pavement performance is dependent on environmental conditions, especially temperature and moisture content. AASHTOWare Pavement ME Design incorporates Enhanced Integrated Climatic Model (EICM) which predicts climatic effects on material properties within each layer and the foundation. In other words, this model is used to predict the effects of temperature, moisture, wind speed and relative humidity on each pavement layer. Therefore, the model requires hourly data for five weather parameters, which includes temperature, precipitation, wind speed, relative humidity, and cloud cover ⁽¹⁰⁾. These effects in turn have impact on the sustainability of the pavement in terms of load application.

The newly released PMED software version 2.5.3 has two types of generated climate database. They are Modern-Era Retrospective analysis for Research and Applications (MERRA) for flexible pavement and North American Regional Reanalysis (NARR) for rigid pavement. It is also expected that AASHTOWare will incorporate MERRA database for rigid pavement in the next global recalibration effort.

MERRA and NARR climate databases are map based. They show nearby climatic stations when searched by name or latitude or longitude. Hence, it is required to know the real project's latitude, longitude and elevation information as Level 1. By using these information, a single station or multiple stations can be selected. Regarding NARR climate database, it is recommended to have multiple stations while selecting a virtual weather station. Detailed descriptions of the selected climate stations are presented in Table 3.4 and Table 3.5 for selected flexible pavements, and in Table 3.6 for rigid pavements.

Table 3.4 Climate Stations for Selected Flexible Pavements in Idaho

District #	MERRA ID	Latitude (Deg)	Longitude (Deg)	Elevation (ft)
D1	152166	47.418	-116.982	2687
	152742	47.511	-116.950	2585
	152742	47.531	-116.927	2580
	152743	47.369	-116.502	2216
	152742	47.482	-116.571	2149
D2	152166	46.934	-116.999	2586
	151590	46.719	-116.971	2629
	152742	46.541	-116.949	2668
	151591	46.533	-116.727	967
	151016	46.074	-115.973	1358
	151016	46.074	-115.973	1358
	151015	46.252	-116.602	3818
D3	149287	43.646	-116.354	2624
	148135	44.039	-116.927	2624
	148135	43.706	-116.912	2410
	148711	44.008	-116.172	2706
	148713	42.840	-115.887	2602
	148135	43.915	-116.198	2634
	146984	42.419	-115.885	5130
	148134	43.605	-116.605	2458
	148138	43.873	-116.972	2254
	148711	43.692	-116.460	2490
D4	146987	42.450	-113.619	4606
D5	146985	42.320	-111.304	5970
D6	148138	43.972	-111.635	5011

Table 3.5 Climate Stations for LTPP Flexible Pavements

LTPP ID	MERRA ID	Latitude (Deg)	Longitude (Deg)	Elevation (ft)
16_1001	153318	47.418	-116.617	2456.71
16_1005	149287	44.516	-116.042	4542.8
16_1007	146985	42.520	-114.872	4264
16_1009	146988	42.306	-113.369	4916.72
16_1010	148142	43.493	-112.041	5038.08
16_1020	146986	42.556	-114.470	3936
16_1021	148142	43.493	-112.041	5038.08
16_9032	152742	47.454	-116.785	2118.88
16_9034	153895	48.277	-116.553	4795.35

Table 3.6 Climate Stations for Rigid Pavements

Climate Stations	Latitude (Deg)	Longitude (Deg)	Elevation (ft)
Pocatello, ID	42.920	-112.571	4440
Logan, UT	41.787	-111.853	4445
Idaho Falls, ID	43.516	-112.067	4730
MEACHAM, OR	45.511	-118.425	3726
Baker City, OR	44.838	-117.810	3361
Boise, ID	43.565	-116.220	2814
Salem, OR	44.908	-122.995	205
Eugene, OR	44.133	-123.214	355
Burley, ID	42.543	-113.772	4137
McCall, ID	44.889	-116.102	5008
Cedar City, UT	37.702	-113.097	5586
Bryce Canyon, UT	37.706	-112.146	7585
Milford, UT	38.443	-113.028	5027
Ogden, UT	41.123	-111.973	4447
Price, UT	39.545	-110.750	5830
Bellingham, WA	48.794	-122.537	153
Spokane, WA	47.621	-117.528	2353
Spokane, WA	47.683	-117.321	1940
Deer Park, WA	47.969	-117.421	2199
Pasco, WA	46.265	-119.118	400
Everett, WA	47.908	-122.280	544
Seattle, WA	47.530	-122.301	16
Renton, WA	47.493	-122.214	19
Portland, OR	45.549	-122.400	23
Portland, OR	45.591	-122.600	20
Vancouver, WA	45.621	-122.657	25
Rock Springs, WY	41.594	-109.065	6742

3.1.3 Materials Data

Material properties input is one of the core requirements for PMED software to characterize pavement behavior and to predict pavement responses. Reasonable and reliable material properties often influence design to be accurate, predictable, and cost-effective. This section describes the material inputs used in the AASHTOWare Pavement ME Design Software for both flexible and rigid pavement.

3.1.3.1 Asphalt Concrete Layer Properties

Site-specific material inputs were provided by the ITD materials engineer. The volumetric properties of asphalt pavement were determined from the Job Mix Formula (JMF). The ITD research project RP193 developed the material database for flexible pavement which was also utilized in this study. AASHTOWare PMED software requires Dynamic Modulus (E^*), Creep compliance and Indirect Tensile Strength (IDT) as level 1 input. RP193 lacked creep compliance and IDT as Level 1 input. Sensing the importance, another ITD research project, RP235, was initiated to develop creep compliance and IDT database as part of their study. Since all of the selected projects do not have the actual mechanical properties, this study looked into the updated RP193 database based on the Idaho asphalt mix types and binder grade. General materials input required for AC layer are presented briefly in Table 3.7.

Table 3.7 General Materials Inputs for AC Layer

Input Groups	Input Parameters	Value Used	Input Level
Asphalt Layer	Thickness (in.)	Actual Project Value	Level 1
Mixture Volumetrics	Air voids (%)	7	Level 3
	Effective binder content (%)	Actual Project Value	Level 1
	Poisson's ratio	0.3	Level 3
	Unit weight (pcf)	150	Level 3
Mechanical Properties	Asphalt binder	Actual Project Value	Level 1
	Creep compliance (1/psi)	Actual Project Value	Level 1
	Dynamic modulus	Actual Project Value	Level 1
	Reference temperature (° F)	70	Level 3
	Indirect tensile strength at 14 °F (psi)	425.25	Level 3
Thermal	Heat capacity (BTU/lb-°F)	0.23	Level 3
	Thermal conductivity (BTU/hr-ft-° F)	0.67	Level 3
	Thermal contraction	Software Calculated Internally	Level 2
AC Layer Properties	AC surface shortwave absorptivity	0.85	Level 3
	Layer interface	Full Friction Interface	Level 3
	Endurance limit (microstrain)	100	Level 3

3.1.3.2 Rigid Pavement Layer Properties

AASHTOWare Pavement ME Design software requires the following listed general input parameters in Table 3.8 for rigid pavement or Portland cement concrete pavement layer properties. This study relied on the ITD provided construction files such as: as-built structure and phase report for rigid pavement structure and material specifications. In addition to that, ITD research project RP253 served as a great source for PCC material database at different hierarchical levels. RP253 utilized eight concrete mixtures from the five districts of Idaho to characterize concrete properties such as compressive strength, flexural strength, modulus of elasticity, Poisson's ratio, modulus of rupture and PCC coefficient of thermal expansion ⁽⁸⁾.

Table 3.8 General Materials Inputs for PCC Surface Layer

Input Groups	Input Parameters	Value Used	Input Level
PCC	Poisson's Ratio	Actual Project Value	Level 1
	Thickness (in.)	Actual Project Value	Level 1
	Unit weight (pcf)	Actual Project Value	Level 1
Thermal	PCC Coefficient of thermal expansion (in./in./deg F x 10 ⁻⁶)	Actual Project Value	Level 3
	PCC heat capacity (BTU/lb-deg F)	0.28	Level 3
	PCC Thermal conductivity (BTU/hr-ft-deg F)	1.25	Level 3
	Aggregate type	Actual Project Value	Level 1
	Cementitious material content (lb/yd ³)	Actual Project Value	Level 1
	Cement type	Actual Project Value	Level 1
	Water to cement ratio	Actual Project Value	Level 1
	Curing method	Actual Project Value	Level 1/Level 3
	Reversible shrinkage (%)	50	Level 3
	Time to develop 50% of ultimate shrinkage (days)	Actual Project Value	Level 1
Strength	PCC strength and modulus	Actual Project Value	Level 1/Level 3
JPCP Design	PCC joint spacing	Actual Project Value	Level 1
	Erodibility index	Actual Project Value	Level 1
	Dowel spacing	Actual Project Value	Level 1
	Dowel diameter	Actual Project Value	Level 1
	Sealant type	Actual Project Value	Level 1
	Tied shoulders	Actual Project Value	Level 1
	Widened slab	Actual Project Value	Level 1

3.1.3.3 Base and Subbase Layer properties

All of the flexible pavements selected in the study are comprised of unbound materials for base and subbase layers. The inputs related to base/subbase layers adopted to execute AASHTOWare PMED software are presents in Table 3.9.

Table 3.9 Base and Subbase Layer Properties Inputs

Input Groups	Input Parameters	Value Used	Input Level
Unbound	Coefficient of lateral earth pressure (k0)	0.5	Level 3
	Layer thickness (in)	Actual Project Value	Level 1
	Poisson's ratio	Actual Project Value	Level 1
Modulus	Resilient modulus (psi)	Actual Project Value	Level 2/Level 3
Sieve	Gradation and other engineering properties	Actual Project Value/Default	Level 1/Level 3

3.1.3.4 Subgrade Layer Properties

AASHTO classifies soil from A1 to A7. Table 3.10 shows the subgrade layer related material inputs which are required for PMED software run.

Table 3.10 Subgrade Layer Properties Inputs

Input Groups	Input Parameters	Value Used	Input Level
Unbound	Coefficient of lateral earth pressure (k0)	0.5	Level 3
	Layer thickness (in)	Semi-infinite	Level 3
	Poisson's ratio	0.4	Level 3
Modulus	Resilient modulus (psi)	Actual Project Value	Level 2/Level 3
Sieve	Gradation and other engineering properties	Actual Project Value/Default	Level 1/Level 3

3.2 Local Experimental Plan

According to the local calibration guide, the objective of this step is to form a sampling template or matrix which will represent the existing and future practice of pavement design in Idaho, in terms of design features, traffic, and site conditions. However, such activity was not done in this study rather referred to a previous research program (RP211A)⁽³⁸⁾ that developed a Roadmap for implementation of the PMED in Idaho. The roadmap recommended a matrix for pavement selection for each of the flexible and rigid pavements as presented in Tables 3.11 and 3.12. Based on the Roadmap research project report RP211A Table 3.11 and Table 3.12 show the selected pavement sections (shaded cells) for flexible pavement and rigid pavement, respectively. It was not possible to find pavement sections in Idaho that cover the entire matrix cells. In collaboration with ITD engineers, we were able to identify pavement sections that can fill the shaded cells shown in Tables 3.11 and 3.12. They represent the most valid and possible pavement conditions in Idaho road network. It is to be noted here that, LTPP sites were included so that the number of test sites in Idaho could be reduced. But it is recommended not to use more than half of the road segments from the LTPP as there is potential differences between LTPP program and ITD's operational policies⁽³⁸⁾.

Table 3.11 Experimental Sampling Matrix for Flexible Pavements

Mix Type	Volume of Truck Traffic	Soil Type	Pavement Structure				
			New Design	Rehabilitation			
			Unbound Aggregate Base	AC Overlay		CIR	FDR Stabilized With Cement
				Flexible	Rigid		
Neat Mixtures	Low	Coarse Grained					
		Low Plasticity					
		High Plasticity					
	High	Coarse Grained					
		Low Plasticity					
		High Plasticity					
Polymer Modified Asphalt	High	Coarse Grained					
		Low Plasticity					
		High Plasticity					

- CIR = Cold-In-Place Recycle; FDR = Full-Depth Reclamation

Table 3.12 Experimental Sampling Matrix for Rigid Pavements

JPCP Joints	Volume of Truck Traffic	Soil Type	Structure				
			New Design		Rehabilitation		
			Unbound Base	Stabilized Base	PCC Overlay		CPR
					Flexible	Rigid	
With Dowels	Low	Coarse Grained					
		Low Plasticity					
		High Plasticity					
	High	Coarse Grained					
		Low Plasticity					
		High Plasticity					
Without Dowels	Low	Coarse Grained					
		Low Plasticity					
		High Plasticity					

- CPR = Concrete Pavement Restoration

3.3 Estimate Sample Size for Specific Distress Predictions Models

Under this step, the least possible road sections essential for validation and local calibration of PMED distress prediction models is estimated. The minimum required road sections is dependent on four factors: design reliability level, confidence Interval, PMED nationally

calibrated models SEE, and design criteria. Table 3.13 represents an estimated minimum number of pavement projects required for the validation and local calibration for both flexible and rigid pavement ⁽¹²⁾.

Note that, IRI is not included in the project selection as it is dependent on other pavement distress predictions' accuracy and site factor. It is not necessary to validate IRI for a wide range of projects if other distress functions satisfy minimum project requirements and their predictions are deemed to be correct and rational.

Table 3.13 Required Minimum Number of Pavement Projects ⁽¹²⁾

Pavement Type	Performance Indicator	Performance Threshold (at 90% Reliability)	Standard Error of the Estimate (SEE)	Minimum Number of Projects Required for Each Pavement Type (n)*
New HMA	Alligator Cracking (%)	20	7	8
	Longitudinal Cracking (ft/mile)	2000	600	11
	Transverse Cracking (ft/mile)	700	250	8
	Rutting (inches)	0.4	0.1	16
	IRI (in./mile)	169	17	99
New JPCP	Faulting (inches)	<0.15	0.05	9
	Transverse cracking (%)	< 10 % slabs	7	2
	IRI (in./mile)	169	17	99

* $n = \left(\frac{Z_{\alpha/2}\sigma}{E}\right)^2$, where, $Z_{\alpha/2} = 1.601$ (for a 90 percent confidence level), σ = performance indicator threshold, and E = tolerable bias at 90 percent reliability ($1.601 \cdot \text{SEE}$).

3.4 Projects Selection

To populate the recommended sampling matrix presented at step 2, this study tried to select potential road sections from the LTPP database and road segments available within Idaho provided by ITD. It is recommended to use both these types of roadway segments to determine the standard error of the estimate for all distress prediction models. It is also suggested to select such road segments which possess the least number of structural layers, for

instance, one or two asphalt layers, one concrete layer, one unbound base layer, and one subbase layer. It will help to decrease the required number of inputs for material characterization. Road sections with non-conventional mixtures should also be included in determining local calibration factors, if needed, because PMED has some limitations in that it only includes conventional HMA and PCC mixtures. It is suggested that if available, the distress/IRI should represent at least 10-years of historical data.

The research team with the valuable guidance from ITD engineers tried to identify and select project sections which represent local climate, traffic, and material specifications. Besides LTPP sections, the other road sections were selected from different districts in Idaho. In the process of selecting roadway segments, following data-information is considered mostly but not limited to:

- Project location (latitude, longitude, and elevation).
- Construction year and month.
- As-built pavement structure (layer type and thickness of each layer).
- AC/PCC/Base/Subbase/Subgrade material properties required by the software.
- Performance data (rutting, longitudinal cracking, alligator fatigue cracking, transverse cracking, joint faulting, transverse slab cracking, and IRI) at different points of time.
- Maintenance history.

Accordingly, a total number of 34 and 39 sites were selected for flexible and rigid pavements, respectively. Among those 34 projects for flexible pavement, six projects were randomly selected for validation purpose. Similarly, seven projects were independently identified for concrete pavement. General descriptions of the projects are tabulated in Table 3.14 and Table 3.15 for flexible pavement. Table 3.16 and Table 3.17 list the sections for rigid pavement. The locations of the selected projects for flexible pavement and rigid pavement are shown on the map in Figure 3.2 and Figure 3.3, respectively.

Table 3.14 Selected Flexible Pavements in Idaho

ITD District #	Construction Year	Route	Beg MP	End MP
D1	2008	US-95	403.5	408.75
	2004	US-95	411.84	415.83
	2002	US-95	415.5	421.3
	2006	SH-3	76.822	84.201
	2013	US-95	477.1	486.36
D2	2008	SH006	100	104.5
	2004	SH008	0	1.76
	2003	US-95	344	344.57
	2007	US-95	319.88	337.67
	2008	SH003	5.00	8.5
	2011	SH013	11.257	18.711
	2010	SH013	18.68	25.378
	2005	US-95	277.28	279.1
	2010	US 95	64.94	67.14
	2011	US 95	0	16.7
	2012	US 95	38.4	46.6
	2011	SH 55	66.1	80.63
	2010	SH 78	0	11.5
	2011	SH 51	60	76.9
	2011	SH 51	47.7	54.6
	2011	SH 78	60	76
	2012	SH 55	13.1	18
	2012	US 20/26	0	1.58
	2012	US 95	47.58	60.87
	2012	SH 16	0	13.392
	2013	SH 52	14.4	30.42
D4	2000	SH 77	18.5	23
D5	2014	US30	328.6	330.7
D6	2012	US20	328.6	335.7

Table 3.15 Selected LTPP Flexible Pavement Sections in Idaho

Segment ID	Construction Year	Route	Milepost
16_1001	1985	U. S.-20	319.6
16_1005	1975	U. S.-95	127.7
16_1007	1972	U. S.-30	205.2
16_1009	1974	Interstate-84	231.7
16_1010	1969	Interstate-15	132
16_1020	1986	U. S.-93	59.8
16_1021	1985	U. S.-20	319.6
16_9032	1987	U. S.-95	424.2
16_9034	1988	U. S.-96	176.2

Table 3.16 Selected Rigid Pavement Sections in Idaho

ITD District #	Construction Year	Route	Beg MP	End MP
D1	1991	I-90	58.5	62.25
D2	1924	US-95	0.06	0.11
	2011	SH008	2.77	3.27
	1976	US-95	251.075	261.588
	2004	US-12	2.197	2.62
D3	1981	I-84	26.35	28.3
	2011	I-84	36	38.7
	2009	I-84	41.3	43.8
	2004	I-84	49.15	49.73
	1996	I-84	49.73	50.21
	1972	I-84	58.8	59
	2001	I-84	70.1	82.3
	1996	I-84	90	94.6
	1983	I-84	94.3	103.5
	1994	I-84	103.5	109.1
	1995	I-84	114.5	121.2
D4	1979	I-84	120.66	127.945
D5	1972	I-15	30.87	36.207
	1960	I-86	14.808	25.98
	1985	US-91	80.15	81.02
	1986	US-91	78.81	79.66

Table 3.17 Selected LTPP Rigid Pavement Sections

Segment ID	Construction Year	Route	Milepost
16_3023	1983	I-84	15.1
49_3010	1978	I-15	83.7
49_3011	1986	I-15	221.2
49_7082	1990	I-15	391.9
49_7085	1991	U.S. - 40	12.6
49_7086	1991	SH - 154	19
53_3013	1970	U.S. - 195	91.6
53_3014	1986	U.S. - 395	26.1
53_3019	1986	I-82	115
53_3813	1966	SH-14	11
53_7049	1981	I-82	49
56_3027	1981	I-80	103.2
32_3010	1982	I-80	348.6
32_3013	1981	I-80	401

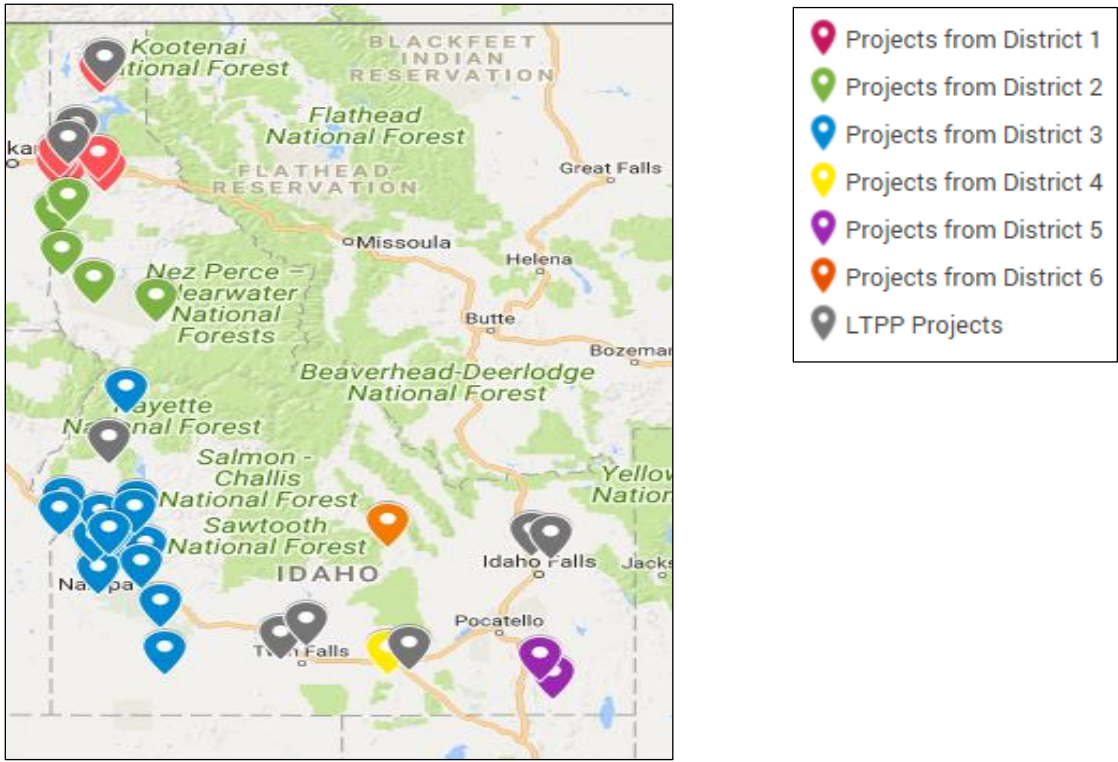


Figure 3.2 Selected Flexible Pavement Sections in Idaho

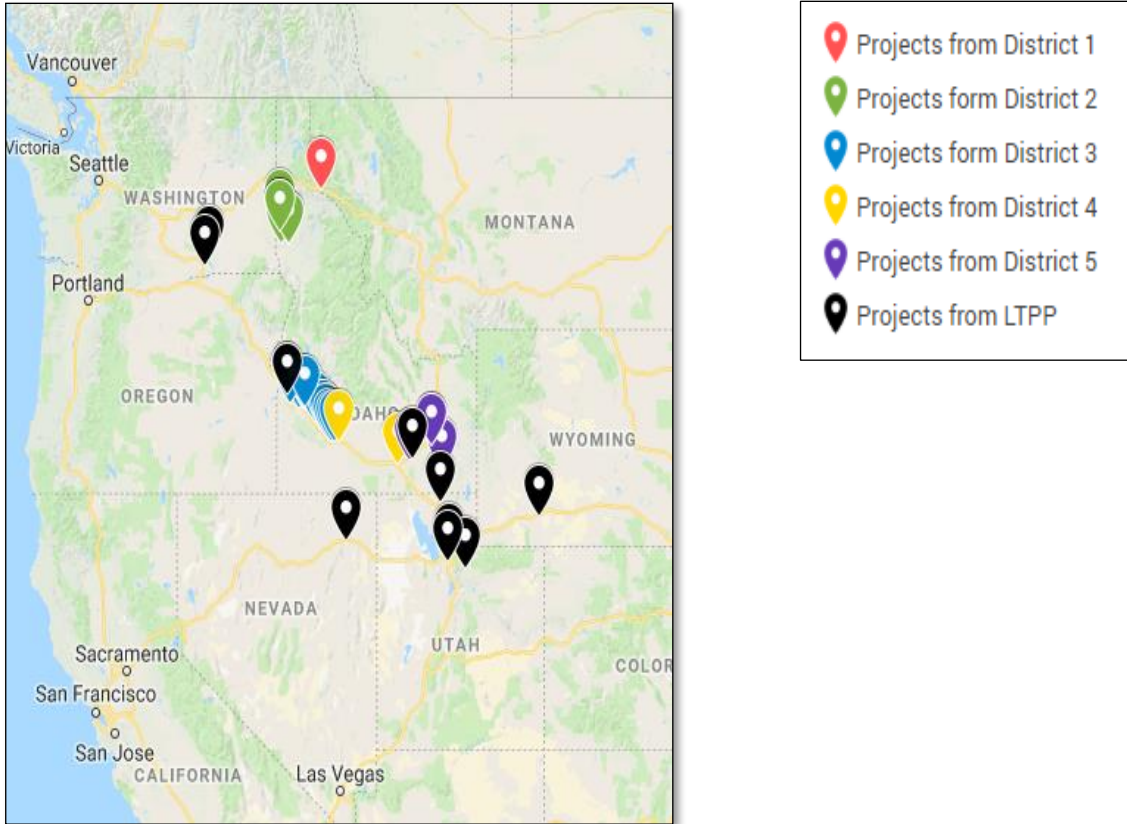


Figure 3.3 Selected Rigid Pavement Sections

3.5 Extract and Evaluate Distress and Project Data

This study developed performance databases for both flexible and rigid pavement. Long Term Pavement Performance (LTPP) and the Idaho Transportation Asset Management System (TAMS) were the sources used to extract distress and IRI data for the selected projects. In appendix Tables A.3 to A.8 report the measured distresses and IRI. All these distresses were reviewed to identify consistency and reasonableness to be readily compared with the PMED output. In this step outliers and anomalies were excluded. As indicated earlier, PMED requires comprehensive data inputs. All the required inputs (traffic, climate, and material) again reviewed here.

3.6 Conduct Field and Forensic Investigation

In this study no field and forensic investigation has been conducted.

3.7 Assess Local Bias Using Global Calibration Coefficients

In this step, considering all the required inputs at different hierarchical levels, the PMED software v2.5.3 with global calibration coefficients was executed at a 50% reliability level as recommended by the local calibration guide ⁽¹²⁾. The extracted prediction results were then compared to the measured data for each distress type to compute bias and the standard error of the estimate. Graphical representations were also made to see the location of the measured values and predicted results around the line of equality.

A hypothesis was checked to identify whether any significant differences existed between the predicted results and the measured data. In order to accomplish this, a paired t-test was conducted. At 95% confidence interval or $\alpha = 0.05$, the hypothesis test was performed. The hypothesis can be explained as follows:

- Null Hypothesis (H_0): Mean measured distress or IRI = mean predicted distress or IRI.
- Alternative Hypothesis (H_A): Mean measured distress or IRI \neq mean predicted distress or IRI.

Bias is assessed based on p-value. Any value of p-value greater than 0.05 implies that there is no significant difference between the measured and predicted value, and the null hypothesis can be accepted. Therefore, the local calibration is not required and the globally calibrated coefficients are robust and yield reasonable predictions. Otherwise, p-value less than 0.05 indicates there are significant differences. In other words, the measured distresses/IRI in Idaho and predicted results are from different populations. As a result, reject the null hypothesis. Rejection of the null hypothesis will lead to step 8 to adjust the calibration factors to local conditions and policies.

3.8 Eliminate Local Bias of Distress and IRI Prediction Models

If the null hypothesis is rejected, the globally calibrated coefficients must be revised and PMED software has to be executed again in this step. In general, the cause of bias and the agency required accuracy influence the calibration process. According to the local calibration guide, to eliminate bias, listed calibration coefficients in Table 3.18 should be considered for adjusting the predictions for flexible and rigid pavement ⁽¹²⁾. Detailed results of the elimination of bias are presented in chapter 4 and chapter 5 for flexible pavement and rigid pavement, respectively.

Table 3.18 Suggested Calibration Coefficients to Eliminate Bias for Flexible and Rigid Pavement ⁽¹²⁾

Pavement Type	Distress		Eliminate Bias
HMA	Total Rutting	AC and Unbound	K_{1r}, β_{1s} or β_{1r}
		Materials Layers	
	Load Related Cracking	Alligator Cracking	C_2 or Kf_1
		Longitudinal Cracking	C_2 or Kf_1
	Roughness, IRI		C_4
JPCP	Faulting		F_1
	Fatigue Cracking		C_1 or C_4
	Roughness, IRI		J_4

3.9 Assess the Standard Error of Estimate

After the elimination of the bias, the standard error of the estimate and the coefficient of determination (R^2) are calculated for each distress prediction model considering the local calibration coefficients. Then the estimated standard error for each distress prediction is compared to those derived from the global calibration effort and reasonability is checked. Therefore, the following probable scenario may occur and decisions can be made accordingly ⁽³⁹⁾.

1. The estimated standard errors of the locally calibrated models are not significantly different from the globally calibrated models. Then, using the locally calibrated models is recommended.

2. The estimated standard errors of the locally calibrated models are significantly different from the globally calibrated model, and the standard error is lesser for locally calibrated models. Then, the locally calibrated models can be accepted.

3. The estimated standard errors of the locally calibrated models are significantly different from the globally calibrated model, and the standard error is greater for locally calibrated models. Then, the locally calibrated models should be adjusted again to reduce the standard error. Or, the locally calibrated models can be accepted considering the higher amount of standard error than the globally predicted performance models.

3.10 Reduce Standard Error of the Estimate

If it is found that the standard error of the estimate is too great to be accepted, and will result in much conservative design at higher reliability levels, the local calibration coefficients should be revised. It is recommended to adjust the following listed parameters in Table 3.19 to reduce the standard error of the estimate for flexible and rigid pavement ⁽¹²⁾.

Table 3.19 Suggested Calibration Coefficients to Reduce Standard Error of the Estimate (SEE) for Flexible and Rigid Pavement ⁽¹²⁾

Pavement Type	Distress		Reduce Standard Error
HMA	Total Rutting	AC and Unbound Materials Layers	Kr ₂ , Kr ₃ , and B _{2r} , B _{3r}
		Load Related Cracking	Alligator Cracking
	Longitudinal Cracking		Kf ₂ , Kf ₃ , and C ₁
	Roughness, IRI		
JPCP	Faulting		C ₁
	Fatigue Cracking		C ₂ , C ₅
	IRI		C ₁

CHAPTER 4: DEVELOPMENT OF THE PMED CALIBRATION FACTORS FOR FLEXIBLE PAVEMENT

This chapter presents the local calibration and validation effort of the PMED flexible performance models to Idaho local conditions. In the process 34 flexible pavement projects were identified, among them 80% project were utilized for local calibration and the remaining 20% kept aside for validation purpose. The performance models included in this chapter are rutting, longitudinal cracking, alligator cracking, transverse cracking and IRI model. The methodology outlined in Chapter 3 was followed to get the calibration results.

4.1 Calibration of Rutting Models

The AASHTOWare Pavement ME Design Software calculates rutting in each layer (AC layer, Base layer, and Subgrade layer) for the entire pavement design life. Total rutting is the summation of rutting occurs in these layers. In PMED rutting is reported in inches.

4.1.1 Verification of Rutting Models Using Global Calibration Factors

The PMED software was executed first using the global calibration factors to find the robustness of the globally calibrated rutting model prediction. Table 4.1 shows the statistical results for the total rutting model prediction using the global calibration factors. The statistical results show that there is not that much significant bias. However, conducting the paired t-test at 95% confidence interval results provided p-value < 0.05, which implied the rejection of the null hypothesis.

Table 4.1 Summary of the Global Calibration Factors of Rutting Models

Calibration Parameters	β_{1r}	β_{2r}	β_{3r}	β_{1s} (Coarse)	β_{1s} (Fine)	N	Bias, $e_{r(\text{mean})}$	Standard Error, S_e	S_e/S_y	R^2 , %	p-value (Paired t-test)
Global Values	0.4	0.52	1.36	1.00	1.00	123	-0.059	0.15	1.795	Poor	2.74E-07

Figure 4.1 shows the predicted total rutting compared to the measured total rutting for the globally calibrated model. The trend of rutting prediction shows that PMED mostly over-predicts total rutting for Idaho local pavements.

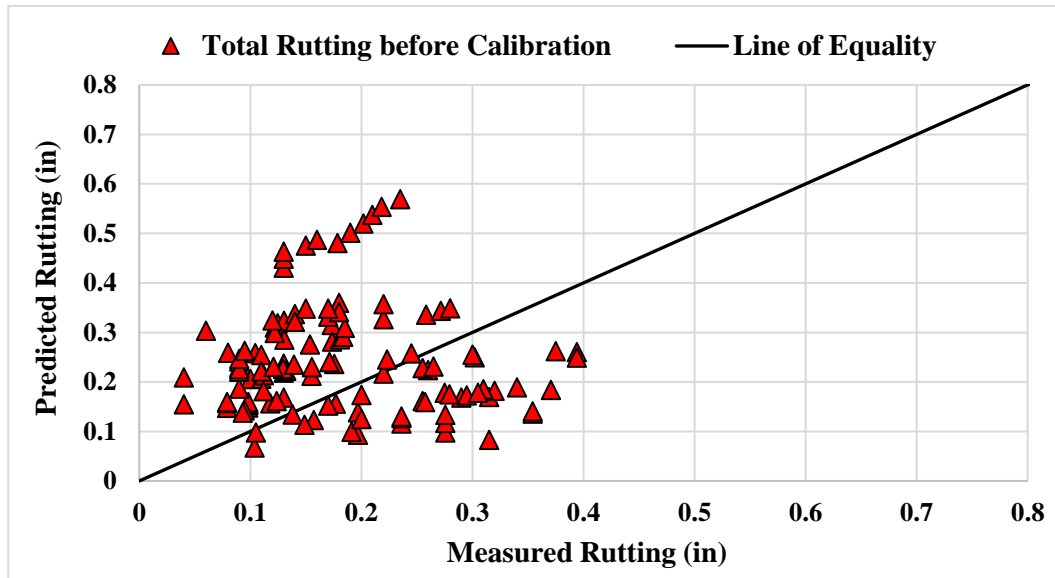


Figure 4.1 Predicted Vs. Measured Total Rutting Using Global Calibration Factors

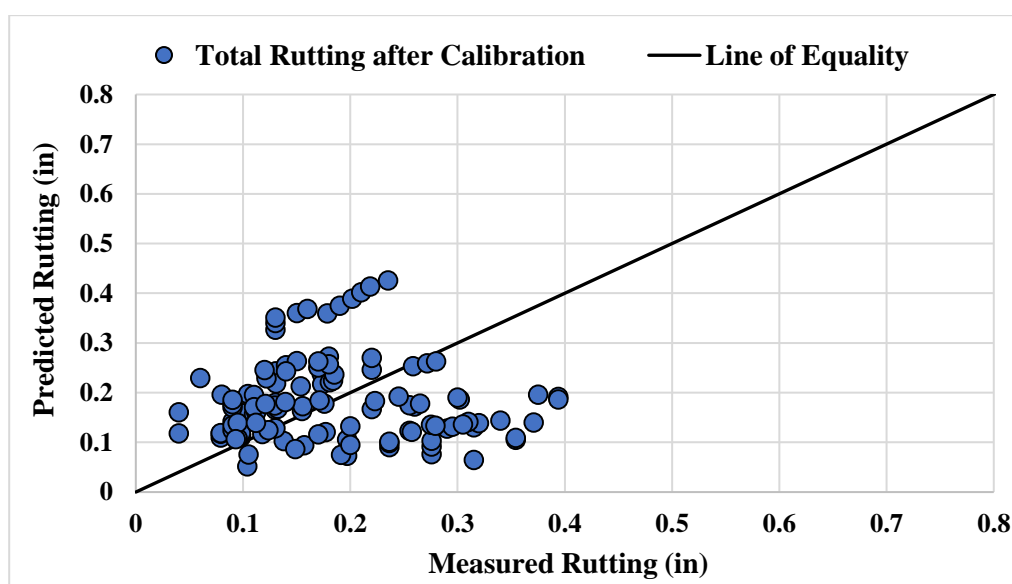
4.1.2 Calibration of Rutting Models

There are five calibration factors related to the total rutting or permanent deformation model in PMED. Among them, β_{1r} , β_{2r} , and β_{3r} are related to AC layer rutting and β_{1s} (coarse) for base layer and β_{1s} (fine) for subgrade layer. An iterative approach had been followed to calibrate the rutting model for Idaho local conditions. According to the local calibration guide, β_{1r} , β_{1s} (coarse) and β_{1s} (fine) were attempted first to optimize for different sets of trials to get the minimum bias. β_{2r} and β_{3r} have the most influence in AC layer prediction. As shown in Equation 2.1, β_{2r} and β_{3r} are the exponents of the number of load repetitions and pavement temperature, respectively. The trial sets of β_{2r} and β_{3r} showed great influences in rutting predictions. For example, changing either of these two terms or both the data points shifted far from the line of equality and subsequently made the null hypothesis rejected. Therefore, β_{2r} and β_{3r} were not adjusted. Table 4.2 demonstrates that after optimization, the null hypothesis was failed to reject with the reduction of bias and standard error of the estimate.

Table 4.2 Summary of the Local Calibration Factors of Rutting Models

Calibration Parameters	β_{1r}	β_{2r}	β_{3r}	β_{1s} (Coarse)	β_{1s} (Fine)	N	Bias, $e_{r(\text{mean})}$	Standard Error, S_e	S_e/S_y	R^2 , %	p-value (Paired t-test)
Local Values	0.3	0.52	1.36	0.86	0.736	123	0.0002	0.10	1.396	Poor	0.49

Figure 4.2 shows that after local calibration there is improvement in prediction compared to the measured value.

**Figure 4.2 Predicted Vs. Measured Total Rutting Using Local Calibration Factors**

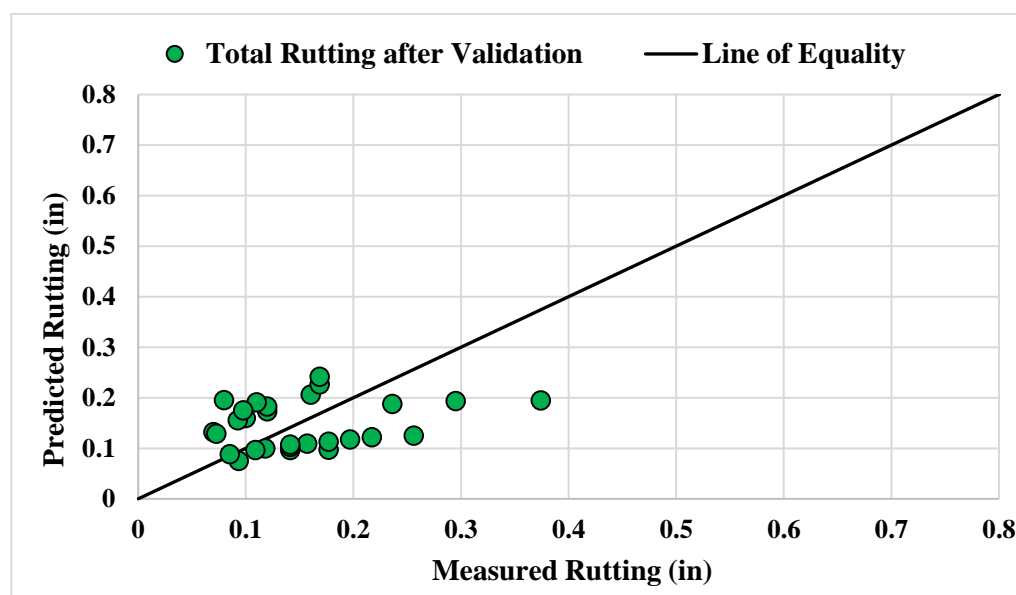
4.1.3 Validation of Rutting Models

After calibration, previously identified six independent projects were utilized as validation sites. The validation effort for the rutting model revealed that there is a good agreement between the calibration results and the validation results. The statistical analysis results in Table 4.3 provided lower bias and standard error of the estimate using the local calibration factors.

Table 4.3 Summary for Rutting Models after Validation

N	Bias, $e_{r(\text{mean})}$	Standard Error, S_e	S_e/S_y	R^2 , %	p-value (Paired t-test)
28	0.0065	0.074	1.03	6	0.33

Figure 4.3 depicts the predicted versus measured rutting using seven random projects which were not included in the calibration effort.

**Figure 4.3 Predicted Vs. Measured Total Rutting Using Local Factors**

4.2 Calibration of Longitudinal Cracking (Top-Down) Cracking Model

Longitudinal cracking is initiated at the surface of the pavement, occurs at the wheel-path and follows parallel to the centerline of the pavement. Longitudinal cracking is predicted in the PMED as ft./mile.

4.2.1 Verification of Longitudinal Cracking Model Using Global Calibration Factors

Longitudinal cracking model with the global calibration factors showed under-prediction for Idaho local pavements with a significant amount of bias and standard error of the estimate. Table 4.4 presents the statistical analysis results for the longitudinal cracking model. The null

hypothesis was rejected at 95% confidence interval because of the p-value lower than 0.05. Hence, local calibration should be done to minimize bias and standard error.

Table 4.4 Summary of the Global Calibration Factors of Longitudinal Cracking Model

Calibration Parameters	B_{f1}			B_{f2}	B_{f3}	C_1	C_2	N	Bias, $e_{r(\text{mean})}$	Standard Error, S_e	S_e/S_y	R^2 , %	p-value (Paired t-test)
	$h_{ac} < 5 \text{ in.}$	$h_{ac} > 12 \text{ in.}$	$5 \text{ in.} \leq h_{ac} \leq 12 \text{ in.}$										
Global Values	0.020 54	0.00103 2	$(5.014 * h_{ac}^{3.416}) * 1 + 0$	1.38	0.88	7.0	3.50	71	132.4	471.7	1.07	Poor	0.008

Figure 4.4 shows the predicted versus measured longitudinal cracking for the globally calibrated longitudinal cracking model.

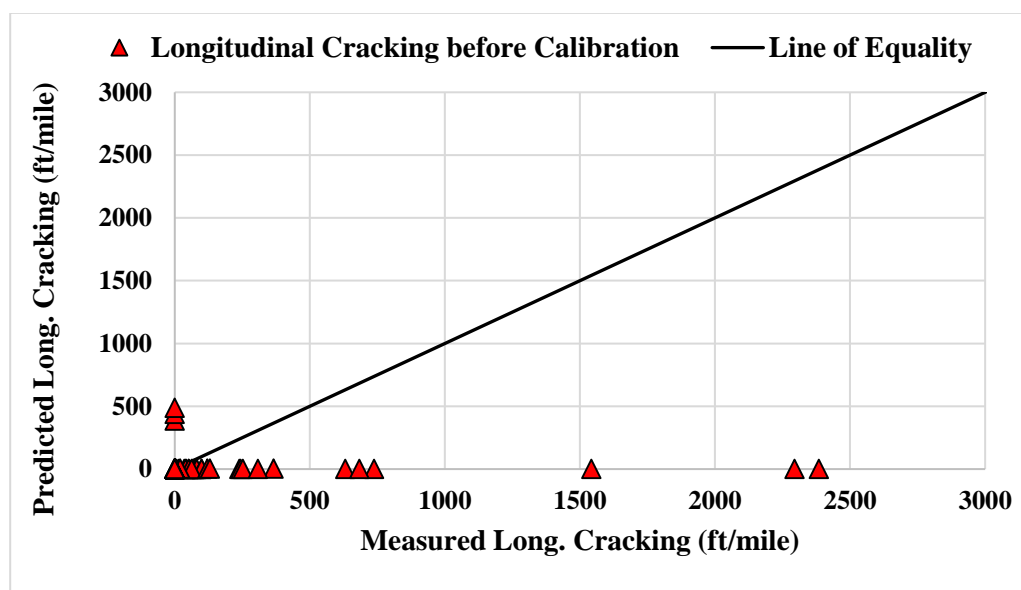


Figure 4.4 Predicted Vs. Measured Longitudinal Cracking Using Global Calibration Factors

4.2.2 Calibration of Longitudinal Cracking Model

As per the local calibration guide, longitudinal cracking model involved only calibration coefficients, C_1 and C_2 to be adjusted. AASHTOWare PMED software was executed numerous times with a large factorial set for C_1 and C_2 to reduce bias and standard error of the estimate. The optimized set of C_1 and C_2 showed significant improvement in bias reduction

from 132.4 to 2.3. Although the standard error was not reduced significantly, the estimated standard error was found reasonable compared to that for global calibration presented in Table 3.13. Table 4.5 lists the statistical results for the longitudinal cracking model after local calibration.

Table 4.5 Summary of the Local Calibration Factors of Longitudinal Cracking Model

Calibration Parameters	B _{f1}			B _{f2}	B _{f3}	C ₁	C ₂	N	Bias, e _{r(mean)}	Standard Error, S _e	S _e /S _y	R ² , %	p-value (Paired t-test)
	h _{ac} < 5 in.	h _{ac} > 12 in.	5 in. ≤ h _{ac} ≤ 12 in.										
Local Values	0.02054	0.001032	$(5.014 \cdot h_{ac}^{-3.416}) \cdot 1 + 0$	1.38	0.88	3.3	1.0	71	2.3	450.2	1.0	Poor	0.48

Figure 4.5 represents the predicted longitudinal cracking compared to the measured data after local calibration.

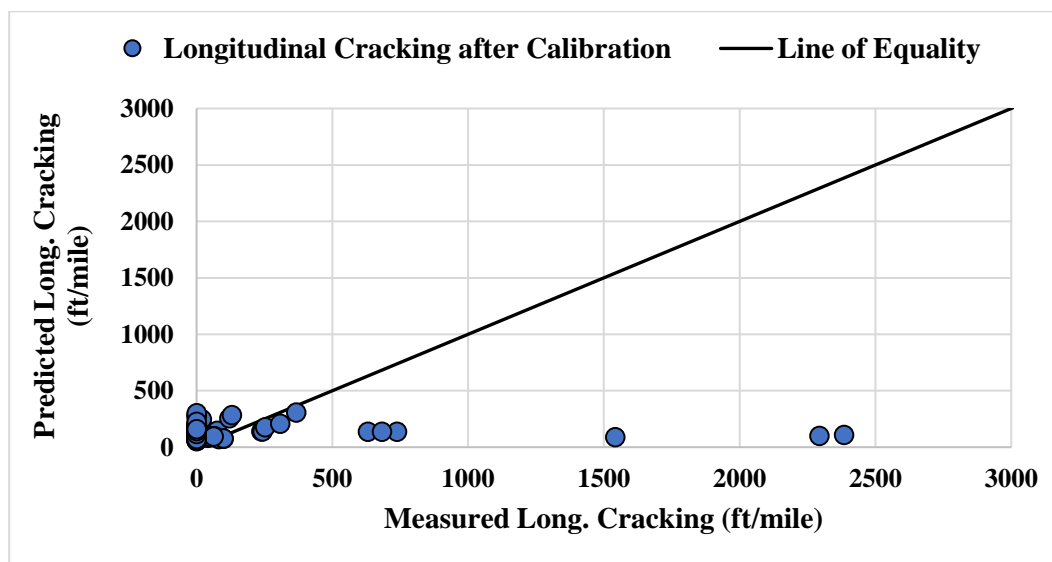


Figure 4.5 Predicted Vs. Measured Longitudinal Cracking Using Local Calibration Factors

4.2.3 Validation of Longitudinal Cracking Model

In order to re-examine the developed local calibration factors for longitudinal cracking model, five random projects were identified and were run as a batch in the PMED software. The

results in Table 4.6 indicates a significant amount of standard error, although the null hypothesis was failed to reject at 95% confidence interval. It can be noted here that, the longitudinal cracking model is still under development in the NCHRP Project 1-52, *A Mechanistic-Empirical Model for Top-Down Cracking of Asphalt Pavement Layers*; hence, it can be expected that the final developed model would generate more robust predictions.

Table 4.6 Summary for Longitudinal Cracking Model after Validation

N	Bias, $\epsilon_r(\text{mean})$	Standard Error, S_e	S_e/S_y	$R^2, \%$	p-value (Paired t-test)
18	-1.7	518	0.82	17	0.5

Figure 4.6 shows predicted versus measured longitudinal cracking using five random projects for validation.

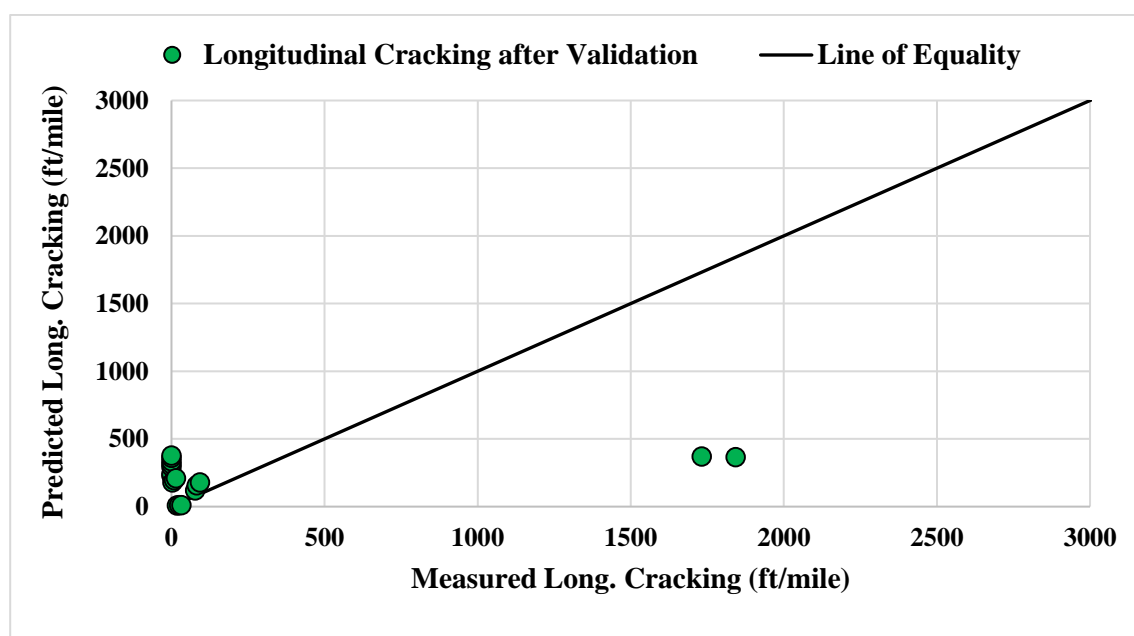


Figure 4.6 Predicted Vs. Measured Longitudinal Cracking Using Local Factors

4.3 Calibration of Alligator (Bottom-Up) Cracking Model

Alligator cracking is initiated from the bottom of the asphalt concrete layer and propagates to the top of the surface. The cracks are interconnected. In PMED, the unit used for the alligator

cracking is “% of total lane area.” A value of 7% for the standard error of the estimate is reasonable for alligator cracking ⁽¹²⁾.

4.3.1 Verification of Alligator Cracking Model Using Global Calibration Factors

Table 4.7 presents the statistical summary for the verification of alligator cracking using the global calibration factors. The globally calibrated alligator cracking prediction model did not show significant bias for Idaho local pavements. However, the p-value was found to be less than 0.05, indicated to reject the null hypothesis. Hence, the local calibration of alligator cracking model was attempted.

Table 4.7 Summary of the Global Calibration Factors of Alligator Cracking Model

Calibration Parameters	C ₁	C ₂ : h _{ac} <5 in.	C ₂ : > 12 in.	C ₂ : 5in. <= h _{ac} <= 12 in.	N	Bias, e _{r(mean)}	Standard Error, S _e	S _e /S _y	R ² , %	p-value (Paired t-test)
Global Values	1.31	2.1585	3.9666	1	70	0.45	1.20	1.07	Poor	0.001

The AASHTOWare Pavement ME Design Software predicts alligator cracking to almost zero. Therefore in Figure 4.7, under-prediction of alligator cracking is observed.

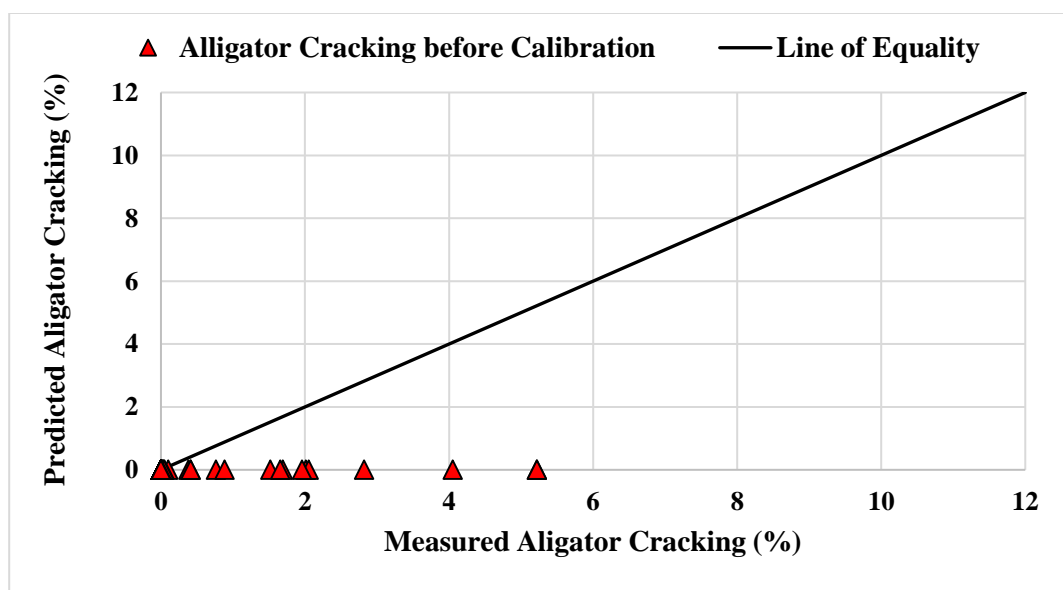


Figure 4.7 Predicted Vs. Measured Alligator Cracking Using Global Calibration Factors

4.3.2 Calibration of Alligator Cracking Model

Alligator cracking model includes three calibration factors C_1 , C_2 , and C_3 . As per the local calibration guide, except for C_3 , the other two coefficients were adjusted in this study. In the AASHTOWare PMED software version 2.5.3, C_2 has three different factors which are dependent on AC layer thickness. Only one project had AC layer thickness greater than 12 inches; hence the factor related to AC layer thickness greater than 12 inches was not adjusted. The PMED software was run for numerous times using different combination sets for C_1 and the two factors for C_2 . The calibration effort reduced bias, as a result, the null hypothesis was failed to reject at 95% confidence interval. The standard error was also found reasonable. The statistical results after local calibration are listed in Table 4.8.

Table 4.8 Summary of the Local Calibration Factors of Alligator Cracking Model

Calibration Parameters	C_1	C2: $h_{ac} < 5$ in.	C2: > 12 in.	C2: 5in. $\leq h_{ac} \leq 12$ in.	N	Bias, $e_{r(\text{mean})}$	Standard Error, S_e	S_e/S_y	R^2 , %	p-value (Paired t-test)
Local Values	0.31	1.1585	3.9666	0.2	70	-0.19	1.07	1.48	Poor	0.18

Figure 4.8 shows the plot of predicted alligator cracking compared to the measured data using the local calibration factors.

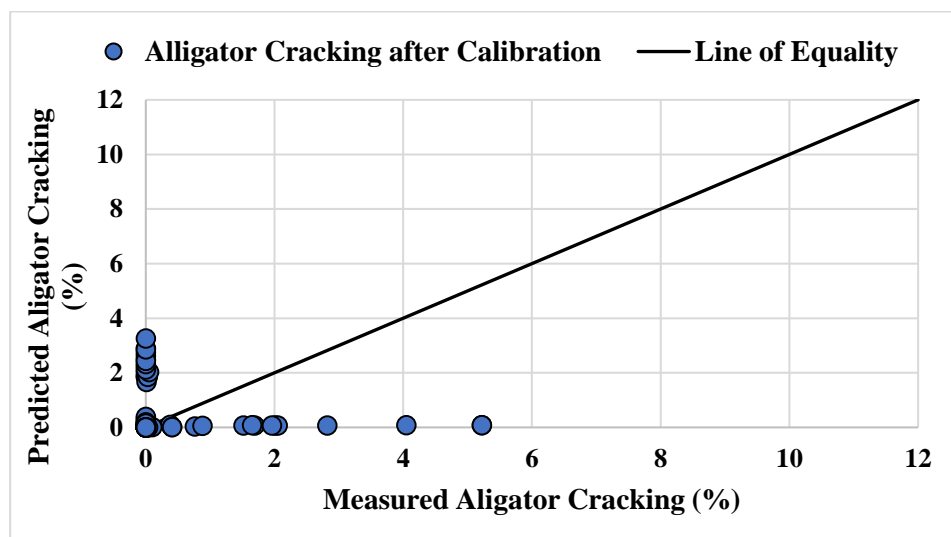


Figure 4.8 Predicted Vs. Measured Alligator Cracking Using Local Calibration Factors

4.3.3 Validation of Alligator Cracking Model

Following the local calibration of the AASHTOWare Pavement ME Design software for alligator cracking, validation was also attempted for five independent projects. Table 4.9 presents the statistical results for the selected projects using the local factors. The null hypothesis was failed to reject with a reasonable amount of bias and standard error of the estimate.

Table 4.9 Summary for Alligator Cracking Model after Validation

N	Bias, $e_r(\text{mean})$	Standard Error, S_e	S_e/S_y	R^2 , %	p-value (Paired t-test)
19	-0.36	3.10	1.03	Poor	0.31

Figure 4.9 depicts the predicted vs. measured alligator cracking using the five independent projects.

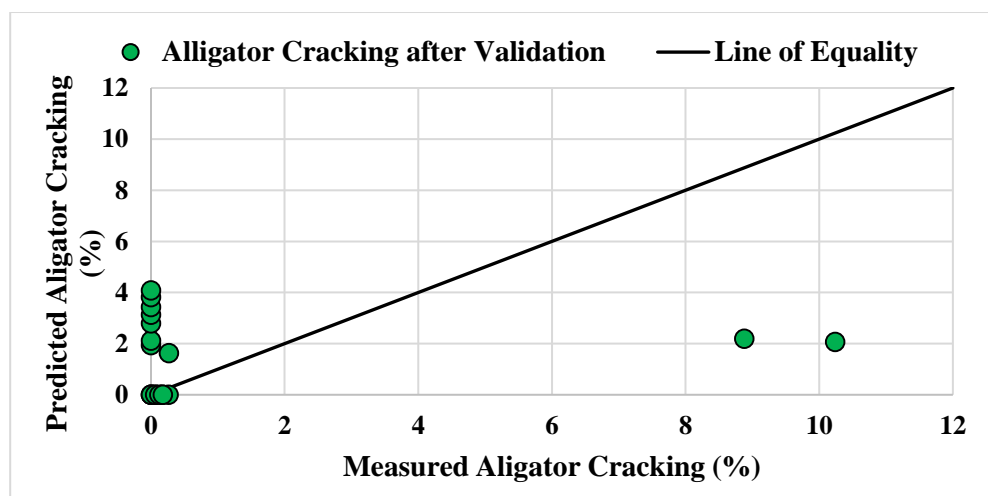


Figure 4.9 Predicted Vs. Measured Alligator Cracking Using Local Factors

4.4 Calibration of Transverse (Thermal) Cracking

Transverse Cracking or thermal cracking is related to low temperature cracking. The thermal cracking model in the PMED software requires creep compliance and indirect tensile strength (IDT) inputs at three different hierarchical levels depending upon the availability. Since level 1 input for IDT was not available, the thermal cracking model was evaluated and calibrated for level 2 and level 3 inputs. The PMED output provides transverse cracking as ft./mile.

4.4.1 Transverse Cracking Model at Level 3

4.4.1.1 Verification of Transverse Cracking Model at Level 3 Using Global Calibration Factors

Transverse Cracking with the global factors showed under-prediction compared to the measured data. Although the statistical results showed that there is no significant difference between the measured and predicted transverse cracking, some bias existed. Therefore, this study attempted to reduce bias optimizing the bold coefficient presented in Table 4.10. The statistical analysis for assessing the transverse cracking model at Level 3 is listed in Table 4.10 with the global factors.

Table 4.10 Summary of the Global Calibration Factors of Thermal Cracking (Level 3) Model

Calibration Parameters	K (MAAT ≤ 57 deg F)	N	Bias, $e_{r(\text{mean})}$	Standard Error, S_e	S_e/S_y	R^2 , %	p-value (Paired t-test)
Global Values	$[3 * 10^{-7} * \text{MAAT}^{4.0319}] * 1 + 0$	67	34.4	469.6	1.67	Poor	0.27

- MAAT = Mean Annual Air Temperature

With the global factors, predicted versus measured thermal cracking at Level 3 is depicted in Figure 4.10.

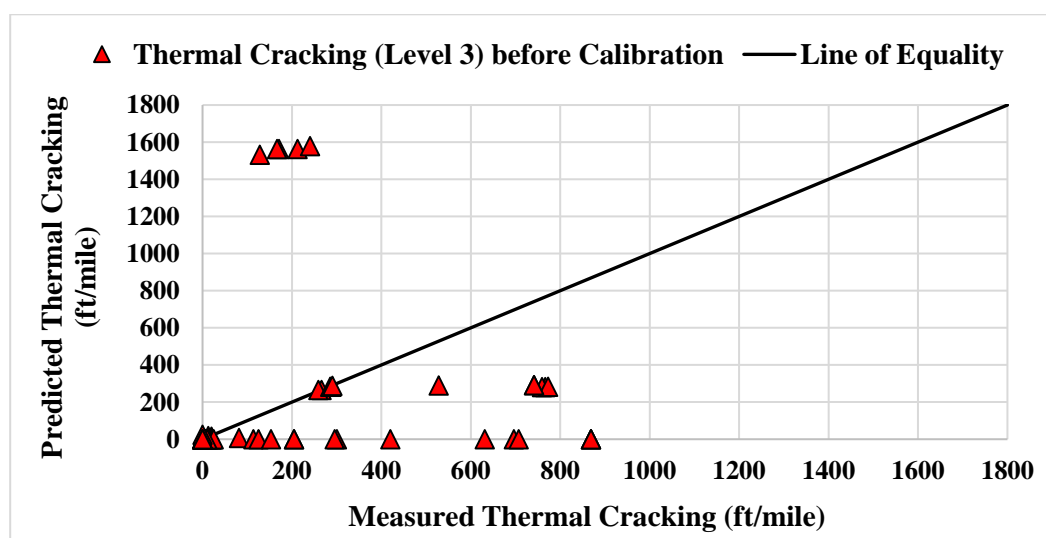


Figure 4.10 Predicted Vs. Measured Transverse Cracking (Level 3) Using Global Calibration Factors

4.4.1.2 Calibration of Transverse Cracking Model at Level 3

The calibration effort for transverse cracking (Level 3) reduced bias, and still, the null hypothesis was failed to reject. However, significant improvements were not observed through the local calibration. Table 4.11 presents the statistical results after local calibration.

Table 4.11 Summary of the Local Calibration Factors of Thermal Cracking (Level 3) Model

Calibration Parameters	K (MAAT ≤ 57 deg F)	N	Bias, $e_{r(\text{mean})}$	Standard Error, S_e	S_e/S_y	R^2 , %	p-value (Paired t-test)
Local Values	$[3.0606 * 10^{-7} * \text{MAAT}^{4.0319}] * 1 + 0$	67	24.2	469.8	1.67	Poor	0.34

- MAAT = Mean Annual Air Temperature

Figure 4.11 shows the plot between predicted and measured thermal cracking (Level 3) after the local calibration.

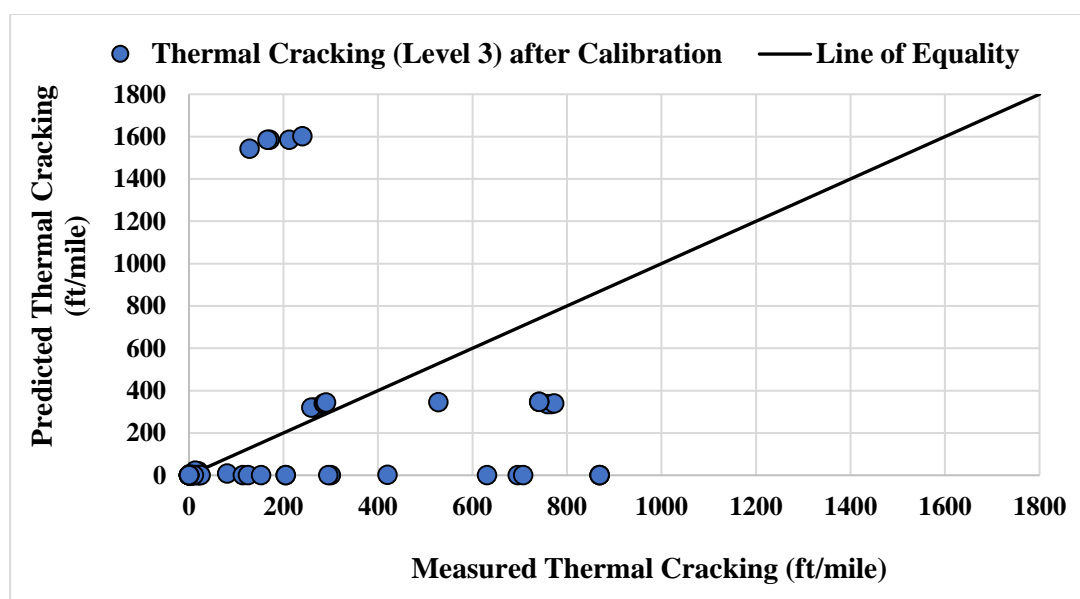


Figure 4.11 Predicted Vs. Measured Transverse Cracking (Level 3) Using Local Calibration Factors

4.4.1.3 Validation of Transverse Cracking as Level 3

The validation results revealed that the null hypothesis was failed to reject, though a significant amount of bias was observed. However, the standard error was found lower

compared to the standard error derived from the local calibration effort. Table 4.12 summarizes the statistical results for validation.

Table 4.12 Summary for Thermal Cracking (Level 3) Model after Validation

N	Bias, $e_r(\text{mean})$	Standard Error, S_e	S_e/S_y	R^2 , %	p-value (Paired t-test)
19	-76.8	260.1	4.01	6.5	0.10

Figure 4.12 shows the predicted thermal cracking (Level 3) compared to the measured data after validation.

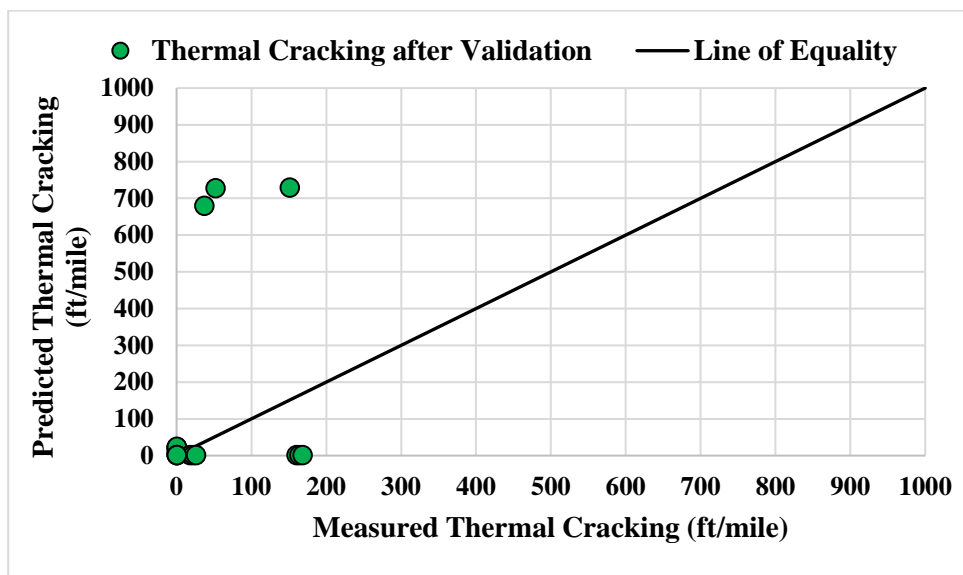


Figure 4.12 Predicted Vs. Measured Transverse Cracking (Level 3) Using Local Factors

4.4.2 Transverse Cracking (Level 2)

4.4.2.1 Verification of Transverse Cracking Model at Level 2 Using Global Calibration Factors

Transverse Cracking at Level 2 with the global factors showed significant bias and standard error, although the p-value was accepted. Therefore, an adjustment was attempted to reduce bias. Table 4.13 shows the statistical analysis for thermal cracking at Level 2 using the globally calibrated factors.

Table 4.13 Summary of the Global Calibration Factors of Thermal Cracking (Level 2) Model

Calibration Parameters	K (MAAT <= 57 deg F)	N	Bias, $e_{r(\text{mean})}$	Standard Error, S_e	S_e/S_y	R^2 , %	p-value (Paired t-test)
Global Values	$[3 * \text{Pow}[10, -7]] * \text{Pow}[\text{MAAT}, 4.0319] * 1 + 0$	35	-174.35	746.201	2.573	10.58	0.09

Figure 4.13 shows the predicted vs measured transverse cracking at Level 2 using the global calibration factors.

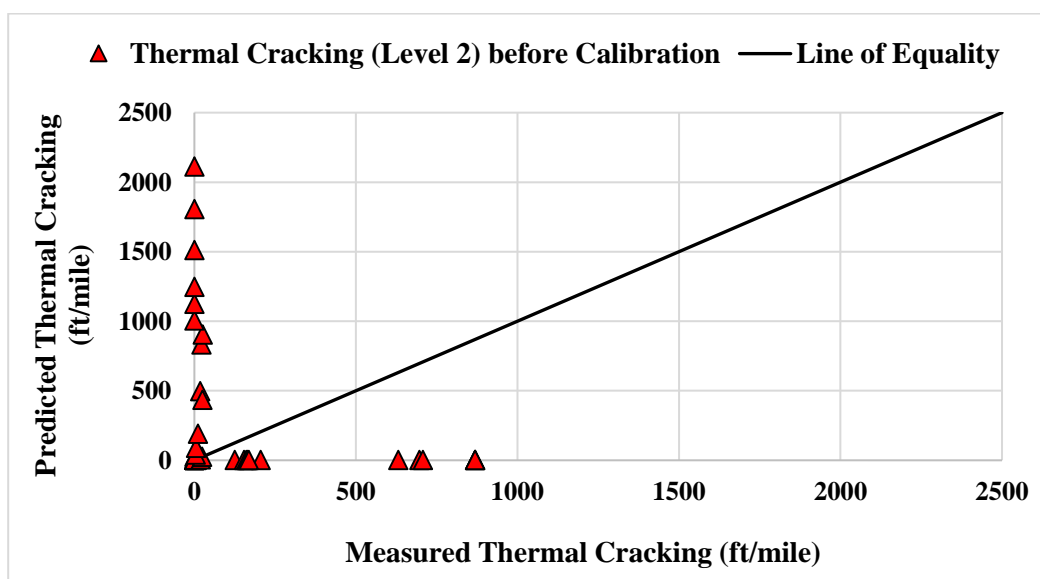


Figure 4.13 Predicted Vs. Measured Transverse Cracking (Level 2) Using Global Calibration Factors

4.4.2.2 Calibration of Transverse Cracking Model at Level 2

The calibration effort reduced bias to almost zero, and the standard error was also reduced. Unlike thermal cracking model calibration with Level 3 inputs, this level showed much improvement after local calibration. Table 4.14 presents the statistical summary for the transverse cracking model at Level 2 inputs after local calibration.

Table 4.14 Summary of the Local Calibration Factors of Thermal Cracking (Level 2) Model

Calibration Factors	K (MAAT <= 57 deg F)	N	Bias, $\epsilon_{r(\text{mean})}$	Standard Error, S_e	S_e/S_y	R^2 , %	p-value (Paired t-test)
Local Values	$[2.591 * \text{Pow}[10, -7]] * \text{Pow}[\text{MAAT}, 4.0319] * 1 + 0$	35	-0.00029	529.394	1.825	5.92	0.5

Figure 4.14 shows the predicted versus measured transverse cracking at Level 2 using the local factors.

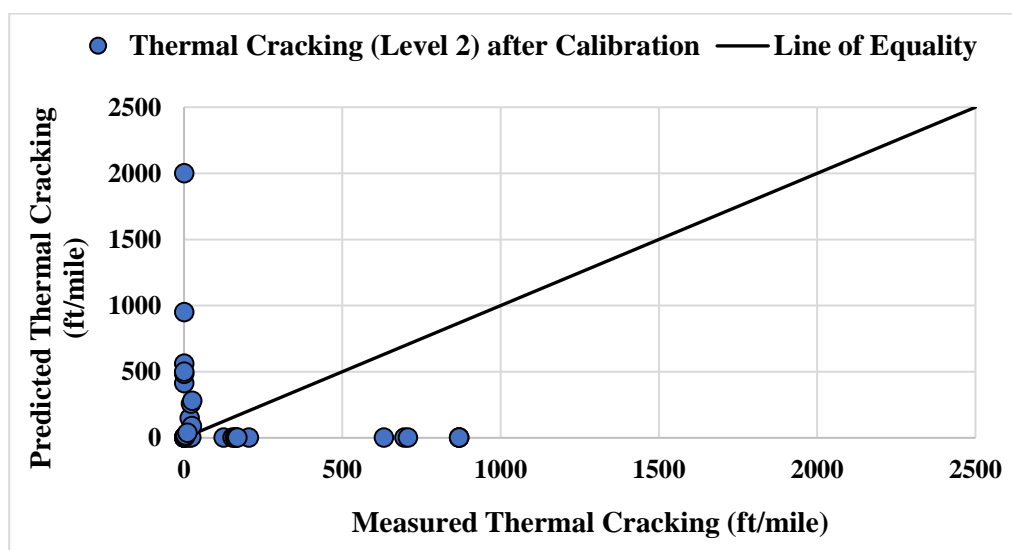


Figure 4.14 Predicted Vs. Measured Transverse Cracking (Level 2) Using Local Calibration Factors

4.4.2.3 Validation of Transverse Cracking Model at Level 2

The transverse cracking model at Level 2 was not validated in this study due to lack of projects with Level 2 low temperature cracking data.

4.5 Calibration of International Roughness Index (IRI) Model

International Roughness Index (IRI) is an indication of smoothness or ride quality of pavement. IRI is a function of other distresses (rut depth, load-related cracking, thermal cracking) and site-factor. IRI is measured as inches/mile.

4.5.1 Verification of IRI Model Using Global Calibration Factors

The statistical summary of the IRI model verification is presented in Table 4.15. A paired t-test at 95% confidence interval showed p-value < 0.001 , which indicated it would reject the null hypothesis. Also, some bias was observed while comparing the measured IRI to the predicted IRI using the global factors.

Table 4.15 Summary of the Global Calibration Factors of IRI Model

Calibration Parameters	C ₁	C ₂	C ₃	C ₄	N	Bias, $e_{r(\text{mean})}$	Standard Error, S_e	S_e/S_y	R ² , %	p-value (Paired t-test)
Global Values	40	0.40	0.008	0.015	94	10.3	19.5	1.08	21	2.10E-08

Figure 4.15 shows that globally calibrated IRI model mostly under-predicted IRI for selected pavements from Idaho. As with Washington state, studded tire also plays a vital role in the deterioration of roads in Idaho. However, PMED does not consider the effect of the studded tire in its prediction for IRI. This may lead to under-prediction of IRI which is also observed in this study.

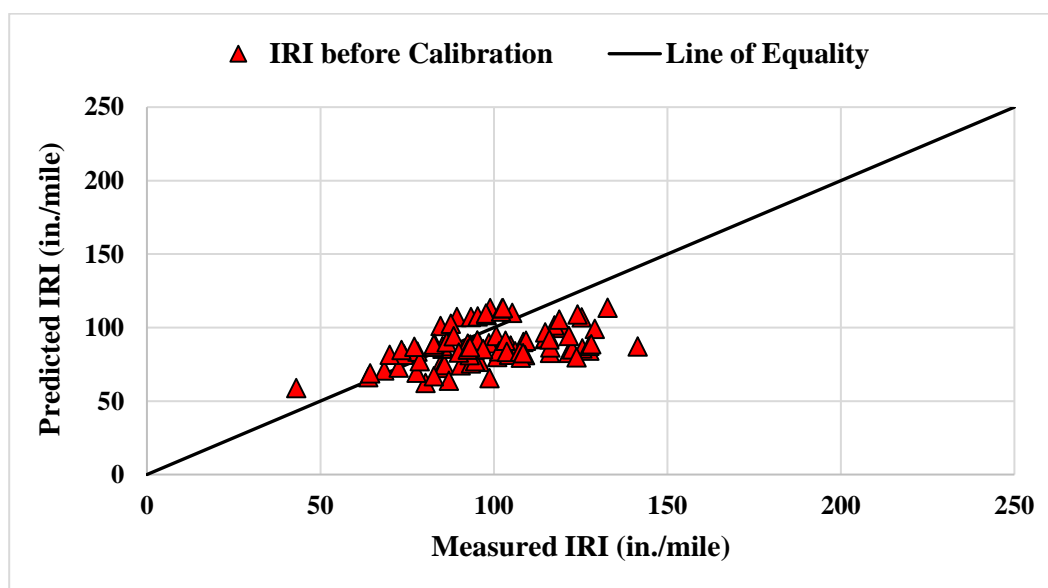


Figure 4.15 Predicted Vs. Measured IRI Using Global Calibration Factors

4.5.2 Calibration of IRI Model

International Roughness Index (IRI) has 4 calibration factors (C_1 , C_2 , C_3 , and C_4). A large factorial of these calibration factors (except C_3 ; was kept as default value) were attempted to calibrate the model. The optimized set of trials improved the model's prediction with reducing bias and standard error of the estimate. The null hypothesis was failed to reject at a 95% confidence interval implying that there is no significant difference between the predicted IRI and the measured IRI. Table 4.16 highlights the statistical results for the IRI model after local calibration.

Table 4.16 Summary of the Local Calibration Factors of IRI Model

Calibration Parameters	C_1	C_2	C_3	C_4	N	Bias, $e_{r(\text{mean})}$	Standard Error, S_e	S_e/S_y	R^2 , %	p-value (Paired t-test)
Local Values	80	0.6	0.008	0.02	94	-1.2	17.5	0.97	24	0.24

Local calibration attempt clustered the data points around the line of equality, as shown in Figure 4.16.

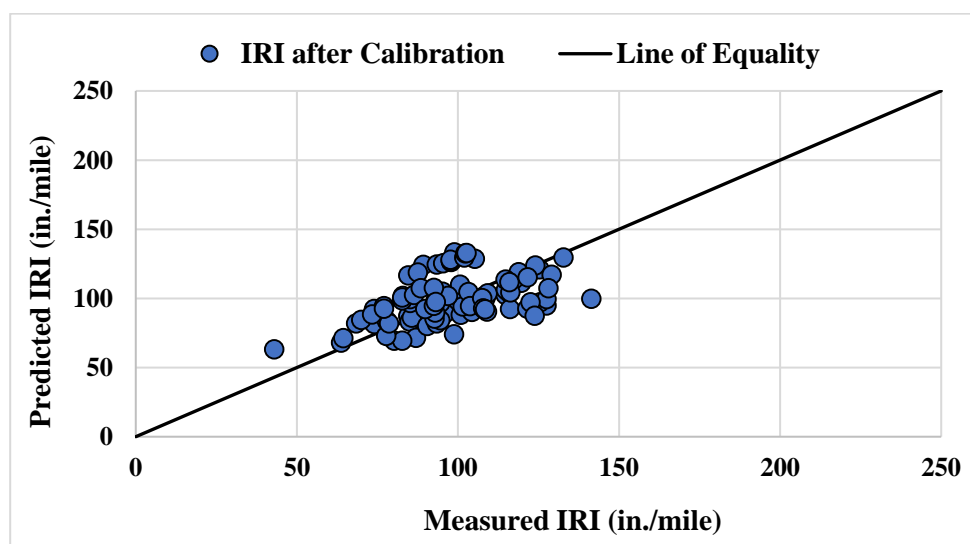


Figure 4.16 Predicted Vs. Measured IRI Using Local Calibration Factors

4.5.3 Validation of IRI

To validate the IRI model for Idaho local conditions, six projects were identified to run the PMED software independently. The statistical analysis results after the validation are reported

in Table 4.17. The p-value was found greater than 0.05, indicated that the null hypothesis was failed to reject. Also, using the local factors resulted in low bias and reasonable standard error.

Table 4.17 Summary of IRI Model after Validation

N	Bias, $e_r(\text{mean})$	Standard Error, S_e	S_e/S_y	R^2 , %	p-value (Paired t-test)
18	3.8	17.6	1.14	21	0.19

Figure 4.17 shows the plot of the measured IRI compared to the predicted IRI for the selected six projects in Idaho.

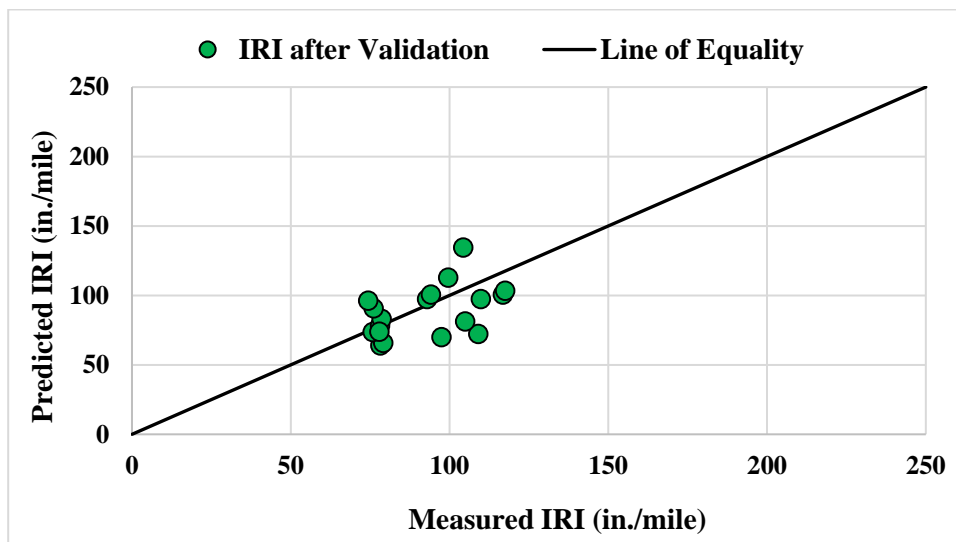


Figure 4.17 Predicted Vs. Measured IRI Using Local Factors

4.6 Calibration Results

Based on the calibration and validation results, the final local factors for flexible pavement in Idaho are tabulated in Table 4.18.

Table 4.18 Developed Local Factors for Flexible Pavement in Idaho

Performance Model	Calibration Parameters	Global Factors (as per PMED V2.5.3)	Local Factors for Idaho
AC Rutting	K1	-2.45	-2.45
	K2	3.01	3.01
	K3	0.22	0.22
	β_{1r}	0.4	0.3
	β_{2r}	0.52	0.52
	β_{3r}	1.36	1.36
Unbound Base Rutting	β_{1s}	1.00	0.86
Subgrade Rutting	β_{1s}	1.00	0.736
Longitudinal Cracking (Top-Down Cracking)	$\beta_{fl}: h_{ac} < 5$ in.	0.02054	0.02054
	$\beta_{fl}: h_{ac} > 12$ in.	0.001032	0.001032
	$\beta_{fl}: 5 \text{ in.} \leq h_{ac} \leq 12$ in.	$(5.014 * h_{ac}^{-3.416}) * 1 + 0$	$(5.014 * h_{ac}^{-3.416}) * 1 + 0$
	β_{f2}	1.38	1.38
	β_{f3}	0.88	0.88
	C ₁	7	3.3
	C ₂	3.5	0.825
Alligator Cracking (Bottom-Up Cracking)	$\beta_{fl}: h_{ac} < 5$ in.	0.02054	0.02054
	$\beta_{fl}: h_{ac} > 12$ in.	0.001032	0.001032
	$\beta_{fl}: 5 \text{ in.} \leq h_{ac} \leq 12$ in.	$(5.014 * h_{ac}^{-3.416}) * 1 + 0$	$(5.014 * h_{ac}^{-3.416}) * 1 + 0$
	β_{f2}	1.38	1.38
	β_{f3}	0.88	0.88
	C ₁	1.31	0.31
	C ₂ : $h_{ac} < 5$ in.	2.1585	1.1585
	C ₂ : $5 \text{ in.} \leq h_{ac} \leq 12$ in.	$(0.867 + 0.2583 * h_{ac}) * 1$	$(0.867 + 0.2583 * h_{ac}) * 0.175$
C ₂ : $h_{ac} > 12$ in.	3.9666	3.9666	
Thermal Cracking (Level 2)	K (MAAT ≤ 57 deg F)	$[3 * 10^{-7} * \text{MAAT}^{4.0319}] * 1 + 0$	$[2.591 * 10^{-7} * \text{MAAT}^{4.0319}] * 1 + 0$
Thermal Cracking (Level 3)	K (MAAT ≤ 57 deg F)	$[3 * 10^{-7} * \text{MAAT}^{4.0319}] * 1 + 0$	$[3.0606 * 10^{-7} * \text{MAAT}^{4.0319}] * 1 + 0$
IRI	C ₁	40	80
	C ₂	0.4	0.6
	C ₃	0.008	0.008
	C ₄	0.015	0.02

CHAPTER 5: DEVELOPMENT OF THE PMED CALIBRATION FACTORS FOR RIGID PAVEMENT

This chapter presents the Jointed Plain Concrete Pavement (JPCP) performance models' verification, calibration, and validation executing the AASHTOWare Pavement ME Design Software version 2.5.3. Three performance models of JPCP pavement such as joint faulting, transverse cracking and smoothness (IRI) were considered in this study. Like flexible pavement performance models, above mentioned activities were also conducted following the steps described in the methodology section of this thesis.

5.1 Calibration of Joint Faulting Model

Faulting is the elevation difference between the joints of two adjacent slabs. Faulting is critical in terms of ride quality as the road users feel bumping while driving on these kind of affected pavements. Faulting is reported as inch in the PMED software.

5.1.1 Verification of Joint Faulting Model Using Global Calibration Factors

To verify the faulting model, the AASHTOWare Pavement ME Design software was run with the global calibration factors. The verification results revealed that the null hypothesis at 95% confidence interval was failed to reject based on $p\text{-value} > 0.05$. Also, bias was found low. However, this study attempted to reduce the standard error further. Table 5.1 presents the statistical analysis results for faulting using the global factors.

Table 5.1 Summary of the Global Calibration Factors of Joint Faulting Model

Performance Model	Parameters	Global Factors	N	Bias, $e_{r(\text{mean})}$	Standard Error, S_e	S_e/S_y	R^2 , %	p-value (Paired t-test)
Faulting	F1	0.595	178	-0.725	0.1	1.39	Poor	0.285
	F2	1.636						
	F3	0.00217						
	F4	0.00444						
	F5	250						
	F6	0.47						
	F7	7.3						
	F8	400						

Figure 5.1 represents the predicted vs measured faulting data using the global factors.

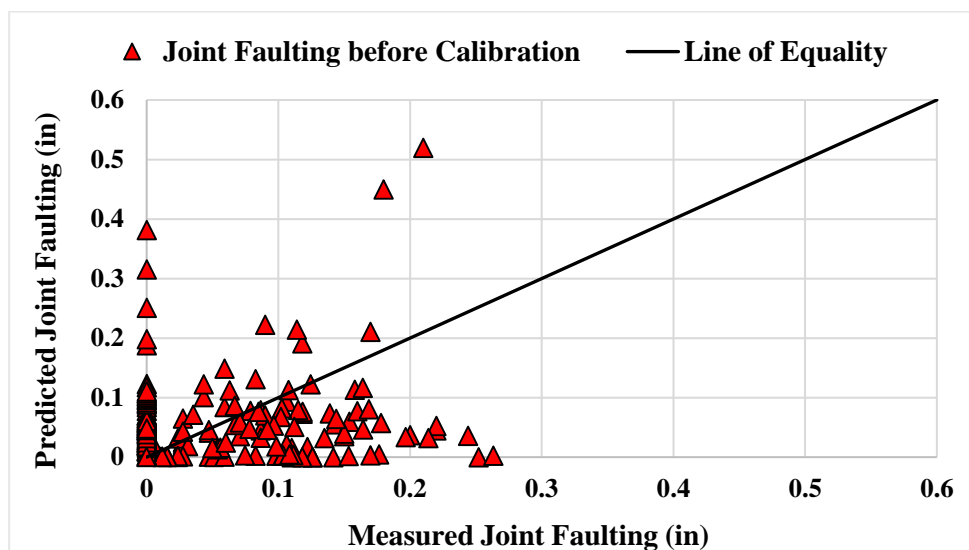


Figure 5.1 Predicted Vs. Measured Faulting Using Global Calibration Factors

5.1.2 Calibration of Joint Faulting Model

According to the AASHTO local calibration guide, only calibration parameter (F1) associated with the faulting model was considered to reduce both bias and standard error. After several trials, the simulation results provided lower bias close to almost zero and the standard error of the estimate was also reduced lower than 0.1 inch. The null hypothesis was still failed to reject. Table 5.2 presents the statistical summary results for faulting after adjusting the factor.

Table 5.2 Summary of the Local Calibration Factors of Joint Faulting Model

Performance Model	Parameters	Global Factors	N	Bias, $e_{r(\text{mean})}$	Standard Error, S_e	S_e/S_y	R^2 , %	p-value (Paired t-test)
Faulting	F1	0.516	178	0.002	0.093	1.37	Poor	0.5
	F2	1.636						
	F3	0.00217						
	F4	0.00444						
	F5	250						
	F6	0.47						
	F7	7.3						
	F8	400						

Figure 5.2 shows the predicted vs measured faulting data using the local factors.

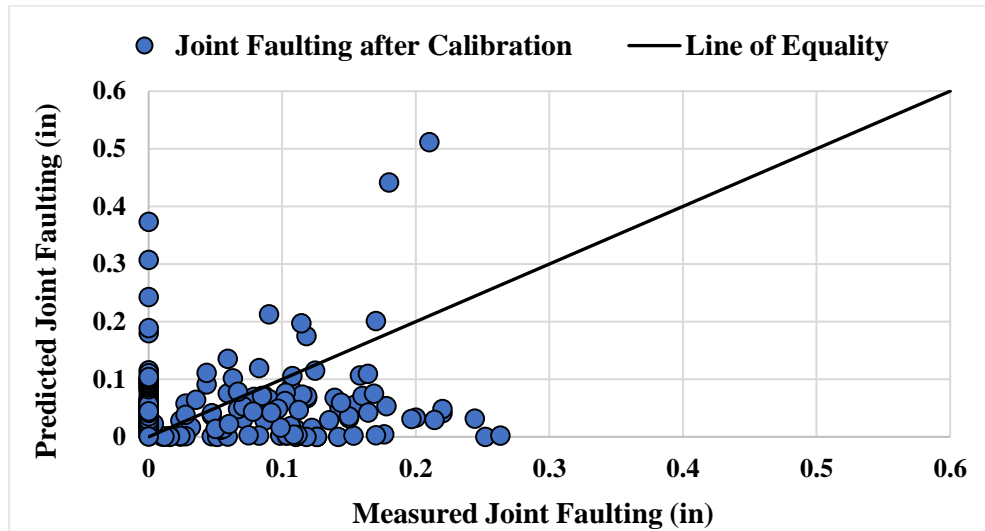


Figure 5.2 Predicted Vs. Measured Faulting Using Local Calibration Factors

5.1.3 Validation of Joint Faulting

Six projects were run as batch to validate the local calibration factors of the faulting model. The simulation results revealed lower bias and standard error of the estimate with the support of accepting the null hypothesis at 95% confidence interval. Table 5.3 lists the summary of the statistical results for the faulting model validation.

Table 5.3 Summary for Joint Faulting Model after Validation

N	Bias, $e_r(\text{mean})$	Standard Error, S_e	S_e/S_y	R^2, %	p-value (Paired t-test)
33	-0.214	0.078	0.747	52.1	0.32

Figure 5.3 shows the predicted versus measured faulting data using the six projects independently for validation.

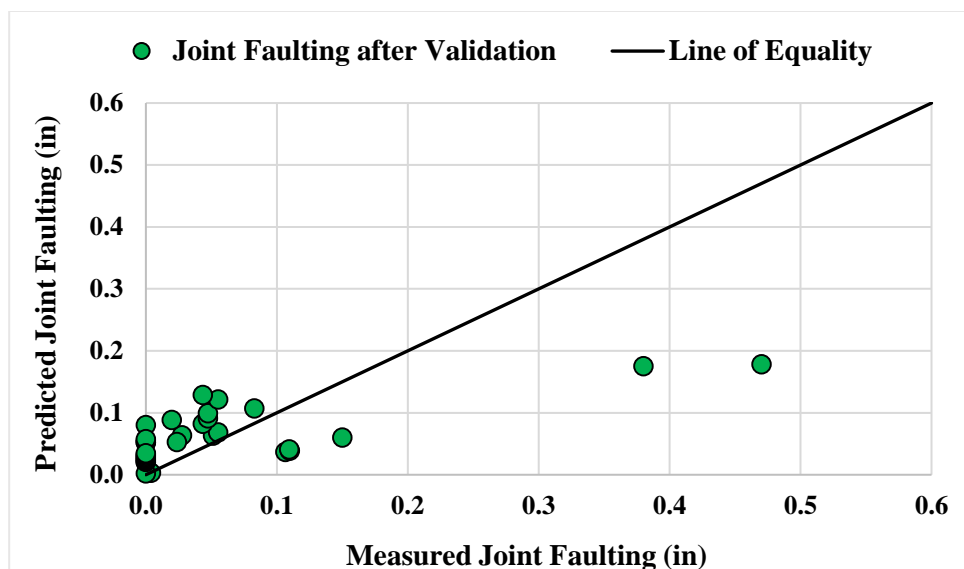


Figure 5.3 Predicted Vs. Measured Faulting Using Local Factors

5.2 Calibration of Transverse Cracking Model

Transverse cracking is the representation of the percent slabs cracked for the jointed plain concrete pavement. Transverse cracking can be initiated either from the bottom of the pavement or at the surface of the pavement. However, both these types of cracking cannot be initiated concurrently for the JPCP pavements. Hence, the cracking model takes account both the top-down and bottom-up cracking and reports as the total transverse cracking. The unit for transverse cracking is “% slabs cracked.”

5.2.1 Verification of Transverse Cracking Model Using Global Calibration Factors

Using the global calibration factors, the transverse cracking verification for Idaho local conditions revealed that the null hypothesis was rejected with a significant amount of bias and standard error of the estimate. Therefore, local calibration was necessitated. Table 5.4 presents the statistical summary for the verification of the transverse cracking model.

Table 5.4 Summary of the Global Calibration Factors of Transverse Cracking Model

Performance Model	Parameters	Global Factors	N	Bias, $e_{r(\text{mean})}$	Standard Error, S_e	S_e/S_y	R^2 , %	p-value (Paired t-test)
Transverse Cracking	C1	2	196	-767.6	18.9	4.450	Poor	0.002
	C2	1.22						
	C4	0.52						
	C5	-2.17						

Using the global factors, the comparison between the predicted transverse cracking and measured data is shown in Figure 5.4.

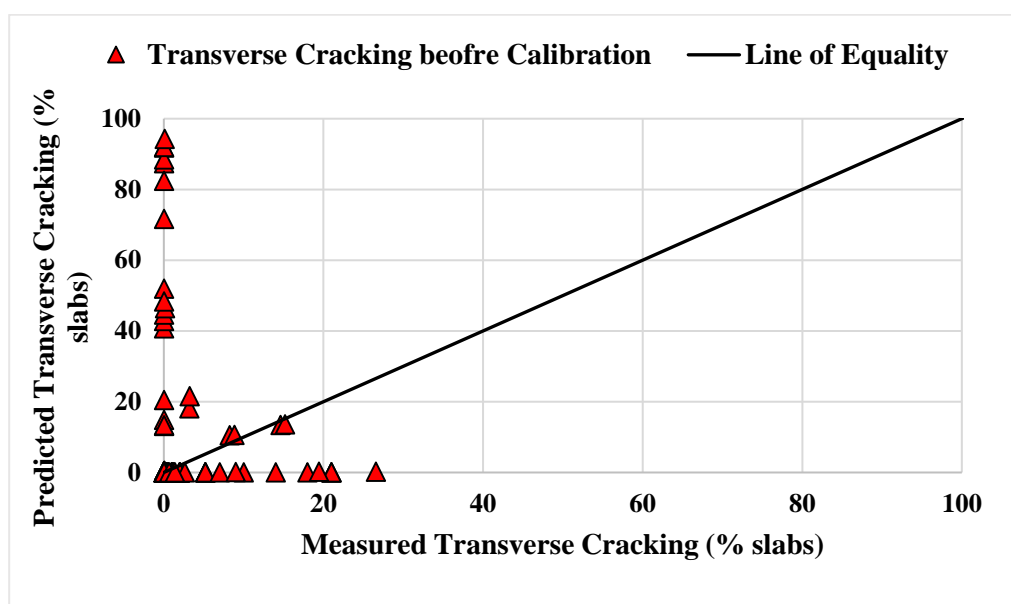


Figure 5.4 Predicted Vs. Measured Transverse Cracking Using Global Calibration Factors

5.2.2 Calibration of Transverse Cracking Model

It is recommended to adjust C_1 or C_4 – term for the transverse cracking model in order to reduce bias as per the AASHTO local calibration guide. After several trials for different set of C_1 the optimized value provided lower bias. Although after adjusting C_1 , the standard error of the estimate was found in the reasonable range, it was tried to minimize it adjusting the recommended calibration factors C_2 and C_5 . However, following so the validation was not accepted in terms of the null hypothesis because there is a poor correlation between the measured and the predicted cracking. Therefore, it was recommended only reducing bias without going further to reduce the standard error. Hence, only C_1 was optimized in this study. The null hypothesis was also failed to reject at 95% confidence interval providing greater p-value than 0.05. The statistical summary results for the transverse cracking model after local calibration is presented in Table 5.5.

Table 5.5 Summary of the Local Calibration Factors of Transverse Cracking Model

Performance Model	Parameters	Local Factors	N	Bias, $e_{r(\text{mean})}$	Standard Error, S_e	S_e/S_y	R^2 , %	p-value (Paired t-test)
Transverse Cracking	C1	2.366	196	-69.02	7.6	1.8	Poor	0.258
	C2	1.22						
	C4	0.52						
	C5	-2.17						

Figure 5.5 shows the improvement in the prediction of transverse cracking after local calibration.

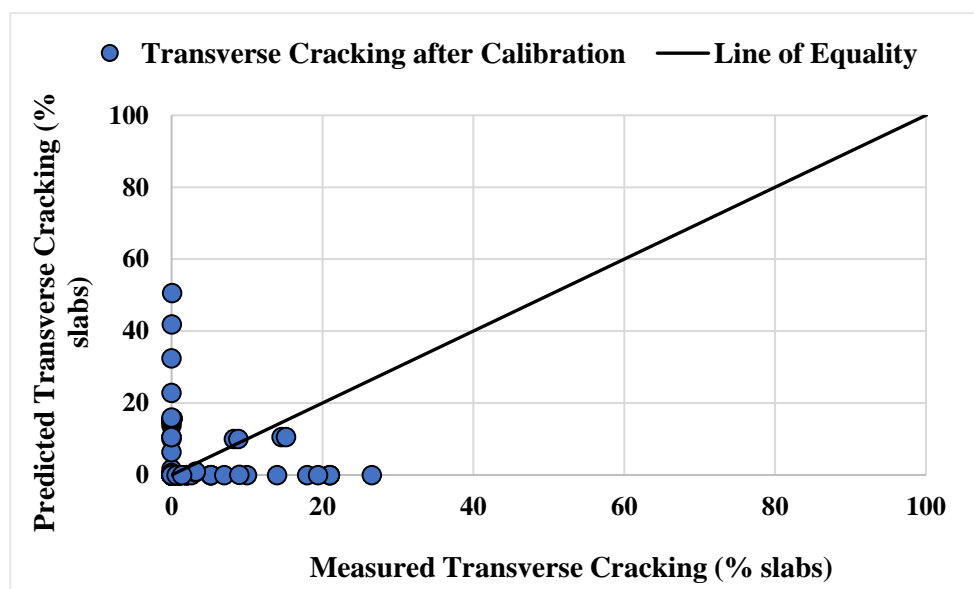


Figure 5.5 Predicted Vs. Measured Transverse Cracking Using Local Calibration Factors

5.2.3 Validation of Transverse Cracking Model

Validation of transverse cracking model could not be achieved as most of the projects that were selected for validation have little to no cracking observed as can be seen in Figure 5.6.

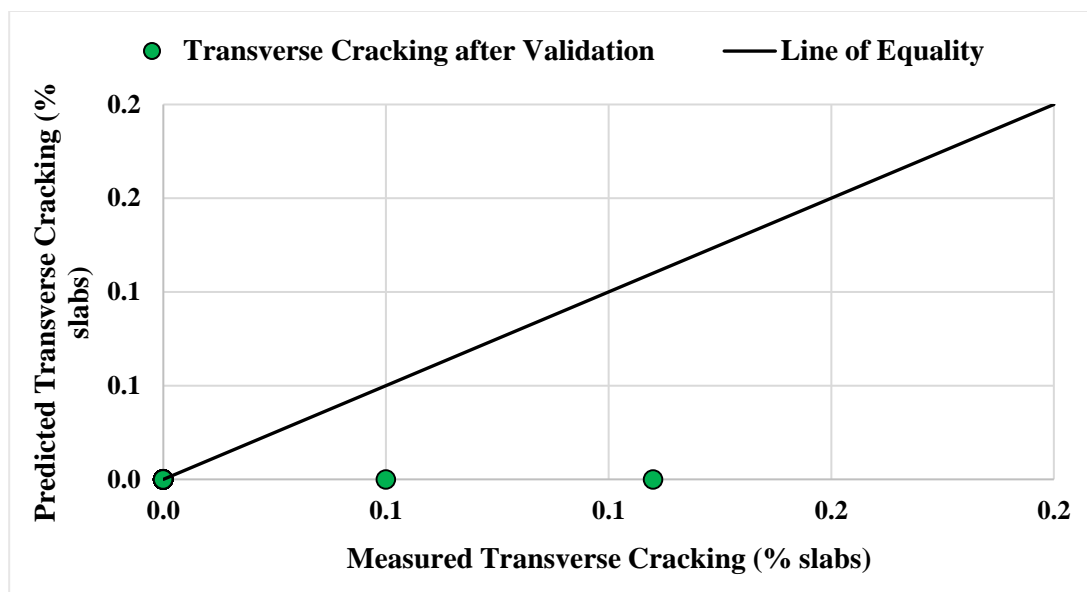


Figure 5.6 Predicted Vs. Measured Transverse Cracking Using Local Factors

5.3 Calibration of International Roughness Index (IRI) Model

Smoothness of the road surface is reported in terms of International Roughness Index (IRI). IRI model for JPCP pavement is dependent on other distress types such as faulting and cracking. In addition to that JPCP-IRI model also includes initial IRI, site factor, and spalling. IRI is reported as inch/mile.

5.3.1 Verification of IRI Model Using Global Calibration Factors

IRI with the global calibration factors showed significant amount of bias and standard error of the estimate. Also, the p-value was found lower than 0.05, which implied to reject the null hypothesis at 95% confidence interval. Hence, local calibration was attempted to reduce bias and standard error. Table 5.6 represents the summary statistics results for the verification of the IRI model.

Table 5.6 Summary of the Global Calibration Factors of IRI Model

Performance Model	Parameters	Global Factors	N	Bias, $e_{r(\text{mean})}$	Standard Error, S_e	S_e/S_y	R^2 , %	p-value (Paired t-test)
IRI	J1	0.8203	213	-1233.6	31.1	1.1	31	0.003
	J2	0.4417						
	J3	1.4929						
	J4	25.24						

Figure 5.7 shows the predicted vs measured IRI data using the global calibration factors.

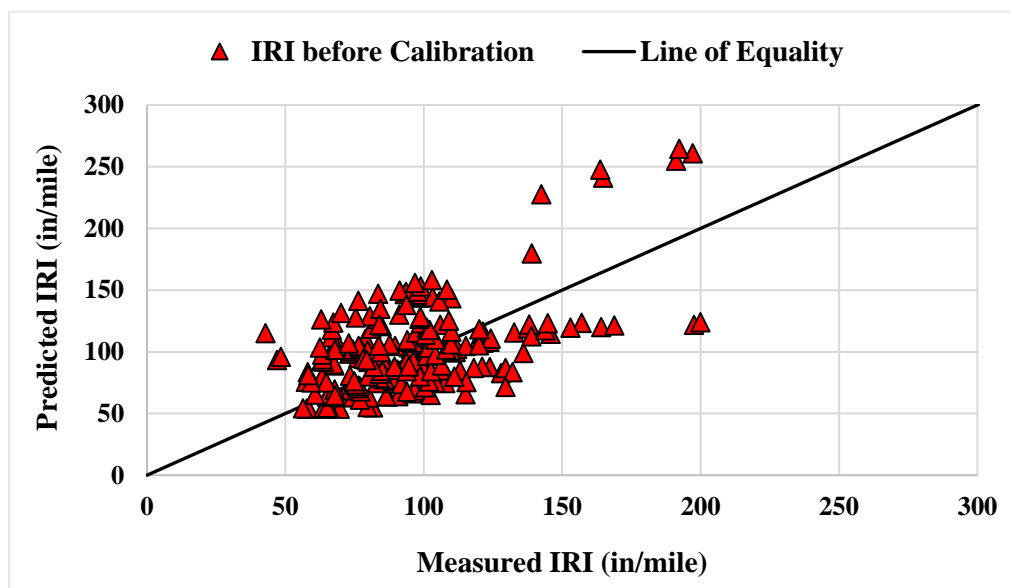


Figure 5.7 Predicted Vs. Measured IRI Using Global Calibration Factors

5.3.2 Calibration of IRI Model

In order to reduce the significant amount of bias and the standard error of the estimate, the calibration factor J4 and J1 was adjusted, respectively. After several trials for J4, bias significantly reduced from -1233.6 to 0.2. Also, the adjustment for J1 reduced the standard error of the estimate. The null hypothesis was failed to reject at 95% confidence interval.

Table 5.7 presents the summary statistical results for IRI after local calibration.

Table 5.7 Summary of the Local Calibration Factors of IRI Model

Performance Model	Parameters	Global Factors	N	Bias, $e_{r(\text{mean})}$	Standard Error, S_e	S_e/S_y	R^2 , %	p-value (Paired t-test)
IRI	J1	0.845	213	0.2	25.3	0.895	32	0.5
	J2	0.4417						
	J3	1.4929						
	J4	28.24						

Figure 5.8 shows the predicted IRI compared to the measured data after considering the local factors.

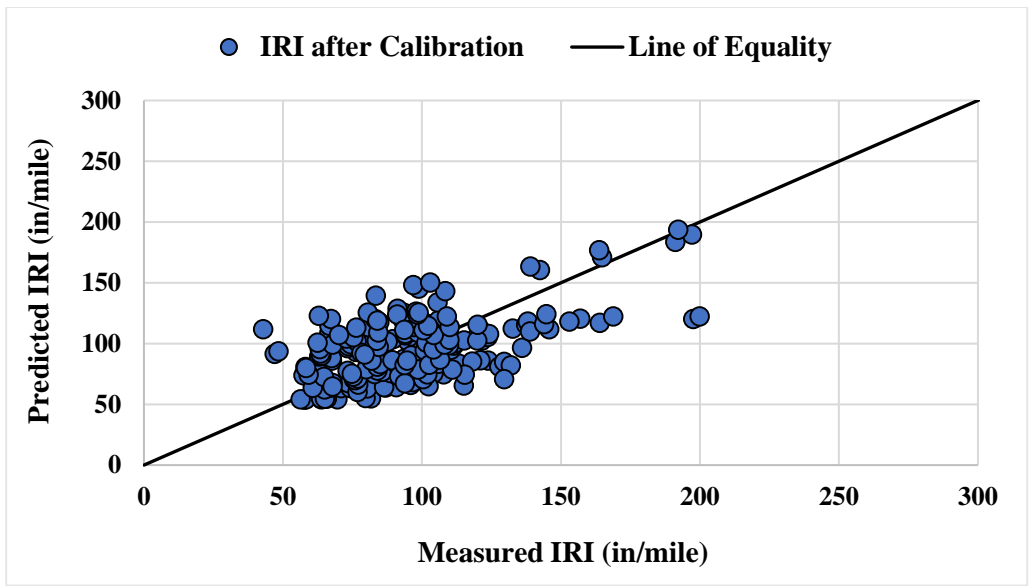


Figure 5.8 Predicted Vs. Measured IRI Using Local Calibration Factors

5.3.3 Validation of IRI Model

Validation of IRI model showed lower standard error and the null hypothesis was failed to reject at 95% confidence interval. Table 5.8 highlights the statistical summary results for IRI after validation.

Table 5.8 Summary of IRI Model after Validation

N	Bias, $e_r(\text{mean})$	Standard Error, S_e	S_e/S_y	$R^2, \%$	p-value (Paired t-test)
59	-11.55	21.04	0.940	15	0.485

Figure 5.9 shows the predicted vs measured IRI after validation using six independently projects.

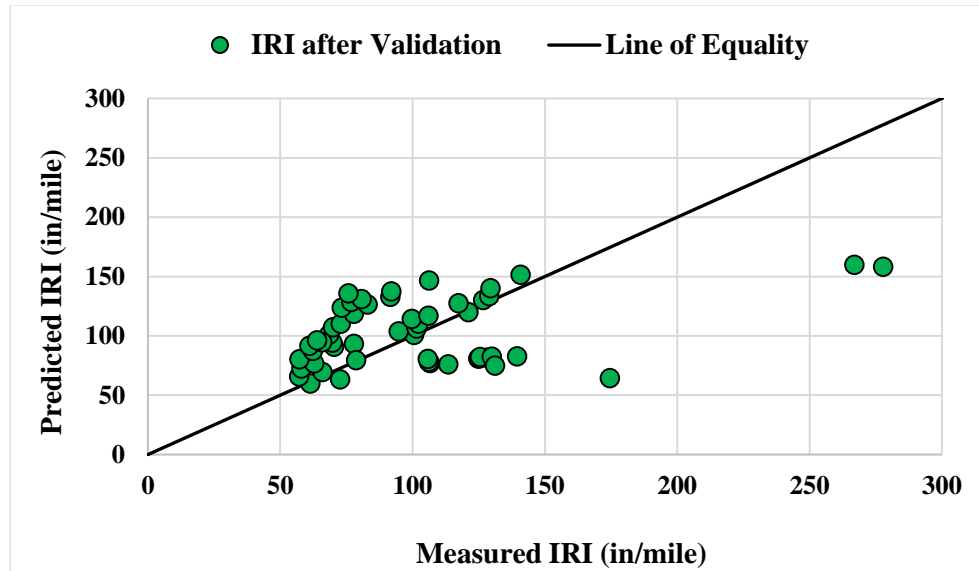


Figure 5.9 Predicted Vs. Measured IRI Using Local Factors

5.4 Calibration Results

Final calibration factors developed for rigid pavement in Idaho are highlighted in Table 5.9.

Table 5.9 Developed Local Factors for Rigid Pavement in Idaho

Performance Model	Calibration Parameters	Global Factors (as per PMED V2.5.3)	Local Factors for Idaho
Faulting	F1	0.595	0.516
	F2	1.636	1.636
	F3	0.00217	0.00217
	F4	0.00444	0.00444
	F5	250	250
	F6	0.47	0.47
	F7	7.3	7.3
	F8	400	400
Transverse Cracking	C1	2	2.366
	C2	1.22	1.22
	C4	0.52	0.52
	C5	-2.17	-2.17
IRI	J1	0.8203	0.845
	J2	0.4417	0.4417
	J3	1.4929	1.4929
	J4	25.24	28.24

CHAPTER 6: SUMMARY, CONCLUSIONS, AND RECOMMENDATIONS

6.1 Summary

The key objective of this study was to improve the PMED models prediction accuracy through local calibration in Idaho. In order to accomplish this, AASHTOWare Pavement ME Design Software version 2.5.3 was executed utilizing a total number of 34 projects for flexible pavement and 39 projects for rigid pavement. All the required inputs were collected at different hierarchical levels from the ITD engineers, and previous research projects RP193, RP253 and RP235. Material inputs were extracted mainly from the job mix formula, as-built structures, and phase reports. Missing inputs were considered following the Idaho PMED User Guide ⁽⁹⁾. Performance databases for both flexible pavement and rigid pavement were developed employing the Transportation Asset Management Systems (TAMS) and the national Long Term Pavement Performance (LTPP) database. In this study, performance models such as: rutting, longitudinal cracking, alligator cracking, thermal cracking, and IRI for flexible pavement and faulting, transverse cracking, and IRI for rigid pavement were considered to be calibrated. In most of the cases, compared to the nationally calibrated models, locally calibrated distress and IRI models improved the prediction accuracy. The local calibration effort reduced bias and standard error of the estimate, as a result, made the calibration factors statistically accepted. Moreover, the traditional splitting approach was followed to validate the calibrated factors in Idaho. Tables 6.1 and 6.2 represent the developed local factors in Idaho for the individual performance models related to flexible and rigid pavement, respectively.

Table 6.1 Summary of Calibration Factors before and after Local Calibration for Flexible Pavement in Idaho

Performance Model	Calibration Parameters	Global Factors (as per PMED V2.5.3)	Local Factors for Idaho
AC Rutting	K1	-2.45	-2.45
	K2	3.01	3.01
	K3	0.22	0.22
	β_{1r}	0.4	0.3
	β_{2r}	0.52	0.52
	β_{3r}	1.36	1.36
Unbound Base Rutting	β_{1s}	1.00	0.86
Subgrade Rutting	β_{1s}	1.00	0.736
Longitudinal Cracking (Top-Down Cracking)	$\beta_{fl}: h_{ac} < 5 \text{ in.}$	0.02054	0.02054
	$\beta_{fl}: h_{ac} > 12 \text{ in.}$	0.001032	0.001032
	$\beta_{fl}: 5 \text{ in.} \leq h_{ac} \leq 12 \text{ in.}$	$(5.014 * h_{ac}^{-3.416}) * 1 + 0$	$(5.014 * h_{ac}^{-3.416}) * 1 + 0$
	β_{f2}	1.38	1.38
	β_{f3}	0.88	0.88
	C_1	7	3.3
	C_2	3.5	0.825
Alligator Cracking (Bottom-Up Cracking)	$\beta_{fl}: h_{ac} < 5 \text{ in.}$	0.02054	0.02054
	$\beta_{fl}: h_{ac} > 12 \text{ in.}$	0.001032	0.001032
	$\beta_{fl}: 5 \text{ in.} \leq h_{ac} \leq 12 \text{ in.}$	$(5.014 * h_{ac}^{-3.416}) * 1 + 0$	$(5.014 * h_{ac}^{-3.416}) * 1 + 0$
	β_{f2}	1.38	1.38
	β_{f3}	0.88	0.88
	C_1	1.31	0.31
	$C_2: h_{ac} < 5 \text{ in.}$	2.1585	1.1585
	$C_2: 5 \text{ in.} \leq h_{ac} \leq 12 \text{ in.}$	$(0.867 + 0.2583 * h_{ac}) * 1$	$(0.867 + 0.2583 * h_{ac}) * 0.175$
$C_2: h_{ac} > 12 \text{ in.}$	3.9666	3.9666	
Thermal Cracking (Level 2)	K (MAAT ≤ 57 deg F)	$[3 * 10^{-7} * \text{MAAT}^{4.0319}] * 1 + 0$	$[2.591 * 10^{-7} * \text{MAAT}^{4.0319}] * 1 + 0$
Thermal Cracking (Level 3)	K (MAAT ≤ 57 deg F)	$[3 * 10^{-7} * \text{MAAT}^{4.0319}] * 1 + 0$	$[3.0606 * 10^{-7} * \text{MAAT}^{4.0319}] * 1 + 0$
IRI	C_1	40	80
	C_2	0.4	0.6
	C_3	0.008	0.008
	C_4	0.015	0.02

Table 6.2 Summary of Calibration Factors before and after Local Calibration for Rigid Pavement in Idaho

Performance Model	Calibration Parameters	Global Factors (as per PMED V2.5.3)	Local Factors for Idaho
Faulting	F1	0.595	0.516
	F2	1.636	1.636
	F3	0.00217	0.00217
	F4	0.00444	0.00444
	F5	250	250
	F6	0.47	0.47
	F7	7.3	7.3
	F8	400	400
Transverse Cracking	C1	2	2.366
	C2	1.22	1.22
	C4	0.52	0.52
	C5	-2.17	-2.17
IRI	J1	0.8203	0.845
	J2	0.4417	0.4417
	J3	1.4929	1.4929
	J4	25.24	28.24

6.2 Conclusions

The following conclusions can be made based on the local calibration and validation effort in Idaho:

- The global rutting prediction model for most of the selected projects over-predicted rutting. Therefore, the local calibration was conducted to reduce bias and standard error of the estimate adjusting the AC and unbound layers related calibration factors. It was found that the locally calibrated rutting model provided a better prediction with lower bias and standard error than the rutting model with the global calibration factors.
- Longitudinal cracking model with the local calibration factors improved prediction with a significant reduction of bias compared to the global prediction model.
- AASHTOWare Pavement ME Design Software v2.5.3 newly introduced three different calibration factors related to C₂ based on the asphalt thickness. The globally calibrated alligator cracking model significantly under-predicted cracking which also true for other studies^(14,16,18,20,23). The local calibration effort minimized bias

successfully and the standard error of the estimate was found within the reasonable range.

- Thermal (transverse) cracking model for flexible pavement was calibrated at Level 2 and Level 3. Due to the unavailability of Level 1 inputs of the indirect tensile strength at low temperatures, the thermal cracking model could not be calibrated at Level 1. Even though significant thermal cracking was observed on some pavement sections, the PMED predicted little to no thermal cracking. Therefore, the globally calibrated model showed a significant amount of bias. Although the thermal cracking model with the local factors at Level 3 did not show considerable improvement, bias and standard error of the estimate reduced significantly for Level 2 inputs. Therefore, it is expected that using Level 1 inputs for thermal cracking model would produce better predictions.
- It was deemed that PMED did not consider the effect of the studded tire in its prediction for IRI, as a result, under-prediction of IRI was observed for the globally calibrated model. Local factors for IRI model provided a satisfactory prediction with a significant reduction in bias and standard error.
- Because ITD did not distinguish the fatigue and reflective cracking separately during the pavement condition survey, there was inadequate data to calibrate the reflective cracking model.
- Faulting model with the global factors showed lower bias and the null hypothesis was also accepted. However, this study attempted to improve the prediction accuracy compared to the measured field data. Thus, local calibration was conducted to reduce bias and proved the model prediction capability.
- The verification results for the PCC transverse cracking revealed that considering the global factors it showed significant amount of bias and standard error of the estimate. The calibration effort reduced bias and also standard error of the estimate was found in the reasonable range.
- IRI model for the JPCP pavement showed significant amount of bias and the null hypothesis was rejected while using the global calibration factors. Hence, the local calibration was necessitated and the results after the calibration effort revealed significant amount of reduction in bias and standard error. The null hypothesis was also accepted at 95% confidence interval.

6.3 Recommendations

- ITD only quantifies rutting as surface rutting. However, previous field investigation reported that rutting also occurred in unbound layers. Therefore, to predict rutting accurately, further trench studies and core extractions should be done.
- Extracted trenches and cores will also help to determine the crack propagation whether initiates from the bottom of the pavement or occurs at the surface of the road.
- Longitudinal cracking model is still undergoing through some refinement in the NCHRP Project 1-52. Therefore, it is suggested to use the model as experimental or informational purposes until the model is improved.
- In order to perform local calibration for the thermal cracking model at Level 1, indirect tensile strength test should be done at low temperatures.
- Calibration is a continuous process with the updated performance models and upgraded PMED version that AASHTO releases. The developed performance databases should be enriched with more years of observations as PMED may include one “automated tool” called “calibrator”. Having a rich database will result in commendable calibration in the state of Idaho.
- The JPCP faulting and IRI performance models have good prediction with the field data, however the JPCP transverse cracking showed poor correlation. Thus further calibration for this model is recommended in the future once more data points are acquired.
- It is expected that the JPCP performance models would be nationally re-calibrated in near future considering the MERRA climate database. Therefore, it is recommended to verify these developed factors, and if needed, conduct further calibration.
- The pavement distress survey should follow the LTPP distress manual to be consistent with the PMED reporting units.
- Traffic database should be refined with the recent data from the WIM stations across the state.

REFERENCES

1. AASHTO. "AASHTO Guide for Design of Pavement Structures." American Association of State Highways and Transportation Officials, Washington, DC. (1993).
2. Kim, Y. R., Jadoun, F. M., Hou, T. & Muthadi, N. "Local calibration of the MEPDG for flexible pavement design." (Report No. FHWA\ NC\ 2007-07, Research and Analysis Group, North Carolina Department of Transportation, Raleigh, North Carolina) (2011).
3. NCHRP. "Guide for the Mechanistic-Empirical Design of New & Rehabilitated Pavement Structures." Final Report for NCHRP Project 1-37A. Transportation Research Board, Washington, DC. (2004)
4. Zhong, J. "Rigid Pavement : Ontario Calibration of the Mechanistic-Empirical Pavement Design Guide Prediction models." (Master's thesis, University of Waterloo) (2017).
5. Long-Term Pavement Performance (LTPP). United States Department of Transportation, Federal Highway Administration. <https://infopave.fhwa.dot.gov/> (2018).
6. Kim, S., Ceylan, H., Ma, D. & Gopalakrishnan, K. "Calibration of Pavement ME Design and Mechanistic-Empirical Pavement Design Guide Performance Prediction Models for Iowa Pavement Systems." Journal of Transportation Engineering. 140, 04014052 (2014).
7. Bayomy, F., El-Badawy, S. & Awed, A. "Implementation of the MEPDG for Flexible Pavements in Idaho." Idaho Transportation Department, (2012).
8. Nassiri, S., Rangelov, M., Ibrahim, A., Bayomy, F., Muftah, A., & Sigdel, B. Portland Cement Concrete Material Characterization for Pavement ME Design Implementation in Idaho (No. RP 253). (Idaho Transportation Department, 2017).
9. Mallela, J., Titus-Glover, L., Bhattacharya, B., Darter, M., & Von Quintus, H. "Idaho AASHTOWare pavement ME design user's guide, version 1.1." (Report No. FHWA-ID/14-211B). (Idaho Transportation Department, 2014).
10. AASHTO. "Mechanistic-Empirical Pavement Design Guide: A Manual of Practice." (American Association of State Highway and Transportation Officials, 2015).

11. AASHTO. "Mechanistic-Empirical Pavement Design Guide, Interim Edition: A Manual of Practice." (2008).
12. AASHTO. "Guide for the Local Calibration of the Mechanistic-Empirical Pavement Design Guide." American Association of State Highway and Transportation Officials (2010).
13. Applied Pavement Technology, Inc. "AASHTO Pavement ME National Users Group Meetings." Technical Report : Second Annual Meeting — Denver, Co. Federal Highway Administration Washington, D.C. (2017).
14. Muthadi, N. R. & Kim, Y. R. "Local Calibration of Mechanistic – Empirical Pavement Design Guide for Flexible Pavement Design." *Transportation Research Record*, 2087(1), 131-141.
15. Miller, J. S., & Bellinger, W. Y. "Distress Identification Manual for the Long-Term Pavement Performance Program." (Report No. FHWA-HRT-13-092). United States. Federal Highway Administration. Office of Infrastructure Research and Development. (2014).
16. Tarefder, R., & Rodriguez-Ruiz, J. I. "Local calibration of MEPDG for flexible pavements in New Mexico." *Journal of Transportation Engineering*, 139(10), 981-991. (2013).
17. Hoegh, K., Khazanovich, L. & Jensen, M. "Local Calibration of Mechanistic – Empirical Minnesota Road Research Project Test Sections." *Transportation Research Record*, 2180(1), 130-141. (2010).
18. Li, J., Pierce, L. M. & Uhlmeier, J. "Calibration of Flexible Pavement in Mechanistic – Empirical Pavement Design Guide for Washington State." *Transportation Research Record*, 2095(1), 73-83. (2009).
19. Hall, K. D., Xiao, D. & Wang, K. C. P. "Calibration of the MEPDG for Flexible Pavement Design in Arkansas." (2015).
20. Souliman, M., Mamlouk, M. & Zapata, C. "Calibration of the AASHTO MEPDG for flexible pavement for Arizona conditions." In *Proceedings of the Transportation Research Board 89th Annual Meeting* (p. 22). Washington, DC, USA: Transportation Research Board. (2010).

21. Darter, M. I., Von Quintus, H., Bhattacharya, B. B., & Mallela, J. "Calibration and implementation of the AASHTO mechanistic-empirical pavement design guide in Arizona." (Report No. FHWA-AZ-14-606). Arizona. Dept. of Transportation. Research Center. (2014).
22. Mallela, J. et al. "Guidelines for Implementing NCHRP 1-37A M-E Design Procedures in Ohio: Volume 1 — Summary of Findings, Implementation Plan, and Next Steps." (Report No. FHWA/OH-2009/9A). Ohio. Dept. of Transportation. (2009).
23. Gong, H., Huang, B., Shu, X. & Udeh, S. "Local calibration of the fatigue cracking models in the Mechanistic-Empirical Pavement Design Guide for Tennessee." *Road Materials and Pavement Design*, 18(sup3), 130-138. (2017).
24. Zhou, C. et al. "Validating MEPDG with Tennessee Pavement Performance Data." *Journal of Transportation Engineering*, 139(3), 306-312. (2013).
25. Li, J., Muench, S. T., Mahoney, J. P., Sivaneswaran, N. & Pierce, L. M. "Calibration of the Rigid Pavement Portion of the NCHRP 1-37A Software for Use by the Washington State Department of Transportation." *Journal of the Transportation Research Board*, (1949), 43-53. (2006).
26. Oh, J. & Fernando, E. G. "Development of Thickness Design Tables Based on the M-EPDG". 308 (2008).
27. Darter, M. I., Titus-Glover, L. & Quintus, H. L. Von. "Implementation of the Mechanistic-Empirical Pavement Design Guide in Utah : Validation, Calibration, and Development of the UDOT MEPDG user's guide." (Report No. UT-09.11). Utah. Dept. of Transportation. Research Division. (2009).
28. Ceylan, H., Kim, S., Kaya, O. & Gopalakrishnan, K. "Investigation of AASHTOWare Pavement ME Design / Darwin-ME Performance Prediction Models for Iowa Pavement Analysis and Design." (2015).
29. Williams, R. C. & Shaidur, R. "Mechanistic-Empirical Pavement Design Guide Calibration for Pavement Rehabilitation" (Report No. SPR 718). Oregon. Dept. of Transportation. Research Section. (2013).

30. Mallela, J., Titus-Glover, L., Sadasivam, S., Bhattacharya, B., Darter, M., & Von Quintus, H. "Implementation of the AASHTO Mechanistic-Empirical Pavement Design Guide for Colorado." (Report No. CDOT-2013-4). Colorado. Dept. of Transportation. Research Branch. (2013).
31. Wu, Z., Xiao, D. X., Zhang, Z. & Temple, W. H. "Evaluation of AASHTO Mechanistic-Empirical Pavement Design Guide for designing rigid pavements in Louisiana." *International Journal of Pavement Research and Technology*, 7(6), 405-416. (2014).
32. Sun, X., Han, J., Parsons, R. L., Misra, A. & Thakur, J. K. "Calibrating the Mechanistic-Empirical Pavement Design Guide for Kansas Calibrating the Mechanistic-Empirical Pavement Design Guide for Kansas." Kansas. Dept. of Transportation. Bureau of Materials & Research. (2015).
33. Smith, B. & Nair, H. "Development of Local Calibration Factors and Design Criteria Values for Mechanistic-Empirical Pavement Design." (Report No. FHWA/VCTIR 16-R1). Virginia Center for Transportation Innovation and Research. (2015).
34. NCHRP. "Changes to the Mechanistic-Empirical Pavement Design Guide Software Through Version 0.900-July, 2006." *Research Results Digest 308*. National Cooperative Highway Research Program 1-40 D. Washington, DC: Transportation Research Board, National Research Council (2006).
35. NCHRP. "National Calibration of MEPDG Rigid Pavement Models Based on Corrected CTE Values." *National Cooperative Highway Research Program 20-07/Task 288*. Washington, DC: Transportation Research Board, National Research Council (2011)
36. Khanum, T., Mulandi, J. N. & Hossain, M. "Implementation of the 2002 AASHTO Design Guide for Pavement Structures in KDOT." (2008).
37. Romanoschi, S., Momin, S., Bethu, S. & Bendana, L. "Development of Traffic Inputs for New Mechanistic-Empirical Pavement Design Guide: Case Study." *Transportation Research Record*, 2256(1), 142-150. (2012).

38. Mallela, J., Quintus, H. L. Von, Darter, M. I. & Bhattacharya, B. B. “Road Map for Implementing The AASHTO Pavement ME Design Software for the Idaho Transportation Department.” (Idaho Transportation Department, 2014).
39. Pierce, L. M. & McGovern, G. “Implementation of the AASHTO Mechanistic-Empirical Pavement Design Guide and Software: A synthesis of Highway Practice.” (Report No. Project 20-05, Topic 44-06) (2014).

APPENDIX

Table A.1 Site Specific Traffic Inputs for Idaho Local Pavements

Project #	District	AADTT	Traffic Growth Rate (%)	Number of Lane	Percent Truck in Design Direction	Percent of Truck in Design Lane	Operational Speed (mph)
1	D1	506	4	2	65	48	60
2	D1	480	4	2	65	48	60
3	D1	570	4	2	65	48	60
4	D1	340	4	1	50	100	60
5	D1	225	4	1	60	100	60
6	D2	88	2.3	1	60	100	50
7	D2	330	3.2	1	60	100	50
8	D2	882	2.6	2	60	50	65
9	D2	430	3	1	60	100	55
10	D2	153	2.2	1	60	100	30
11	D2	152	2.5	1	60	100	40
12	D2	515	2.1	1	60	100	65
13	D3	359	1.2	1	60	100	35
14	D3	737	3.8	2	51	95	45
15	D3	584	3.25	1	60	100	65
16	D3	724	1.8	1	60	100	55
17	D3	530	1.9	2	50	60	55
18	D3	530	3	1	60	100	60
19	D3	80	1.6	1	60	100	55
20	D3	1040	2.8	1	60	100	55
21	D3	430	3	1	60	100	35
22	D3	290	1.3	1	60	100	55
23	D4	570	3.5	1	60	48	60
24	D5	880	3	1	60	48	60
25	D6	1070	3	1	60	48	60

Table A.2 Site Specific Traffic Inputs for LTPP Sections

Project #	LTPP ID	AADTT	Traffic Growth Rate	Number of Lane	Percent Truck in Design Direction	Percent of Truck in Design Lane	Operational Speed (mph)
1	1001	120	3	2	50	95	65
2	1005	70	3	1	50	100	65
3	1007	67	3	1	50	100	60
4	1009	1048	3	2	50	95	75
5	1010	1000	3	2	50	95	75
6	1020	87	3	1	50	100	65
7	1021	527	3	2	50	95	65
8	9032	123	3	1	50	100	65
9	9034	196	3	1	50	100	65

Table A.3 Measured Rutting and IRI Data for Idaho Local Pavements

Project #	District	Year	AC Rutting (inches)	Base Rutting (inches)	Subgrade Rutting (inches)	Total Rutting (inches)	IRI (inch/mile)
1	D1	2011	0.035	0.023	0.042	0.100	-
		2012	0.055	0.035	0.065	0.155	-
		2013	0.078	0.050	0.092	0.220	-
		2014	0.093	0.059	0.108	0.260	68.409
		2015	0.091	0.058	0.106	0.255	72.500
		2016	0.095	0.059	0.111	0.265	84.591
2	D1	2011	0.033	0.026	0.071	0.130	-
		2012	0.051	0.040	0.109	0.200	-
		2013	0.072	0.054	0.149	0.275	-
		2014	0.085	0.062	0.173	0.320	85.000
		2015	0.082	0.060	0.168	0.310	85.682
		2016	0.092	0.065	0.183	0.340	95.909
3	D1	2011	0.023	0.018	0.054	0.095	
		2012	0.041	0.032	0.096	0.170	
		2013	0.064	0.048	0.143	0.255	
		2014	0.074	0.054	0.162	0.290	80.250
		2015	0.076	0.055	0.164	0.295	87.000
		2016	0.079	0.057	0.170	0.305	98.750
4	D1	2011	0.034	0.014	0.130	0.178	-
		2012	0.036	0.015	0.139	0.190	-
		2013	0.038	0.016	0.148	0.202	-
		2014	0.040	0.016	0.154	0.210	100.682
		2015	0.042	0.017	0.159	0.218	114.773
		2016	0.047	0.018	0.170	0.235	129.091
5	D1	2014	0.018	0.011	0.065	0.093	97.500
		2015	0.017	0.010	0.059	0.085	109.091
		2016	0.023	0.012	0.074	0.109	110.909
6	D2	2014	0.029	0.013	0.081	0.122	100.909
		2015	0.030	0.013	0.082	0.125	104.318
		2016	0.031	0.013	0.086	0.130	116.136
7	D2	2013	0.049	0.015	0.160	0.223	109.000
		2014	0.067	0.020	0.215	0.302	121.500
		2015	0.069	0.020	0.212	0.300	127.500
		2016	0.057	0.016	0.172	0.245	125.500

Table A.3 Measured Rutting and IRI Data for Idaho Local Pavements (Cont.)

Project #	District	Year	AC Rutting (inches)	Base Rutting (inches)	Subgrade Rutting (inches)	Total Rutting (inches)	IRI (inch/mile)
8	D2	2012	0.030	0.022	0.121	0.173	-
		2013	0.039	0.028	0.153	0.220	-
		2014	0.048	0.033	0.178	0.258	74.000
		2015	0.052	0.034	0.186	0.272	77.000
		2016	0.054	0.035	0.191	0.280	94.500
9	D2	2013	0.030	0.020	0.080	0.130	101.500
		2014	0.031	0.019	0.080	0.130	85.200
		2015	0.032	0.019	0.079	0.130	85.200
		2016	0.038	0.022	0.090	0.150	82.900
		2017	0.041	0.023	0.097	0.160	103.300
10	D2	2012	0.034	0.011	0.025	0.070	-
		2013	0.051	0.015	0.033	0.100	-
		2014	0.063	0.018	0.039	0.120	109.886
		2015	0.064	0.017	0.039	0.120	116.818
		2016	0.059	0.016	0.035	0.110	117.500
11	D2	2011	0.019	0.006	0.015	0.040	-
		2012	0.046	0.013	0.031	0.090	-
		2013	0.059	0.015	0.037	0.110	-
		2014	0.070	0.017	0.043	0.130	82.727
		2015	0.071	0.017	0.042	0.130	95.000
		2016	0.071	0.017	0.042	0.130	95.227
12	D2	2013	0.045	0.040	0.069	0.154	-
		2014	0.052	0.045	0.077	0.174	103.750
		2015	0.054	0.046	0.080	0.181	122.500
		2016	0.056	0.047	0.081	0.184	141.429
13	D3	2013	0.045	0.020	0.039	0.104	-
		2014	0.058	0.025	0.048	0.131	-
		2015	0.054	0.023	0.045	0.122	-
		2016	0.083	0.035	0.068	0.185	-
14	D3	2011	0.016	0.012	0.052	0.080	-
		2012	0.014	0.009	0.038	0.060	-
		2013	0.029	0.018	0.074	0.120	-
		2014	0.034	0.021	0.085	0.140	107.500
		2015	0.037	0.022	0.091	0.150	116.250
		2016	0.045	0.026	0.108	0.180	128.056
15	D3	2012	0.011	0.010	0.019	0.040	-
		2013	0.025	0.022	0.043	0.090	-
		2014	0.025	0.022	0.043	0.090	90.455
		2015	0.024	0.022	0.044	0.090	93.409
		2016	0.031	0.026	0.053	0.110	94.545

Table A.3 Measured Rutting and IRI Data for Idaho Local Pavements (Cont.)

Project #	District	Year	AC Rutting (inches)	Base Rutting (inches)	Subgrade Rutting (inches)	Total Rutting (inches)	IRI (inch/mile)
16	D3	2013	0.047	0.010	0.055	0.112	-
		2014	0.057	0.012	0.064	0.132	82.727
		2015	0.067	0.014	0.075	0.156	86.364
		2016	0.076	0.015	0.084	0.176	88.409
17	D3	2013	0.034	0.018	0.089	0.140	107.800
		2014	0.043	0.021	0.105	0.170	96.900
		2015	0.047	0.023	0.111	0.180	92.500
		2016	0.045	0.021	0.104	0.170	116.000
		2017	0.058	0.027	0.134	0.220	121.600
18	D3	2014	0.017	0.015	0.129	0.160	105.000
		2015	0.019	0.016	0.134	0.169	127.727
		2016	0.021	0.015	0.133	0.169	130.227
19	D3	2013	0.014	0.019	0.057	0.090	74.091
		2014	0.016	0.019	0.055	0.090	77.955
		2015	0.017	0.020	0.058	0.095	92.727
20	D3	2014	0.115	0.046	0.096	0.257	-
		2015	0.128	0.048	0.103	0.279	-
		2016	0.171	0.064	0.136	0.371	-
21	D3	2014	0.018	0.006	0.048	0.073	77.917
		2015	0.023	0.008	0.062	0.093	92.917
		2016	0.024	0.008	0.066	0.098	94.167
		2017	0.021	0.006	0.052	0.080	99.583
22	D3	2014	0.042	0.030	0.070	0.141	108.409
		2015	0.042	0.029	0.070	0.143	-
		2016	0.043	0.029	0.069	0.145	-
23	D4	2013	0.024	0.029	0.058	0.110	123.844
		2014	0.028	0.033	0.068	0.129	92.969
		2015	0.026	0.031	0.063	0.121	89.844
		2016	0.030	0.036	0.074	0.139	92.500
		2017	0.037	0.043	0.091	0.171	93.125
24	D5	2014	0.018	0.025	0.061	0.104	63.750
		2015	0.030	0.039	0.122	0.191	64.375
		2016	0.024	0.029	0.096	0.149	70.000
		2017	0.034	0.038	0.127	0.200	73.333
25	D6	2014	0.034	0.031	0.040	0.105	82.727
		2015	0.026	0.025	0.042	0.093	77.727
		2016	0.034	0.032	0.058	0.124	78.636
		2017	0.032	0.028	0.052	0.112	77.045

Table A.4 Measured Rutting and IRI Data for LTPP Sections in Idaho

Project #	LTPP ID	Year	AC Rutting (inches)	Base Rutting (inches)	Subgrade Rutting (inches)	Total Rutting (inches)	IRI (inch/mile)
1	1001	1994	0.061	0.044	0.131	0.236	-
		1997	0.078	0.055	0.163	0.295	-
		1998	0.099	0.069	0.205	0.374	-
2	1005	1989	0.057	0.083	0.175	0.315	93.160
3	1007	1997	0.055	0.000	0.339	0.394	89.290
4	1009	1994	0.096	0.029	0.269	0.394	98.880
5	1010	1983	0.018	0.005	0.057	0.079	84.590
		1984	0.022	0.006	0.070	0.098	87.610
		1987	0.023	0.006	0.069	0.098	93.390
		1987	0.023	0.006	0.069	0.098	95.360
		1987	0.023	0.006	0.069	0.098	97.900
		1987	0.024	0.006	0.068	0.098	97.820
		1988	0.024	0.006	0.068	0.098	97.680
		1988	0.029	0.007	0.082	0.118	105.290
		1988	0.019	0.005	0.055	0.079	102.010
		1989	0.024	0.006	0.068	0.098	102.300
6	1020	1990	0.020	0.005	0.055	0.079	102.620
6	1020	1990	0.030	0.052	0.095	0.177	43.000
7	1021	1990	0.048	0.022	0.107	0.177	78.220
		1991	0.033	0.014	0.071	0.118	79.110
		1995	0.045	0.019	0.094	0.157	75.850
		1997	0.051	0.021	0.105	0.177	78.140
		1999	0.058	0.023	0.115	0.197	78.670
		2002	0.067	0.025	0.124	0.217	76.130
		2004	0.083	0.029	0.144	0.256	74.400
8	9032	1991	0.056	0.109	0.150	0.315	104.861
		1992	0.038	0.066	0.093	0.197	98.588
		1993	-	-	-	-	108.472
		1994	0.051	0.093	0.131	0.276	114.745
		1995	-	-	-	-	115.949
		1996	-	-	-	-	119.687
		1997	0.049	0.077	0.110	0.236	117.406
		1998	0.056	0.090	0.129	0.276	-
		1999	-	-	-	-	118.863
		2000	0.051	0.075	0.110	0.236	125.263
		2001	0.052	0.074	0.110	0.236	124.059
		2002	0.061	0.086	0.128	0.276	-
		2003	0.080	0.110	0.164	0.354	132.739
2005	0.083	0.108	0.163	0.354	-		
9	9034	1994	0.052	0.031	0.074	0.157	106.080
		1997	0.046	0.027	0.065	0.138	109.220
		1998	0.068	0.038	0.091	0.197	114.830

Table A.5 Measured Longitudinal, Alligator and Thermal Cracking Data for Idaho Local Pavements

Project #	District	Year	Longitudinal Cracking (ft/mile)	Alligator Cracking (%)	Thermal Cracking (ft/mile)
1	D1	2014	-	0.000	0.000
		2015	0.000	0.000	0.000
		2016	0.000	0.000	0.000
2	D1	2014	81.868	0.000	4.739
		2015	98.944	0.012	6.727
		2016	100.005	0.020	7.247
3	D1	2014	40.768	0.000	113.906
		2015	51.751	0.000	204.517
		2016	62.733	0.000	295.127
4	D1	2014	0.000	0.009	5.897
		2015	0.550	0.029	12.520
		2016	2.716	0.049	18.827
5	D1	2014	18.212	0.068	17.806
		2015	25.580	0.167	21.871
		2016	32.948	0.266	25.936
6	D2	2014	0.000	0.000	0.000
		2015	0.000	0.000	0.000
		2016	2.286	0.000	6.467
7	D2	2014	0.000	0.000	-
		2015	0.000	0.000	0.000
		2016	0.000	0.000	0.000
8	D2	2014	3.599	0.000	0.000
		2015	8.269	0.000	0.000
		2016	15.199	0.000	0.000
9	D2	2011	0.000	0.000	0.000
		2012	0.000	0.000	0.000
		2013	0.000	0.000	0.000
		2014	7.100	0.000	20.000
		2015	15.927	0.000	23.012
		2016	19.825	0.001	24.555
10	D2	2014	0.000	0.000	0.000
		2015	0.000	0.000	0.000
		2016	0.000	0.000	0.000
11	D3	2014	0.000	0.000	3.463
		2015	0.000	0.000	4.728
		2016	1.375	0.000	10.450

Table A.5 Measured Longitudinal, Alligator and Thermal Cracking Data for Idaho Local Pavements (Cont.)

Project #	District	Year	Longitudinal Cracking (ft/mile)	Alligator Cracking (%)	Thermal Cracking (ft/mile)
12	D3	2014	121.132	0.000	630.907
		2015	130.085	0.011	695.960
		2016	366.535	0.037	707.049
13	D3	2014	0.000	0.000	124.757
		2015	0.000	0.000	152.910
		2016	0.000	0.000	204.433
14	D3	2014	0.000	0.000	0.000
		2015	0.000	0.000	0.000
		2016	0.000	0.000	0.000
15	D3	2014	77.195	0.063	159.964
		2015	82.385	0.125	163.905
		2016	92.875	0.180	168.019
16	D3	2013	0.000	0.000	0.000
		2014	0.000	0.000	0.000
		2015	0.000	0.000	0.000
17	D3	2014	243.518	0.761	868.863
		2015	252.722	0.883	868.863
		2016	307.954	1.654	868.863
18	D3	2014	0.000	0.000	-
		2015	0.000	0.000	-
		2016	0.000	0.000	-

Table A.6 Measured Longitudinal, Alligator and Thermal Cracking Data for LTPP Sections in Idaho

Project #	LTPP ID	Year	Longitudinal Cracking (ft/mile)	Alligator Cracking (%)	Thermal Cracking (ft/mile)
1	1001	1994	2103.000	0.270	37.000
		1997	1843.000	10.240	52.000
		1998	1732.000	8.880	151.000
2	1005	1989	0.000	0.000	81.000
3	1007	1997	0.000	-	300.000
4	1009	1994	0.000	0.380	420.000
5	1010	1983	0.000	0.000	266.000
		1984	0.000	0.000	259.000
		1987	0.000	1.690	766.000
		1987	73.000	2.010	759.000
		1987	52.000	2.050	773.000
		1987	631.000	1.520	285.000
		1988	738.000	1.960	288.000
		1988	683.000	2.820	290.000
		1988	239.000	4.050	528.000
		1989	35.000	5.220	741.000
1990	76.000	5.220	741.000		
6	1020	1990	0.000	0.000	0.000
7	1021	1990	0.000	0.000	0.000
		1991	0.000	0.000	0.000
		1995	0.000	0.000	0.000
		1997	0.000	0.000	0.000
		1999	0.000	0.000	0.000
		2002	0.000	0.000	0.000
		2004	0.000	0.000	0.000
8	9032	1996	0.000	0.000	128.189
		1999	0.000	0.000	170.919
		2000	0.000	0.000	166.299
		2003	66.982	0.000	212.493
		2004	42.730	0.102	240.210
9	9034	1994	1542.000	0.000	3.000
		1997	2294.000	0.410	20.000
		1998	2384.000	0.410	13.000

Table A.7 Measured Faulting, Transverse Cracking and IRI Data for Rigid Sections in Idaho

Project #	District	Year	Faulting (inch)	Transverse Cracking (% slabs)	IRI (inch/mile)
1	D1	2013	-	0	175.13
		2014	-	0	153.51
		2016	0.26	0.60	182.08
		2017	0.18	1.25	145.79
2	D2	2015	0.15	1.08	-
		2016	0.10	1.21	-
		2017	0.17	0.00	-
3	D2	2009	0.00	0.00	-
		2010	0.00	0.00	-
		2011	0.00	0.00	-
		2012	0.00	0.00	82.92
		2013	0.00	0.00	85.96
		2016	0.18	0.03	57.68
		2017	0.21	0.08	85.52
4	D3	2012	0.00	0.00	-
		2013	0.00	0.00	-
		2014	0.00	0.00	145.56
		2015	0.20	0.00	130.47
		2016	0.22	0.27	127.84
		2017	0.22	2.63	129.53
5	D3	2015	0.10	0.00	102.39
		2016	0.11	0.00	115.07
		2017	0.11	0.00	96.00
6	D3	2014	0.00	0.00	76.00
		2015	0.05	0.00	76.80
		2016	0.06	0.00	75.40
		2017	0.10	0.11	59.29
7	D3	2007	0.00	0.00	87.00
		2008	0.00	0.00	86.00
		2009	0.00	0.00	84.00
		2010	0.00	0.00	80.00
		2011	0.00	0.00	47.00
		2012	0.00	0.00	76.29
		2013	0.00	0.00	100.00
		2014	0.00	0.00	73.14
		2015	0.14	0.00	73.57
		2016	0.18	0.00	74.40
2017	0.15	0.00	77.00		

Table A.7 Measured Faulting, Transverse Cracking and IRI Data for Rigid Sections in Idaho (Cont.)

Project #	District	Year	Faulting (inch)	Transverse Cracking (% slabs)	IRI (inch/mile)
8	D3	2007	0.00	0.00	88.75
		2008	0.00	0.00	85.75
		2009	0.00	0.00	84.00
		2010	0.00	0.00	80.00
		2011	0.00	0.00	58.33
		2012	0.00	0.00	84.00
		2013	0.00	0.00	132.00
		2014	0.00	0.00	85.00
		2015	0.21	0.00	90.40
		2016	0.20	0.00	118.00
9	D3	2015	0.00	0.00	139.00
		2016	0.17	3.18	261.00
		2017	0.09	3.22	233.50
10	D3	2014	0.00	0.00	96.70
		2015	0.05	0.00	100.47
		2016	0.00	0.00	91.84
		2017	0.06	0.02	74.81
11	D3	2007	-	0.00	79.63
		2008	-	0.00	76.46
		2009	0.00	0.00	68.47
		2010	0.00	0.00	66.67
		2011	0.00	0.00	42.84
		2012	0.00	0.00	66.74
		2013	0.00	0.00	84.72
		2014	0.00	0.00	67.34
		2015	0.11	0.00	62.89
		2016	0.00	0.00	80.53
12	D3	2007	0.00	0.00	81.87
		2008	0.00	0.00	67.54
		2009	0.00	0.00	63.87
		2010	0.00	0.00	63.49
		2011	0.00	0.00	48.38
		2012	0.00	0.00	63.28
		2013	0.00	0.00	84.48
		2014	0.00	0.00	67.84
		2015	0.12	0.00	62.42
		2016	0.12	0.00	83.75
		2017	0.12	0.10	72.85

Table A.7 Measured Faulting, Transverse Cracking and IRI Data for Rigid Sections in Idaho (Cont.)

Project #	District	Year	Faulting (inch)	Transverse Cracking (% slabs)	IRI (inch/mile)
13	D3	2007	0.00	0.00	105.87
		2008	0.00	0.00	100.07
		2009	0.00	0.00	98.96
		2010	0.00	0.00	96.16
		2011	0.00	0.00	78.20
		2012	0.00	0.00	101.04
		2013	0.00	0.00	136.00
		2014	0.00	0.00	109.73
		2015	0.14	0.00	101.58
		2016	0.16	0.00	119.88
		2017	0.17	0.36	111.70
14	D3	2007	-	0.00	122.43
		2008	-	0.00	121.61
		2009	-	0.00	123.35
		2010	-	0.00	132.39
		2011	0.00	0.00	67.84
		2012	0.00	0.00	93.91
		2013	0.00	0.00	129.55
		2014	0.00	0.00	101.91
		2015	0.14	0.00	98.63
		2016	0.15	0.00	93.81
		2017	0.16	0.04	94.63
15	D4	2007	0.00	0.00	115.35
		2008	0.00	0.00	110.96
		2009	0.00	0.00	102.61
		2010	0.00	0.00	106.51
		2011	0.00	0.00	79.38
		2012	0.00	0.00	104.16
		2013	0.00	0.00	108.12
		2014	0.00	0.00	109.84
		2015	0.09	0.26	104.22
		2016	0.08	0.33	100.59
		2017	0.10	0.50	102.11
16	D5	2007	0.00	0.00	75.40
		2008	0.00	0.00	70.14
		2014	0.00	0.00	84.33
		2016	0.14	0.16	93.69
		2017	0.10	0.00	76.37

Table A.7 Measured Faulting, Transverse Cracking and IRI Data for Rigid Sections in Idaho (Cont.)

Project #	District	Year	Faulting (inch)	Transverse Cracking (% slabs)	IRI (inch/mile)
17	D5	2008	0.00	0.00	138.83
		2009	0.00	0.00	145.83
		2010	0.00	0.00	110.00
		2011	0.00	0.00	120.00
		2012	0.00	0.00	164.00
		2013	0.00	0.00	84.00
		2014	0.00	0.00	157.00
		2015	0.00	0.00	109.00
		2016	0.16	0.67	98.40
		2017	0.16	1.38	98.80
18	D5	2016	0.00	8.26	268.83
		2017	0.11	8.86	144.80
		-	0.10	-	-
19	D5	2007	-	-	144.00
		2008	-	-	153.00
		2016	0.09	14.60	197.56
		2017	0.08	15.18	199.89

Table A.8 Measured Faulting, Transverse Cracking and IRI Data for LTPP Rigid Sections in Idaho

Project #	LTPP ID	Year	Faulting (inch)	Transverse Cracking (% slabs)	IRI (inch/mile)
1	16_3017	1991	-	-	100.46
		1992	-	-	94.68
		1993	0	0	101.47
		1994	-	-	102.17
		1995	-	-	99.70
		1996	-	-	105.92
		1997	-	-	121.03
		1999	0	0	117.28
		2000	-	-	126.62
		2001	0.028	0	128.91
		2003			129.35
		2005	0	0	106.11
		2007	0.020	0	140.72
2	16_3023	1995	-	0	98.107
		1996	-	-	97.980
		1997	-	-	102.99
		1997	-	-	95.440
		1999	-	-	94.551
		2000	-	-	89.598
		2002	0.03	0	96.329
		2003	-	-	93.98
		2004	0.03	0	93.98
		2006	-	-	101.028
		2007	0.02	0	100.838
		2009	0.07	0	97.2185
		2012	0.05	0	101.028
		2014	0.09	0	105.918
2015	-	-	98.996		
3	49_3011	1988	-	-	83.8
		1989	-	-	103.3
		1990	0.03	-	103.0
		1991	-	0	113.1
		1992	-	0	123.8
		1993	0.09	0	-
		1994	0.24	18	-

Table A.8 Measured Faulting, Transverse Cracking and IRI Data for LTPP Rigid Sections in Idaho (Cont.)

Project #	LTPP ID	Year	Faulting (inch)	Transverse Cracking (% slabs)	IRI (inch/mile)
4	49_3015	1988	-	-	124.841
		1989	-	-	124.904
		1990	-	-	125.603
		1991	0	0	128.206
		1992	-	-	125.349
		1993	-	0	129.857
		1994	-	-	139.446
5	49_7082	1990	0.00	-	57.721
		1991	-	-	69.596
		1992	-	-	63.881
		1993	-	-	58.293
		1994	-	-	56.324
		1996	0.02	0.00	63.754
		1997	0.01	0.00	65.786
		1998	-	-	65.0875
		2000	-	-	81.661
		2001	0.05	0.00	-
		2002	-	-	79.692
		2003	0.03	0.00	-
		2006	0.02	5.20	-
		2008	0.08	5.20	-
		2009	0.10	5.20	-
2011	0.07	5.20	-		
6	49_7083	1992	-	-	80.264
		1993	-	-	70.993
		1994	-	-	74.358
		1996	-	-	66.929
		1998	0.01	-	86.995
		1999	-	-	90.805
		2000	0.02	-	86.423
7	49_7085	1992	-	-	89.6
		1993	-	14	89.3
		1994	-	-	87.2
		1996	0.02	21	103.8
		1997	-	-	100.3
		1998	0.05	10	108.5

Table A.8 Measured Faulting, Transverse Cracking and IRI Data for LTPP Rigid Sections in Idaho (Cont.)

Project #	LTPP ID	Year	Faulting (inch)	Transverse Cracking (% slabs)	IRI (inch/mile)
8	49_7086	1992	-	-	90.424
		1993	-	0	107.823
		1994	0.01	0	82.995
		1996	-	-	104.140
		1998	0.06	0	-
9	53_3013	1989	-	-	109.919
		1990	0.11	-	98.616
		1991	-	-	97.028
		1993	0.12	-	97.600
		1996	-	-	93.091
		1997	0.11	0	97.854
		1999	0.14	0	-
		2001	0.13	0	-
		2006	0.11	0	-
10	53_3014	2007	0.13	0	-
		1988	-	-	61.278
		1989	-	-	72.581
		1990	-	-	57.087
		1991	-	-	65.913
		1992	-	-	57.976
		1993	-	-	62.738
		1994	-	-	57.150
		1996	0.024	0	62.294
		1997	-	-	70.295
		1998	0.051	0	69.660
		2000	-	-	68.390
		2002	0.055	0	69.914
		2003	-	-	72.835
		2004	0.043	0	-
		2006	0.047	0	77.788
		2008	0.047	0	73.216
		2009	-	-	82.995
		2010	-	-	76.835
		2011	-	-	80.709
2012	0.083	0	91.567		
11	56_3027	1988	-	-	142.431
		1989	-	-	164.783
		1990	-	-	163.767
		1991	0.118	0	191.135
		1992	-	-	197.168
		1993	0.114	0	192.215
		1996	0.252	0	-